ABSTRACT

YOON, YEOBEOM. Design and Analysis of an Advanced Double Skin Façade System as a Window Retrofit in Old Apartments for Energy Savings. (Under the direction of Dr. Soolyeon Cho).

Due to rapid industrialization, fossil fuel consumption and CO_2 emissions have increased. One of the most effective solutions to reduce carbon dioxide emissions and fossil fuel consumption is to decrease energy consumption. In South Korea, buildings consume about 17% of total energy; therefore, efforts to save energy in the building sector are inevitable. This study focuses on high-rise apartment buildings, which account for 60% of domestic residential buildings. The number of high-rise apartments has increased exponentially since the late 1970s to address housing problems caused by high population density. In 2018, 47.7% of high-rise apartments were more than 20 years old, a 1.2% increase from 2017. At present, aging high-rise apartments have become a more serious problem.

To overcome this building problem, this study proposes a double-skin façade (DSF) system as a window retrofit method. The DSF system can enhance the insulation performance of windows and walls and serve as a thermal buffer. Photovoltaic (PV) systems are integrated into the DSF system to further reduce energy consumption by utilizing the electricity produced by the former. The EnergyPlus program was used to build simulation models. Experimental studies were conducted to improve the reliability of simulation results. Measured data were collected to analyze and calibrate the simulation model. Results revealed that installing the DSF system can significantly reduce heating and cooling energy.

When proposing a DSF system, a short payback period is as important as energy savings. Accordingly, a life cycle cost analysis was performed for DSF systems, which included the costs of manufacturing, construction, transportation, and installation. Energy cost

savings were calculated based on the simulation results of the EnergyPlus model that had been calibrated according to measured data. Subsidies from the government or the city were also considered. The energy consumption and life cycle cost analysis helped determine whether the installation of DSF systems is a more realistic way of retrofitting old high-rise apartments than replacing windows or upgrading HVAC systems.

Design and Analysis of an Advanced Double Skin Façade System as a Window Retrofit in Old Apartments for Energy Savings

by
Yeobeom Yoon

A dissertation submitted to the Graduate Faculty of
North Carolina State University
in partial fulfillment of the
requirements for the degree of
Doctor of Philosophy

Design

Raleigh, North Carolina
2021

APPROVED BY:

_____	_____
Dr. Soolyeon Cho Committee Chair	Dr. Wayne Place
_____	_____
Dr. Traci Rose Rider	Dr. Stephen Terry

DEDICATION

I dedicate this dissertation to my beloved parents, Seokcheol Yoon and Miwol Cho, and my sister, Jihye Yoon. I could not have finished this dissertation without your continuous support, love, and encouragement that boosted my self-confidence.

I also dedicate this dissertation to my lovely wife, Jiyoung Kim, and my sweet daughter, Jiah Yoon, who have supported me. Thank you for standing by my side and for giving me space to finish this dissertation on time.

I also thank my friends in Raleigh, Byeongmo Seo, Jinoh Park, Byungsoo Kim, Dongjae Yi, Hany Gaballa, Renae Mantooth, Helia Taheri, Payod Panda, Xing Huang, Anantaya Wonaphotimuke, Elif Sener, and all other Ph.D. in Design students.

Thank you for the encouragement and support during my Ph. D. studies and all the good memories we have had together.

BIOGRAPHY

Yeobeom Yoon received both his bachelor's and master's degrees in architectural engineering from the Hanbat National University in Daejeon, South Korea. He joined the Building Energy Technology (BET) lab in the College of Design at North Carolina State University in 2016. As a graduate teaching assistant, he taught and contributed to making and developing building simulation models using the EnergyPlus simulation program and the OpenStudio simulation program. Under the guidance of Dr. Soolyeon Cho, Yeobeom conducted several researches to save building energy consumption by integrating a high-performance HVAC system and ensuring its optimal control through artificial intelligence technology.

ACKNOWLEDGMENTS

First, I want to express my sincere appreciation to my advisor and committee chair, Dr. Soolyeon Cho, for his extensive guidance, support, and encouragement. Dr. Cho's broad knowledge and wise direction have helped me during my research and in completing this dissertation. I also thank my committee members, Dr. Traci Rose Rider, Dr. Wayne Place, and Dr. Stephen Terry, for their advices, valuable comments, and help.

Second, I am grateful to Dr. Kwang Ho Lee, Dr. Yujin Nam, Dr. Sunglok Do, Dr. Hongwook Kim, Dr. Dongsu Kim, and Dr. Junghyun Moon for encouraging and inspiring me during my Ph.D. study. Moreover, I thank my labmates, Mr. Byeongmo Seo and Dr. Hany Gaballa, for their insights about the research and their kind help throughout the years.

Third, I also thank my friends, Minjae Kim, Dongju Lee, Jangyong Shim, and Jungyun Jeon, for sharing good memories and their lives with me both in Korea and the United States.

Fourth, I give my heartfelt gratitude to my family, Seokcheol Yoon, Miwol Cho, Sunok Noh, Myeongbae Kim, Jihye Yoon, and all my relatives who have always supported me during my studies.

Last, my deepest appreciation goes to my wife, Jiyoung Kim, and my daughter, Jiah Yoon, for all that they have done for me. Without you, this would not have been possible.

TABLE OF CONTENTS

LIST OF TABLES

LIST OF FIGURES

Chapter 1 **INTRODUCTION**

South Korea imports 95% of its energy from overseas. The country has an energy-intensive industrial structure; thus, enhancing energy efficiency is important (Sung and Faith, 2019).

The building sector is one of the main consumers of total energy in South Korea, with buildings accounting for about 17% of total energy in 2015 (KEEI, 2016). Building energy consumption has steadily increased due to industrial development and the increasing number of buildings. Increased use of energy sources in buildings, such as gas and electricity, stimulate the emission of greenhouse gases and contribute to global warming. In 2015, the international community adopted the Paris Agreement to reduce the greenhouse gas emission (Kim et al., 2016).

South Korea ranked 7th for CO_2 emissions in 2016. Reducing CO_2 emissions is a serious concern for the country, prompting more intensive use and development of renewable energy and high-performance buildings. However, South Korea currently ranks 8th for electricity production from fossil fuels, is unranked for solar power production, and is 10th for other renewable energy resources (Olivier et al., 2017). Based on size, South Korea ranks 107th in the world, with an area of about 100,000 km^2, while based on population, it ranks 28th, with approximately 51.7 million people residing in the country as of 2020 (KOSIS, 2020). South Korea has a high population density, and many high-rise apartment buildings have been built to solve the uneven ratio of population in certain areas. South Korea has also had a dramatic economic growth (Chang, 2006).

High-rise apartment buildings are one of the most dominant types of housing in the country (Yuen and Yeh, 2011). The Ministry of Land, Infrastructure, and Transport—the government body that provides statistics on construction in South Korea—publishes on their website the Apartment House Living Condition Statistics. These statistics show living conditions in residential buildings in South Korea, including the number of floors in each (MOLIT, 2016). At present, South Korea has 125,944 high-rise apartment buildings, of which the 15-story apartment is the most common, followed by 5-story, 20-story, and 25-story apartments (Figure 1-1).

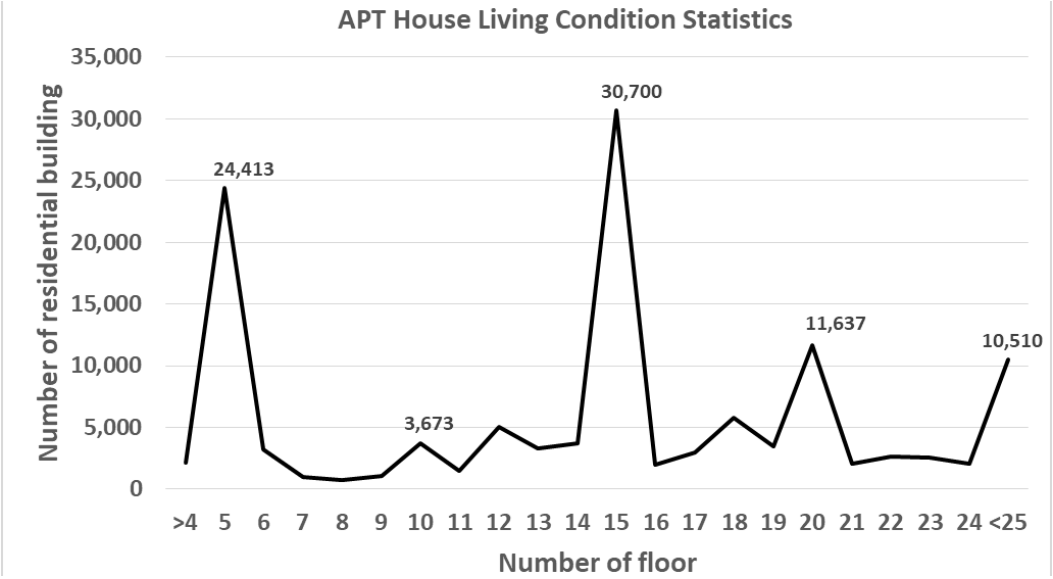

Figure 1-1: Apartment house living condition statistics

According to Statistics Korea, there are 10.8 million apartment units in high-rise apartment buildings in South Korea, comprising 61.4% of all housing in the country, and this number is steadily increasing. Of the total number of apartments, 39.6% or 4.3 million were built 20 years ago or earlier (Statistics Korea, 2019). Of this number, only about 2,000 units or

around 5% have been retrofitted through a government incentive program starting in 2014 (Yoon et al., 2018).

To reduce CO_2 emissions and energy consumption, the South Korean government revised building regulations and policies in 2001, requiring apartment buildings to be energy efficient. From 2001 to 2014, 1,380 residential buildings received preliminary Building Energy Efficiency Certification. In 2001, only one residential building received certification, but since then, the number of certified buildings increased every year. In 2014, 267 new residential buildings obtained this certificate (Park et al., 2015).

Most regulations and efforts to reduce building energy consumption, however, focus on new buildings instead of existing buildings. New buildings consume relatively less energy than buildings built in the past due to added efforts, such as utilizing highly efficient insulation, lighting, and equipment. During the construction of old buildings, construction codes were not strict, nor did they require buildings to have insulation with low U-value, and this resulted in high cooling and heating energy usage.

The Green retrofitting support project, a government project that supports retrofitting, was implemented for existing buildings. The project started in 2014 and initially covered 352 buildings. This number increased in the following years, with 2,753 and 7,742 buildings receiving support in 2015 and 2016, respectively. Of the 10,847 buildings that received green remodeling support, 10,773 were residential buildings, and only 74 were non-residential buildings (Lim et al, 2017). Notably, of the 10,847 buildings, 10,701 buildings simply changed windows, 8 reinforced insulation, 50 reinforced insulation and windows, 15 replaced windows and equipment, and 73 reinforced insulation and replaced windows and equipment.

As shown in Figure 1-2, 99% of green remodeling projects involved only window replacement, while 1% involved remodeling without window replacement. Accordingly, it can be concluded that most of the remodeling involved replacing windows that have high U-value with those that have high efficiency.

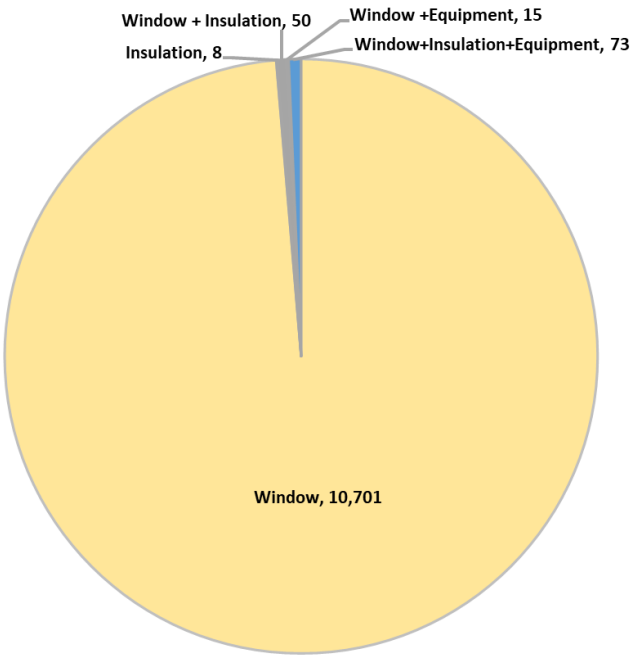

Figure 1-2: Green remodeling statistics

Not all retrofitting, however, can lower building energy consumption. Residents retrofit to extend their living space to the balcony area to create a more conditioned zone (see Figure 1-3), as seen in more than 2.6 million apartments (i.e., 26% of the total number of apartments) (Song and Choi, 2012). Expansion of living space to the balcony area adversely affects energy consumption and indoor thermal comfort. Most apartments in South Korea are south facing, so such expansion means that solar radiation directly enters the room, resulting in increased

use of air conditioners since indoor temperature is higher. Similarly, such expansion means the loss of a passive buffer area within the apartment.

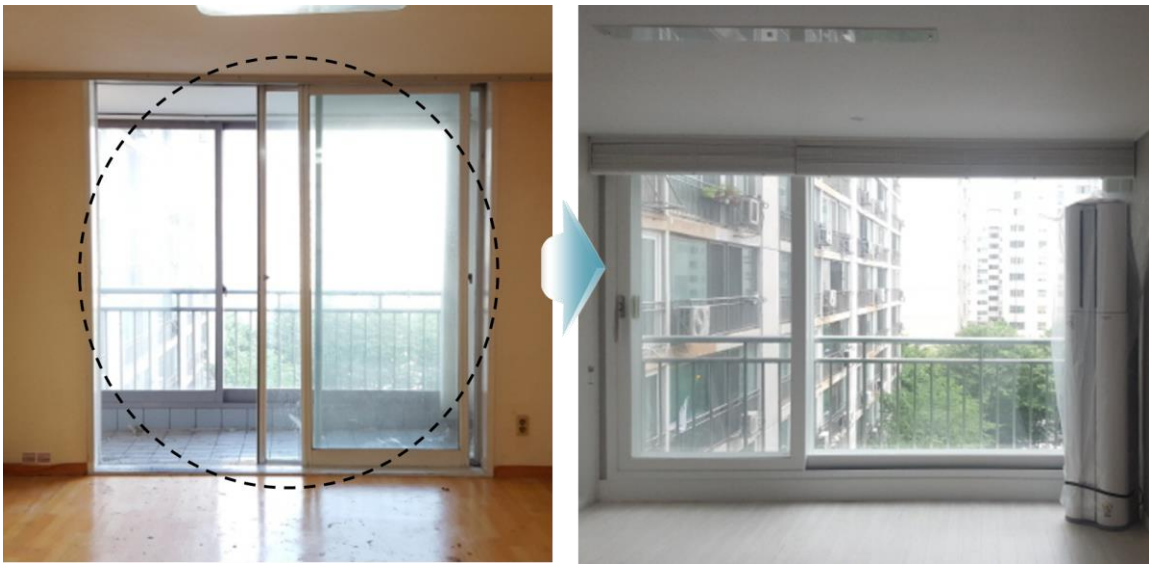

Figure 1-3: Example of a balcony area expansion

The loss of buffer area and the increased conditioned space explain why energy consumption in high-rise apartment buildings is higher than expected. The following can be done to reduce energy consumption in high-rise apartment buildings:

- enhancing the U-value of walls and windows,
- adopting a high-efficiency heating, ventilation, and air conditioning (HVAC) system, and
- installing a renewable energy system.

Although ideally effective, these options are realistically difficult to apply. For example, to enhance the U-value of walls, insulation must be added, and windows must be changed to low-emissivity (Low-E) windows or high-efficiency windows with double or triple glazing. For high-rise apartment buildings, the area of the outer wall and the outer window is smaller than that of a detached house; hence, it is difficult to reduce energy by changing the walls and windows. While window replacement is a simple and common retrofitting method, wall replacement is more difficult because the walls of the entire building must be reinforced.

While replacing windows and walls involve difficulties, adopting a high-efficiency HVAC system is even more complex. High-rise apartment buildings usually have more than 15 stories, and each story has at least two apartment units—this means that the size of the HVAC system for these high-rise apartment buildings is larger than that of single residential buildings. Moreover, replacing the HVAC system entails an extensive amount of time and expensive replacement costs.

The last option is the installation of a renewable energy system. There are a number of renewable energy sources: solar, wind, water, and geo-thermal energy. Except for solar energy, it is difficult to install other renewable energy systems due to high costs or geographical problems. As explained previously, the outer walls of high-rise apartment buildings have a smaller area than that of detached houses; therefore, the installation of a photovoltaic (PV) system is not enough to cover the energy demand of the building. Installing a PV system alone cannot significantly reduce the energy consumption of a building.

Given the above reasons, this research proposes the installation of enhanced walls and windows and a renewable energy system in an apartment unit as a retrofitting method to reduce building energy consumption.

To enhance the U-value of the exterior wall, additional insulation or other building materials should be used. It is difficult to do so for the exterior walls of high-rise apartment buildings because the entire wall of the building needs to be strengthened. Similarly, installing a DSF system can reduce the energy consumption of each apartment unit but not the entire high-rise apartment building.

The installation of the DSF system can reinforce walls and windows due to its outer structure. It also has an air cavity that can work as a thermal buffer area. The DSF system is an efficient way to reduce heating energy because the temperature inside the system is higher than the outside temperature in the winter season. It can effectively reduce energy consumption in apartment buildings, which are heating-oriented buildings. In addition, the PV system in the DSF system can generate electrical energy, which can be used in the apartment building.

1.1 Research Significance and Objectives

This research is significant for two reasons: (1) it proposes the installation of a DSF system and a PV system in high-rise apartment buildings to save energy, and (2) it improves the appearance of a high-rise apartment building. Although reducing energy consumption in high-rise apartment buildings in South Korea is necessary, this may be difficult to achieve due to the lack of exterior walls and windows and the fact that, due to poor construction, high-rise apartment buildings built 20 years ago or earlier consume more energy than newer residential buildings.

Furthermore, 26% of residential units in high-rise apartment buildings have extended living space to the balcony area. The disappearance of the balcony area increases heating and cooling energy consumption. The balcony area is an unconditioned zone because it prevents

solar radiation from directly entering the room. The air layer in the balcony also acts as a thermal buffer, which can reduce cooling and heating energy consumption. Old high-rise apartment buildings already consume much heating and cooling energy, but with the disappearance of balconies, energy consumption rose even more.

The replacement of exterior windows is a typical retrofitting method to reduce building energy consumption. However, this is not enough to reduce building energy consumption.

The objectives of this research are two-fold: (1) to reduce energy consumption in high-rise apartment buildings using a new retrofitting method, that is, the installation of the DSF system to the south façade and the installation of the PV system to the DSF system and (2) to improve the appearance of high-rise apartment buildings (see Figure 1-4). The image on the left side shows the appearance of the old high-rise apartment building, while the image on the right side shows the expected appearance of the same building after the installation of the DSF and PV systems. The outdoor unit is usually installed randomly in each apartment unit, which negatively affects the appearance of the high-rise apartment building. Accordingly, the outdoor unit is installed in the DSF system.

Figure 1-4: Appearance of a high-rise residential building without (left) and with DSF system (right)

1.2 Research Questions

The primary goal of this research is to increase building energy savings in existing apartment buildings through the installation of the DSF and PV systems as a combined unit. This research proposes an optimal design for the DSF system, investigates its effect on building energy consumption, and addresses the following research questions:

- How much energy savings can be achieved through the installation of an advanced DSF system in an existing apartment unit?
- What is the optimal design of the DSF system to achieve maximum energy savings?
- Which parameters should be considered to optimally control the DSF system?

Three publications were analyzed to answer the above research questions. Each publication underwent the following phases:

- **First Phase:** This phase focuses on the effect of the DSF system on the number of floors in the building. Most high-rise apartment buildings in South Korea have more than 15 stories, and outdoor conditions (e.g., outdoor air temperature and wind speed) may be different in each floor. This phase determines how much heating and cooling energy can be saved through the installation of the DSF and PV systems and identifies which layer shows the greatest reduction. The objectives of the first research phase are as follows:
  - To analyze changes in outdoor conditions according to the number of floors,
  - To analyze changes in heating and cooling energy consumption according to the number of floors,
  - To determine how much heating and cooling energy can be saved in each floor through the installation of the DSF system, and
  - To explain how the installation of the DSF system can reduce heating and cooling energy consumption.

- **Second Phase:** While the first phase ascertains how the installation of the DSF system reduces heating and cooling energy consumption in each floor, in the second phase, analyses are conducted at the system level to explain how the installation of the DSF system reduces building energy consumption. Residential buildings are heating-oriented buildings. In South Korea, residential buildings are heated by an expansive floor heating system. Cooling systems are not usually installed, so residents buy and install air conditioners or air fans. Since cooling systems may vary due to the individual preferences of residents, the second phase only focuses on the heating system (i.e., radiant heating system). The objectives of the second research phase are as follows:

- To analyze the energy consumption of boilers with the installation of the DSF system, and
- To analyze the annual heating energy consumption according to the thermal performance of the DSF system and the characteristics of the boiler's part load ratio (PLR).

- **Third Phase:** In the first and second phases, the effect of the DSF system and the heating system on each floor is analyzed, and reductions in heating and cooling energy consumption are determined. Meanwhile, in the third phase, life cycle cost analysis is performed. The payback period is calculated according to (1) the installation cost of the DSF system and (2) the heating and cooling energy cost savings. Furthermore, this phase suggests a way to reduce the payback period. The objectives of the third research phase are as follows:

  - To analyze how much the installation of the DSF system costs and calculate payback period, and
  - To identify government subsidies related to DSF system installation, PV system installation, and retrofitting.

1.3 Dissertation Overview

This paper is a publication-based dissertation that explores three different publications. Chapter 2 provides a literature review on retrofitting, the DSF system, and the PV system. Chapter 3 describes the methodology of this research and explains the simulation research method and the experimental research method. Chapter 4 discusses the first publication, which is about the effect of the DSF system on the number of floors in high-rise apartment buildings.

This publication describes how much heating and cooling energy can be saved through the installation of the DSF and PV systems at a geometric level. Chapter 5 reviews the second publication, which focuses on the heating energy consumption of boilers with the installation of the DSF system. In this publication, heating energy savings of boilers with the installation of the DSF and PV systems were analyzed at the system level. Chapter 6 describes the third publication in which a payback analysis was performed to calculate the payback period by considering the manufacturing, installation, and maintenance costs of the DSF and PV systems and the energy savings. This publication also proposed a way to reduce the payback period. Chapter 7 presents the conclusions and recommendations for future studies, while Chapter 8 provides the list of references.

Chapter 2 **LITERATURE REVIEW**

2.1 Introduction

The primary goal of this research is to increase building energy savings in existing high rise apartment buildings through the proper installation of the DSF and PV systems. Retrofitting, PV system, and DSF system are keywords in this research and thus constitute the sections of the literature review. The chapter discusses current research trends related to these topics, explains the importance of this research, and differentiates it from previous studies.

2.2 Retrofitting

This section discusses previous research related to retrofitting in high-rise apartment buildings. Morelli et al. (2012) conducted research on three retrofitting measures implemented in a test apartment. The three types of retrofitting used in an old Danish multi-family building to make it a nearly zero-energy building were (1) changing interior insulation, (2) hanging exterior windows, and (3) installing a decentralized mechanical ventilation system with heat recovery. The results revealed that it is difficult to achieve a nearly zero-energy building without generating renewable energy on site even though the three methods of retrofitting can reduce 68% of building energy consumption. Meanwhile, Dallo et al. (2012) studied a methodology for evaluating energy savings from retrofitting residential buildings. This methodology, which entailed surveying and changing windows, roofs, insulation, and facades, can reduce the energy consumption of residential buildings in the European Union (EU) by up to 24.8% in 2020. Similarly, Arumagi and Kalamees (2014) analyzed building energy use for

historic wooden apartment buildings and found that building energy use can be reduced by 20 to 65% by improving the HVAC system and the building envelope.

In Jang et al.'s (2016) research, they changed glazing from a 5-mm clear single glazing to a 22-mm Low-e double glazing and 16-mm double clear glazing to reduce annual building energy consumption by 2.1%. Meanwhile, Chan and Chow (2010) studied the energy and environmental impact of the provision of a balcony in residential apartments in Hong Kong for different balcony orientations and window glazing materials. The building case in which the balcony faced southwest, and a clear glazed window was used has the highest saving of 12.3% in annual air conditioning consumption. In Iran, Raeissi and Taheri (1998) investigated the optimum dimensions of an overhang to increase energy saving in the air conditioning system. By using the appropriate size, the cooling load can be reduced by 12.7% during the summer season, whereas winter heating demand has an insignificant increase of 0.6%.

Based on previous studies in which retrofitting was performed to reduce energy consumption in residential buildings, one of the most frequently applied methods, especially for apartments, is window replacement because the construction period is relatively short. Previous studies also examined alternative methods, such as installing a high-efficiency HVAC system or replacing the exterior wall. Other researchers conducted a comparative analysis of high-efficiency HVAC systems and envelopes versus conventional ones. However, only a few studies have conducted a comprehensive analysis of HVAC systems, windows, and walls when retrofitting.

2.3 Installation of the Photovoltaic System into the Balcony

This section discusses previous research related to PV systems in residential buildings. Chin and Yoon (2010) proposed a movable PV design for the balcony, featuring a changeable PV angle (Figure 2-1). The researchers analyzed building energy consumption and the amount of electricity generated from the PV system in apartments that range in size from 33 m^2 to 168 m^2. Bigger apartments have bigger balconies, thus increasing the PV installation area. As such, the largest apartment generates the most amount of electricity. The results also showed that the PV system can generate 30.25% of electricity. If the PV system is installed in the upper part of the balcony, it has a shading effect, which can save up to 28.3 kWh of cooling load per year (Chin and Yoon, 2010).

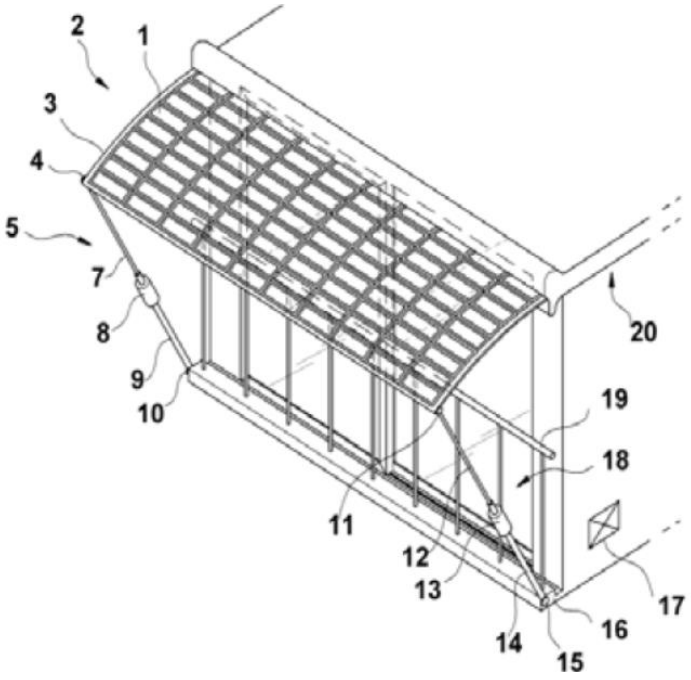

Figure 2-1: Design for movable BIPV shading device (Chin and Yoon, 2010)

Chin et al. (2010) proposed a design for the façade balcony window-style PV system (Figure 2-2). To generate maximum electricity from the PV system, it should be tilted at 30~60° angles. This design generates electricity by operating the PV system when residents are not home or when they do not need natural light; thus, it considers the living pattern of residents. As shown in Figure 2-3, the PV modules installed on the balconies are designed to open and close like a sliding window according to the needs of residents (Chin et al., 2010).

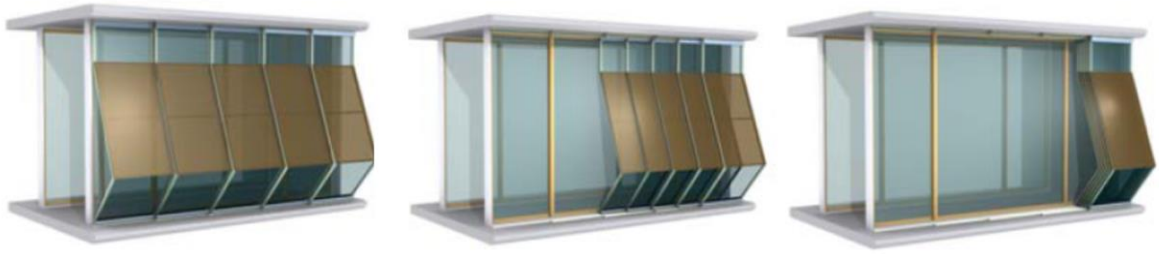

Figure 2-2: Design of sliding PV system integrated into a balcony (Chin et al., 2010)

Karteris et al. (2014) studied the façade PV system for multifamily buildings and proposed a method for predicting the PV potential of building façade surfaces. The researchers explored typical façade PV installations for Greek multi-family buildings to reduce building energy consumption and CO_2 emission. They tested five optimal façade PV system designs according to different orientations and other environmental factors and created the Geographical Information Systems (GIS) model to ensure proper PV installation for multi-family buildings. One interesting result was that 97% of the 25,670 multi-family buildings in Thessaloniki and 79.9% of multi-family buildings in Kalamaria, Greece are suitable for façade PV application because of natural barriers (e.g., trees), building orientation, urban area features, and building typology.

For apartments, PV can be installed on the wall or the balcony. Doing so, however, may have disadvantages; for instance, it may disrupt the view of residents or darken the living room due to the color of the PV panel. To overcome these problems, researchers have proposed a movable PV system (Chin and Yoon, 2010; Chin, 2009). Although the PV system produces electricity and can supplement the electric energy need of buildings, it also has disadvantages, such as limitations on building azimuth angles and installation angles of inclination (Kim et al., 2009).

Overall, previous studies on residential buildings have affirmed that PV systems can reduce building energy consumption without installing high-efficiency equipment or high thermal insulation materials. However, PV systems can only be installed in apartment walls and balconies. In fact, many studies have explored the installation of PV systems on balconies.

2.4 Double-Skin Facade

This section discusses previous research on DSF systems. The DSF system is one of the most widely used technical solutions for reducing building energy consumption. It creates thermal buffer areas and natural ventilation and blocks solar radiation coming through the window in modern and high-rise buildings (GhaffarianHoseini et al., 2016). The DSF system has two glazed surfaces with a central cavity. It can be a sealed box or open to air circulation, either of which affects the air temperature of the system (Alberto et al., 2017). With the aim of reducing building energy consumption, many researchers have investigated the optimal design of the DSF system; some designs incorporate other systems, such as PV systems or blind systems.

Park et al. (2007) conducted an experimental study on the DSF system in Seoul, South Korea. When DSF was installed, room temperature decreased by about 5 °C, and cooling energy consumption in the summer decreased by about 55~80% when compared to the curtain wall system. Meanwhile, a comparative research on DSF with an outer louver and double glazing with internal blind showed that when the reflectivity of the louver is high, cooling energy can be reduced by up to 48.3%, while heating energy can be reduced by up to 67.2% (Kim and Park, 2010). These previous studies focused on office buildings, not residential buildings. Many office buildings operate during daytime and use a curtain wall system, so cooling energy increases. Joe et al. (2014) compared DSF and double glazing in residential buildings. For the summer design day, DSF can reduce cooling energy by more than 60%, while for the winter design day, DSF can reduce heating energy by more than 30%.

Gelesz and Reith (2015) studied the thermal, energy, and comfort performance of DSFs by comparing double-glazed and triple-glazed single-skin façades in a highly glazed office in Central Europe. The simulation study revealed that the buffer mode box-type window performs better than the double-glazed façade, but triple-glazed façades are even better in terms of energy consumption and thermal performance. The outdoor air curtain ventilated box-type window with shading showed, on average, 7% cooling energy savings compared to double glazing; it also performed better than the triple-glazed façade while maintaining the same thermal comfort.

Joe et al. (2013) conducted a study on the actual behavior of a multi-story DSF in South Korea. The DSF building registered a 15.8% heating and 7.2% cooling energy consumption reduction compared to the single-skin façade building. The researchers also proposed a new DSF model where heated air in the cavity was introduced to an outdoor air mixing box of an

HVAC system during heating season and flowed into an indoor space through inner layer openings for natural ventilation. They controlled outdoor air supply in an AHU based on the amount of natural ventilation during cooling season. Compared to a regular DSF, this model resulted in 28.2% heating and 2.3% cooling energy consumption reduction.

Meanwhile, Kim et al. (2018) compared the energy consumption of a building with a DSF system with an interior or exterior blind system and a building where no passive technologies had been applied. Compared to the base model, the DSF system with the blind system saves up to 52% of the total energy consumption.

Alberto et al. (2017) conducted a parametric study on the DSF system to reduce building energy consumption according to the thickness of the air gap. Study results indicated that changing from a 25-cm cavity to a 100-cm cavity can decrease energy demand by up to 9.5%. In another study, Kim et al. (2012) attached the DSF system to a five-story residential building located in the Korean peninsula. The researchers found that the DSF system, which had a 90-cm air cavity, can reduce the heating and cooling energy consumption of old residential buildings by 38%. Regarding the payback period, the researchers found that the DSF system with a 60-cm cavity is the best option for South Korea. Similarly, Luo et al. (2017) proposed a DSF system integrated with PV slat blinds. In the said system, which they called photovoltaic blind double-skin façade (PVB-DSF), building energy consumption is reduced through the DSF system while electricity is generated by the PV slat-blind. Compared with conventional DSF systems with and without shading blinds, the PVB-DSF saves about 12.16% and 22.57% of energy in the summer season.

Souza et al. (2018) conducted an experimental study on temperature differences between outside air temperature, inside temperature, and DSF system temperature using a DSF

system that had a 100-mm air cavity. Results showed that when the outdoor air temperature is 23.1 °C, the temperature of the DSF system is 25.6 °C, while the inside temperature of the test cell is 23.6 °C. Results also revealed that the DSF system can capture the heat inside it, and this has a positive effect on the inside temperature.

The majority of previous studies focused on how the DSF system itself or the attached PV system or blind system in the DSF system reduces energy consumption. However, many of these studies concentrated on office buildings and not residential buildings. Studies that analyze wind speed and solar radiation fluctuations according to the DSF system location and studies that compare PV system power generation and building energy consumption are still lacking.

2.5 Literature Review Summary

The literature review on the key topics of this study affirms that most researchers have tried to reduce residential building energy use by improving the efficiency of the building envelope and the HVAC system. Many researchers suggested using the PV system as a means to reduce building energy consumption without replacing the building envelope and the HVAC system with high-efficiency ones. Most researchers studied the DSF system itself or the attached PV system or blind system to the DSF system to reduce the energy consumption in an office building and found that the DSF system reinforces the building envelope due to its outer structure (e.g., wall and window) and its air cavity, which can work as a thermal buffer area.

The literature review underlines the importance of improving the indoor thermal environment by enhancing the efficiency of the building envelope and the HVAC system and

of installing a PV system when retrofitting old high-rise residential buildings, as doing so can reduce energy consumption. However, improving the efficiency of the HVAC system may be difficult for multi-family residential buildings, especially high-rise apartment buildings. The larger the number of households is, the larger the size of the HVAC system should be; hence, the more complex the system becomes.

Theoretically, it is possible to save heating and cooling energy, but in reality, it is not easy to replace the HVAC system. Therefore, to reduce energy consumption in an old high-rise residential building, it is worth installing both the DSF and PV systems because they can improve not only indoor thermal conditions but also energy efficiency.

Chapter 3 **METHODOLOGY**

3.1 Overview

This research combines both experimental and simulation methods (Figure 3-1). Through experimental research, actual data were collected, and the thermal behavior of the DSF system was analyzed. It was, however, difficult to analyze various scenarios simultaneously due to constraints in time, space, and cost. Simulation research was thus conducted to overcome these difficulties. Conversely, even in the same building, simulation results may differ, depending on the subjective judgment and assumptions of the user (Augenbroe et al., 2008).

If research analysis is based on a hypothetical model without calibration or validation with experimental data, discrepancies in simulation results increase as a consequence of unreliable input variables and assumptions inherent in the simulation model construction process. Therefore, hypothetical results may differ significantly from the actual energy consumption pattern (Kim and Park, 2010). To increase the reliability of research results, a calibrated simulation model based on the measured data is needed.

In the case study, the old high-rise apartment building was referred to as the Base Case. Window replacement, a typical retrofitting method, was selected for Case 1, whereas the DSF system with PV system attached to the Base Case—the proposed retrofitting method in this research—was selected for Case 2. Heating and cooling energy consumption reduction analysis, carbon dioxide analysis, and life-cycle cost analysis (LCCA) were conducted on these three cases.

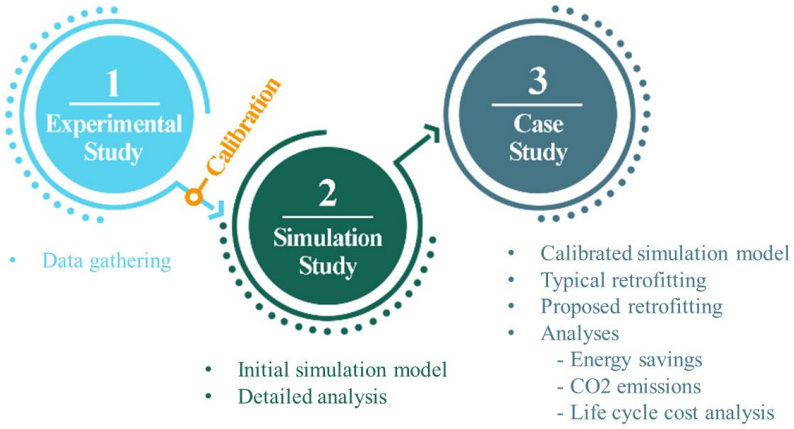

Figure 3-1: Research method

3.2 Theoretical Perspective

As described previously, this study uses simulation and experimental methods to achieve its goal. The theoretical perspective in this study is that of positivism. Auguste Comte coined the term "positivism," which has various meanings. Positivism refers to a theory of history, as all knowledge passes through three phases: theological, metaphysical, and positive states (Given, 2008). Positivism asserts that only claims based on experience can be considered genuine knowledge (Patton, 2001).

Guba and Lincoln explained how each paradigm responds to questions related to the ontological, epistemological, and methodological points of view (Creswell, 1994). Table 3-1 outlines the basic beliefs of positivism.

Table 3-1: Basic beliefs of positivism

Item	Positivism
Ontology	Naïve realism— "real" reality but apprehendable
Epistemology	Dualist/objectivist; finding true
Methodology	Experimental/manipulative; verification of hypotheses; chiefly quantitative methods

Ontology is defined as the "science or study of being." It addresses the nature of existence and the structure of reality (Crotty, 1998). In a broader perspective, this research is based on realistic ontology. Actual data were gathered to understand building energy consumption changes caused by the installation of the DSF system. These data (i.e., building information and output data from the installed equipment) comprised the reality in this study.

The basic epistemological question is: What is the relationship of the researcher to that being researched? Positivism assumes that there is knowledge, known or unknown, and this view is called objectivism. Inquiry occurs through a one-way mirror. Prescribed processes are rigorously followed to ensure that values and biases do not influence outcomes. Accordingly, replicable findings are considered true (Guba and Lincoln, 1994).

This research uses an objectivistic approach from the epistemological point of view. In this study, an experimental research was conducted, and actual data were gathered without interpretation (i.e., related to human response). To prevent subjective judgments and assumptions, which is a disadvantage of simulation research, an epistemological basis is important. To use a real building as a simulation model, the value input by default and the value determined by the subjective judgment of the user must be minimized. It is therefore necessary to collect, through experimental research, values that change in relation to

independent variables and to analyze the building information and the installed equipment when creating a simulation model.

The basic methodological question is: What is the process of research? In methodology, the assumption is that there is a special way of finding knowledge or reality. The methodology is the research procedure—the way of finding out what the researcher knows to be true or to exist. In positivism, the researcher conducts an experimental study (Denzin and Lincoln, 2011).

This study follows a quantitative strategy. To find knowledge or reality, actual data were collected through an experimental study. All data were collected directly from the sensor. By analyzing these data, the thermal behavior of the DSF system and the change in indoor thermal environments when the DSF system is installed in the building can be understood.

Interconnections between the positivist system of research and design are revealed in two different ways: (a) research about a subject related to design and (b) research about the design products. For example, if lighting, energy efficiency, construction, and other building systems in the building have been studied from a positivist perspective, then knowledge in these areas is based on experimental data. The output of positivist research is either true or false, but the output of design research has indefinite possibilities.

Experimental research is important before conducting simulation research even though the main analysis involves the latter. In this research, the energy simulation program was based on formulas. Because simulation research is founded on formulas, it is difficult to simulate an actual building. For example, when using a simulation program for predicting or analyzing building energy consumption, a researcher first inputs the weather file in the simulation model. This weather file is based on hourly data, but in real conditions, weather changes more frequently, and the simulation program cannot deal with this gap. All the schedules for lighting,

equipment, and system operation also have the same problem, which is why a simulation program cannot perfectly imitate real buildings.

Researchers often think about how they can reduce the gap between the simulation model and the actual building. They normally follow codes or guidelines published by a national laboratory or organization based on the manufacturer's data, actual data, and building codes and standards. Many companies make lighting, equipment, and HVAC systems. All buildings are different, and building codes and standards only provide minimum requirements, energy performance standards, and energy codes, not actual building information. There is a significant amount of building information, but there is no single data that can accurately simulate an actual building or a target building. Building simulation models are therefore constructed according to the subjective judgment and assumptions of the researcher. To avoid these problems, both simulation and experimental research methods were used in this study.

3.2.1 Quality Standard

Quality standard indicates whether an outcome is valid and reliable. According to Groat and Wang (2013), the quality considerations proposed by Guba (1981) are aligned with post-positivism standards of internal and external validity, reliability, and objectivity.

Table 3-2 shows these quality standards of the positivist/post-positivism paradigm alongside Guba's proposed standards. Notably, the standards on the left side of Table 3-2 are generic terms that are not associated with any particular system of inquiry. Doing so prevents attaching privilege to terms and concepts associated with any one paradigm (Guba, 1981).

Table 3-2: Comparative analysis of quality standards (Guba, 1981)

Standard	Positivism/Post-positivism	Naturalistic
Truth value	*Internal validity* Equivalence of data of inquiry and phenomena they represent	*Credibility* Check data with interviewees; triangulation—multiple data sources of data collection
Applicability	*External validity* Generalizability	*Transferability* Thick description of context to assess similarity
Consistency	*Reliability* Instruments must produce stable results	*Dependability* Trackability of expected instability of data
Neutrality	*Objectivity* Methods explicated; replicable; investigator one step removed from object of study	*Confirmability* Triangulation of data; practice of reflexivity by investigator

Internal validity indicates confidence that the causality being tested is reliable and not affected by other factors or variables. Internal validity has many sub-categories, but the underlying question is whether the key concepts and operations of the study truly represent the subject under study (Groat and Wang, 2013). To ensure internal validity in this study, both simulation and experimental methods were used to evaluate energy savings from the installation of the DSF system.

External validity indicates the degree to which the results of the study can be applied or generalized to different situations or events. External validity is applied in different ways, depending on the research topic (Creswell, 2009); it shows whether the findings are applicable

to other setting. In this study, the DSF system was installed in an actual building, and actual data were collected to calibrate the simulation model for detailed analysis. Detailed analysis was performed for one region only, so external validity could not be ascertained. Future studies can further the analysis done in this study by analyzing potential energy savings with the DSF system in simulation models for different climate zones beyond South Korea, for example, the eight climate zones in the United States.

Reliability refers to the consistency of measurements or results. Within the objective paradigm, it is assumed that the research method will yield the same results under the same conditions. Other architectural studies using objective survey systems often require a greater examination of reliability due to the focus, conditions, or social phenomena of the study. As such, lack of consistent and stable results is due to fundamental changes in research conditions rather than a lack of reliability in research tools.

The goal of reliability is to minimize errors and biases in a study (Yin, 2017). For this purpose, the experiment in this study involved attaching the DSF system to the sandwich panel (i.e., unconditional zone) before attaching it to the actual building. In addition, the experiments were conducted from autumn to winter to gather enough actual data for analysis and understand the effects of the DSF system on building energy in a cold climate. Similarly, the reliability of the simulation data was ensure by calibrating the simulation model based on the collected data. However, to make the results more reliable, future studies can conduct the experiments for one whole year, not only during fall and winter.

Consistent with the objective system of inquiry, objectivity ensures that the research process excludes potential biases or interventions from the researcher. This can be achieved by strictly specifying and managing relevant procedures. Researchers generally use standardized

measurement instruments, such as questionnaires and calibrated equipment. The sequence and process of experimental manipulation are also highly regulated (Groat and Wang, 2013). To exclude potential biases or interventions from the researcher in this study, detailed information on building materials, infiltration, internal heat gain, and building system are needed. To determine infiltration value, for instance, the infiltration test was conducted, using the blower door test. In addition, the HVAC system was directly installed so that HVAC system information and actual HVAC system data could be utilized. By implementing the simulation model based on the experimental values and building information, potential biases and interventions from the researcher were avoided.

3.2.2 Statistical index used for validity and reliability

To ensure validity and reliability, the measurement and verification (M&V) standard was used in this research. The accuracy of the simulation model was assessed by comparing the simulation results with actual experimental data. The ASHRAE Guideline 14-2014, the International Performance Measurement and Verification Protocol (IPMVP), and the Federal Energy Management Program (FEMP) are representative M&V guides and indicators that safeguard the accuracy of simulation models. M&V guides set the normalized mean bias error (NMBE) and the coefficient of variation of the root mean squared error (CV(RMSE)). Table 3-3 shows the tolerance range of each M&V guide (ASHRAE, 2014; IPMVP, 2002; and FEMP, 2015). The allowable error rate of the tolerance range varies, as it depends on the M&V guide. When correction is performed with monthly data, the allowable tolerance range differs

for each guide. However, if the simulation model is calibrated with hourly data, the tolerance range is ± 10% for NMBE and 30% for CV(RMSE), and all three M&V guides are the same.

In this research, the simulation model was calibrated with hourly data. The tolerance range used was based on NMBE ± 10% and CV(RMSE) 30%, which are the same for all three indicators.

Table 3-3: Tolerance range of each M&V guide

Data interval		Tolerance range		
		ASHRAE Guideline 14-2014	IPMVP	FEMP
Monthly	NMBE	±5%	±20%	±5%
	CV(RMSE)	15%	5%	15%
Hourly	NMBE	±10%		
	CV(RMSE)	30%		

Equations 3-1 to 3-4 were used for calculating NMBE and CV(RMSE).

$$NMBE(\%) = \frac{\sum_{period}(S-M)_{interval}}{\sum_{period} M_{interval}} \times 100 \quad \text{Eq. 3-1)}$$

$$RMSE_{period} = \frac{\sqrt{\sum (S-M)^2_{interval}}}{N_{interval}} \quad \text{Eq. 3-2)}$$

$$A_{period} = \frac{\sum_{period} M_{interval}}{N_{interval}} \quad \text{Eq. 3-3)}$$

$$CV\left(RMSE_{period}\right)(\%) = \frac{RMSE_{period}}{A_{period}} \times 100 \quad \text{Eq. 3-4)}$$

where,

S : Simulation data

M : Measured data

$N_{Interval}$: Number of data

A_{period} : Average data

3.3 Experimental Study

The goal of the experimental study in this research is to understand the thermal behavior of the DSF system in a real building and calibrate or validate the simulation model for detailed analysis.

3.3.1 Pre-Experimental Study

To understand the thermal characteristics of the DSF system, an experimental study was conducted from August 17 to September 21, 2018 in which a DSF system was attached to a sandwich panel. Outdoor and indoor data were collected in this experimental study. Outdoor weather data included outdoor air temperature, humidity, and solar radiation. Meanwhile, indoor data consisted of the indoor air temperature and humidity in the DSF system and the temperature and humidity of the sandwich panel. The temperature sensor installed was a T1 sensor manufactured by T company. The sensor operates between -35 and 55 ℃, with an error rate of ± 5 ℃. Figure 3-2 shows the actual experimental view and the position of the sensor installed.

Figure 3-2: Pre-experimental view (left) and location of the sensor installation (right)

3.3.2 Experimental Study

3.3.2.1 Test Building

After analyzing the thermal behavior of the DSF system through the pre-experiment study, the DSF system was installed in a real building. As previously mentioned, the goal of this study is to propose a new retrofitting method for old high-rise apartment buildings; hence, the building type tested was an old high-rise apartment building. Unexpected problems may arise when the DSF system under development is attached to an old high-rise apartment building. For this reason, the test building (see Figure 3-3), which was built for experimental purpose, was selected as the experimental building.

Figure 3-3: Test building

To minimize the impact of external weather (e.g., ground temperature and roof), the second floor was selected as target. The experimental study was conducted from October 1, 2019 to January 15, 2020. Figure 3-4 shows the floor plan of the test building.

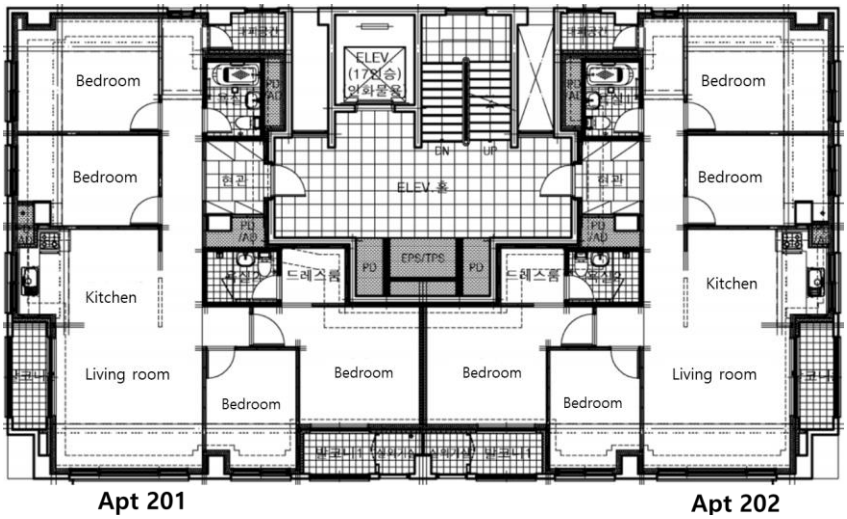

Figure 3-4: Floor plan of the test building

Figure 3-5 shows the stand-type heat pump system of C company used in the actual experiment. The rated capacity of the heat pump system was 5,200 W for cooling and 6,000 W for heating. To compare the results, the same heat pump was installed in apartments 201 and 202. The heating set temperature was 20 °C, while the cooling set temperature was 26 °C.

Figure 3-5: Installed stand-type heat pump system

3.3.2.2 Data Point

Before proceeding with the actual experiment, preliminary experiments were conducted for about a month to check and ensure that the conditions of apartments 201 and 202 are the same.

Apartment 201 was assumed to be an apartment unit, whereas apartment 202 was assumed to be an apartment unit with DSF system attached. The experiment was conducted for about three months. Figure 3-6 shows the preliminary experiment on the test building

before the DSF system was attached and the exterior of apartment 202 in the experimental building where a DSF system was attached after the preliminary experiment.

Figure 3-6: Experimental set-up (left) and exterior view of the test building with DSF system (right)

Figure 3-7 presents the sensor list and sensor location. Three types of data were collected: dry bulb temperature, humidity, and wind speed. All sensors, except those used in the DSF system in apartments 202, were installed in the same location. To prevent external factors in the experiment, a partition wall was installed in the room where the DSF system did not have any direct effect. Two computers were used for data collection; they were designated as PC1 and PC2 to distinguish the location of the data collected on each.

Figure 3-8 shows the location of the sensors in the DSF system installed in apartment 202. To simulate the exact thermal behavior of the DSF system, which is the main purpose of the actual experiment, the dry bulb temperature of the upper, middle, and lower hollow layers of the DSF system, the temperature of the inner and outer surfaces of the indoor and outer

windows, the wind speed, and the temperature of the dry bulb in front of the ventilation system were measured.

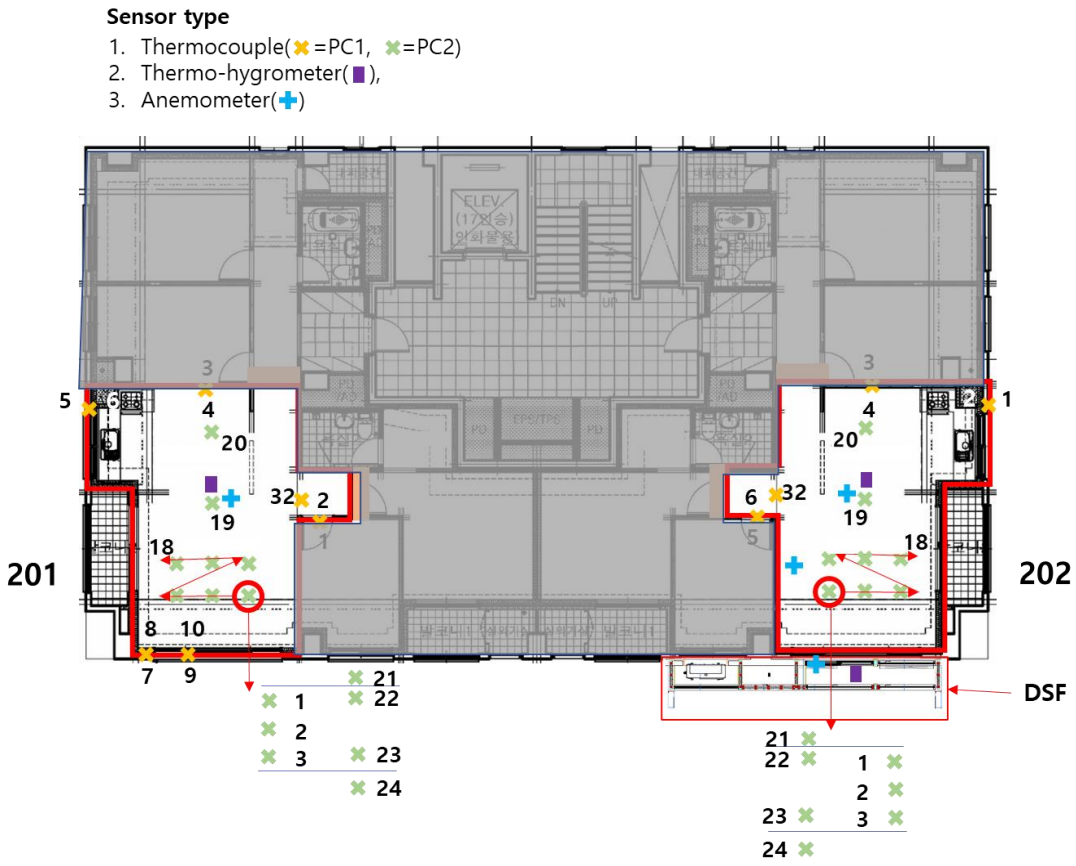

Figure 3-7: Sensor list and sensor location

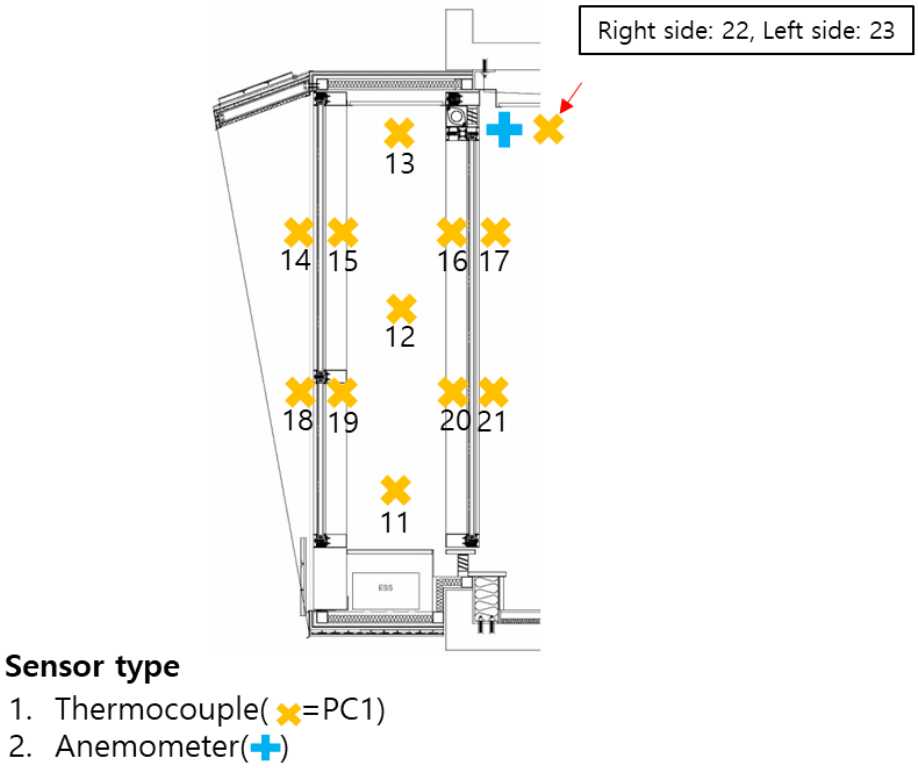

Figure 3-8: Sensor location in the DSF system

3.4 Simulation Study

3.4.1 Simulation Program

The simulation program used in this project was EnergyPlus version 9.0 developed by the U.S. Department of Energy (U.S. DOE). The EnergyPlus program combines the advantages of BLAST and DOE-2 and uses the heat balance method recommended by the American Society of Heating, Refrigerating, and Air-Conditioning Engineers (ASHRAE).

To verify the reliability of the EnergyPlus simulation program, simulation tools were developed and evaluated using ASHRAE Guideline 14-2014 (U.S. DOE., 2014). Eighty scenarios were tested and assessed using three categories: building air-conditioning load, heating equipment, and cooling equipment. The EnergyPlus program was further reviewed and

verified by the International Energy Agency (IEA) Building Energy Simulation Test (BES Test). Zone simulation analysis based on integrated thermal and material equilibrium, which is not possible with the DOE-2 program, is possible in the EnergyPlus program. In addition, the EnergyPlus program complements the analysis of flow between multiple zones, pollutants generated in buildings, and renewable energy systems. Given these points, the EnergyPlus simulation program was deemed suitable for this research, which combined the DSF system with the PV system in a simulation model.

3.4.2 Simulation Model

3.4.2.1 Simulation Conditions

To simulate an old high-rise apartment building, the DOE Ref Pre-1980 Template, which is capable of representing an old residential building, was used. The aforementioned template is one of many templates related to residential buildings in the EnergyPlus simulation program. This template provides a construction set for buildings built around 1980. The building material information for the DOE Ref Pre-1980 Template is shown in Table 3-4, where OSB stands for oriented strand board, CRC stands for cellulose fiber reinforced cement, and Skytech is a kind of insulation.

Table 3-4: Building material information

Material	Conductivity (W/m·K)	Density (kg/m^3)	Specific heat (J/kg·K)
Wood siding	0.11	544	1,210
Insulation	0.049	265	836
Gypsum board	0.16	785	830
Metal decking	45	7,680	418
Roof insulation	0.049	265	836
Roof membrane	0.16	1,121	1,460
CRC	0.24	32	920
OSB	0.13	600	1,460
Skytech insulation	0.032	135	750
Low-e insulation	0.0135	16	1,865
PF board	0.02	520	1,200

Tables 3-5 and 3-6 refer to the construction made by combining the building materials in Table 3-4. The numbers in parentheses indicate the thickness of the material. The U-value of the exterior wall was 1.011 $W/m^2 \cdot K$. For the DSF system, the U-value of the side wall was 0.324 $W/m^2 \cdot K$, the south wall was 0.176 $W/m^2 \cdot K$, while the roof and floor had 0.456 $W/m^2 \cdot K$.

Table 3-5: Construction of the old high-rise apartment building (DOE Ref Pre-1980)

Construction	Exterior to interior thickness in mm		
Exterior wall	Wood siding (10)	Insulation (33)	Gypsum board (12.7)
Interior wall	Gypsum board (19)	Air space	Gypsum board (19)
Floor and ceiling	Acoustic Tile (19)	Ceiling air space	Concrete (100)

Table 3-6: Construction of the DSF system

Construction	Exterior to interior thickness in mm				
Side wall	CRC board (6)	OSB (11.5)	Skytech insulation (13)	Low-e insulation (200)	Skytech insulation (30)
Floor and roof	CRC board (6)	OSB (11.5)	Skytech insulation (13)		Low-e insulation (60)
South wall	CRC board (6)	OSB (11.5)	Skytech insulation (13)		PF board (100)

Table 3-7 presents the properties of the windows. The U-value of the windows was 5.84 $W/m^2 \cdot K$, which was also applied to the old high-rise apartment building. Meanwhile, a 22-mm double low-E window filled with argon gas was applied to the DSF system.

Table 3-7: Window properties

Windows	U-value ($W/m^2 \cdot K$)	Solar Heat Gain Coefficient (SHGC)
DOE Ref Pre-1980 Window (Old high-rise residential building)	5.84	0.54
22-mm double Low-E Glazing with Argon (DSF system)	0.96	0.347

Table 3-8: Internal heat gain and heating and cooling set points

Internal heat gain	People	0.035 person/m^2	
	Lights	10 W/m^2	
	Equipment	3.90 W/m^2	
Infiltration		1 Air change per hour (for old high-rise residential building) 0.25 air change per hour (for room with attached DSF system) 0.2 air change per hour (for DSF system)	
Set point	Heating (November to March)	20 ℃	0:00~24:00
	Cooling (May to October)	26 ℃	00:00~24:00

3.4.2.2 Calibration Results

Figures 3-9 and 3-10 show the calibration results of the simulation model using hourly measured data. In the actual experiment conducted from October 1, 2019 to January 15, 2020, electric energy consumption was collected from November 4 to November 11, 2019 and from December 1, 2019 to January 15, 2020. About three weeks of actual data were used for the calibration, except for periods during which power consumption data collection was not smooth due to external factors (e.g., power outage). For the heat pump system used in the experiment, the manufacturer did not provide data regarding performance and conditions excluding the rated cooling and heating capacities. For this reason, default performance formulas of the EnergyPlus program that were calculated using the performance formulas of the heat pump systems of various manufacturers were used.

Compared to the actual electricity consumption data of the heat pump installed in apartment 201, the CV(RMSE) of the simulation results was 26.8%, while the NMBE was

3.9%. In apartment 202, the CV(RMSE) was 22.7%, while the NMBE was 5.9%. Both simulation models satisfy NMBE ± 10% and CV(RMSE) 30%, which are the acceptance criteria of the hourly error indicator, confirming the accuracy of the simulation model in this study. In apartment 201, the CV(RMSE) of the hourly heat pump electric consumption was 26.8%, while the NMBE was 3.9%. Apartment 202 obtained a CV(RMSE) of 22.7% and an NMBE of 5.9%. The values of both the CV(RMSE) and the NMBE were in the tolerance range (i.e., NMBE ± 10% and CV(RMSE) 30%), which indicate that the simulation model is calibrated.

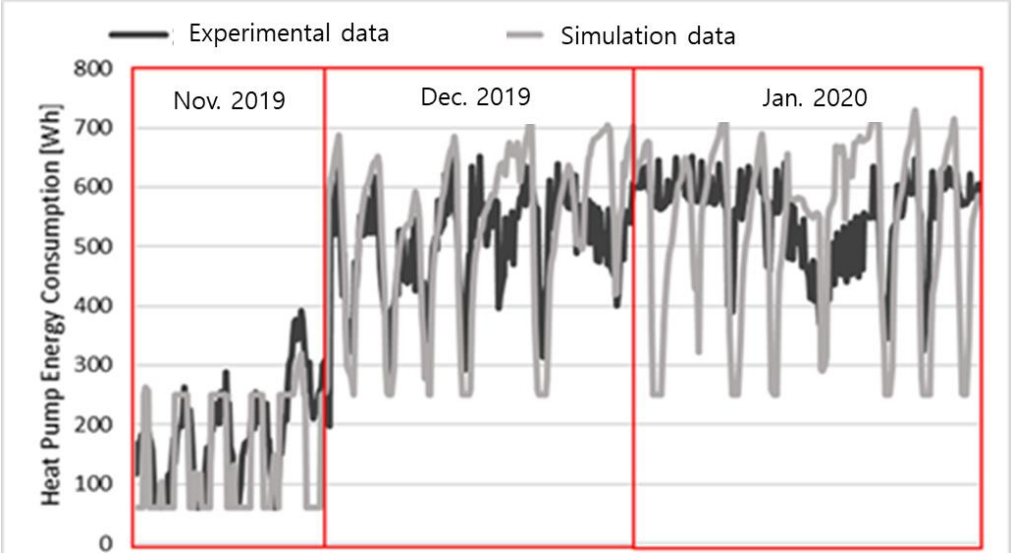

Figure 3-9: Simulation calibration results for apartment 201

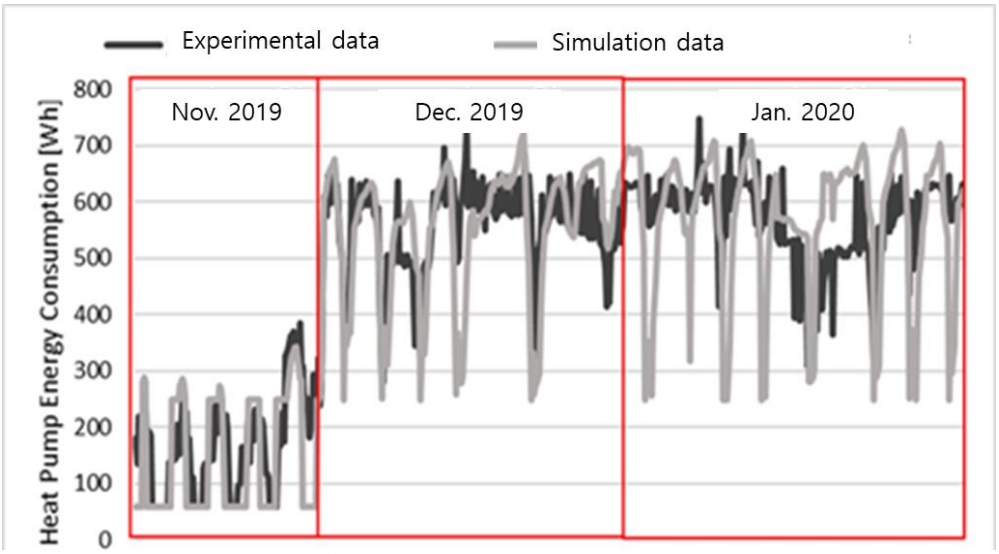

Figure 3-10: Simulation calibration results for apartment 202

3.5 Methodology Summary

The thermal behavior of the DSF system was analyzed through the pre-experimental study and the experimental study. The DSF system was attached to the actual building during the experimental study. Sensors were installed inside the building and in the DSF system to collect data. For the simulation, model calibration was performed using actual data, which in turn increased accuracy. The simulation model was used in this research to conduct a detailed analysis.

In the following chapters, the energy-saving potential in different floor levels of a high-rise independent building is analyzed. How the heating system behavior changes with the installation of the DSF system is also explained. The payback-period is an important aspect when utilizing the DSF system as a retrofitting method for high-rise apartment buildings; hence, life cycle cost analysis was also conducted.

Chapter 4 PERFORMANCE ANALYSIS OF A DOUBLE SKIN FAÇADE SYSTEM INSTALLED ON DIFFERENT FLOOR LEVELS OF HIGH-RISE APARTMENT BUILDING

This chapter introduces a double-skin façade (DSF) system that can be installed in existing apartments in South Korea as a replacement of poorly performing old balcony windows. The DSF system can bring thermal benefits, especially in heating dominant climate areas. The DSF system works as a thermal buffer area and passive heating system. The goal of this research is to evaluate the thermal performance of a DSF system installed in apartments on different floor levels. A typical 25-story apartment building is used as a case study to test the thermal performance of a DSF system in different floors. Heating energy savings are the focus since the location, Seoul, is a heating dominant climate area. The main parameters are temperature, wind speed, and pressure differences on different floor levels. A thermal simulation model for a Base-Case is developed and calibrated to measured data gathered from a real-scale DSF system physical model. Two other simulation models are developed on top of the Base-Case model to compare performances of the DSF system installed in apartments on different floor levels.

4.1 Introduction

There are more than 10 million apartment units in South Korea accounting for about 60% of all residential units. Most apartment buildings are of ten stories or more. 15-story apartment buildings are most common, followed by 5-story, 20-story, and 25-story buildings (MOLIT, 2019). About 36% of them are 20 years or older (Statistics Korea, 2019). The old

apartments have similar envelope figures like new ones, but newer buildings have been constructed with much advanced building codes such as more stringent energy codes. Energy efficiency measures have been implemented to old apartments as a form of retrofitting mostly on windows, which have been carried out on about 2% of existing apartments (Lim et al., 2017). Replacing old, inefficient windows with high-efficiency windows has been one of the most popular retrofitting methods (Jang et al., 2016). However, the apartment owners focused mainly on extending the balcony areas into conditioned spaces to increase the value of the apartments, not very much considering energy performance impact from it (Song and Choi, 2012). Enclosing the balcony space to convert it into an indoor space resulted in the loss of a thermal buffer area. The balcony extension may cause thermal discomfort, glare, and increase of heating and cooling loads. As an advanced window retrofit idea, a double-skin façade (DSF) system has been introduced. It is similar to window replacement but brings the thermal buffer area back along with other functions. It could save energy substantially more than the simple window replacement.

Since the DSF system will eventually be installed in multi-story apartment buildings, it is necessary to evaluate the thermal performance in different floor levels, such as first floor, fifth floor, twentieth floor, and so forth. The thermal loads are different in different floors due to the differences of temperature, wind speed, and air pressure. The heating energy consumption is the main interest since it has the largest energy consumption portion of apartments in Seoul climate in South Korea. Figure 4-1 shows the pre- and post-installation of the DSF system in an old apartment complex in South Korea.

Nomenclatures			
$\dot{m}_i$	Air mass flow rate at i-th linkage [kg/s]	z_m	Exit elevations [m].
C_i	Air mass flow coefficient [m^3]	$P_{t,n}$	Total pressures at node n [Pa]
ΔP_i	Pressure difference across the i-th linkage [Pa]	$P_{t,m}$	Total pressures at node m [Pa]
μ	Air viscosity [Pa-s]	P_s	Pressure difference due to density and Height differences [Pa]
P_n	Entry static pressures [Pa],	P_w	Pressure difference due to wind [Pa]
P_m	Exit static pressures [Pa]	C_p	Wind surface pressure coefficient [Dimensionless]
V_n	Entry airflow velocities [m/s]	V_{ref}	Reference wind speed at local height [m/s]
V_m	Exit airflow velocities [m/s]	V_{met}	Wind speed at local height by the standard meteorological wind speed measurement [m/s]
ρ	Air density [kg/m^3]	δ	Local atmospheric boundary layer depth [m]
g	Acceleration due to gravity [9.81 m/s^2]	z	The height difference [m]
z_n	Entry elevations [m].	α	Power law exponent difference [Dimensionless]

Figure 4-1: Pre- and Post-installation of the DSF system in an old-apartment complex

4.2 Literature Review

DSF system is one of the widely used technical solutions to save energy by utilizing the thermal buffer area, natural ventilation, and solar radiation block in modern and high-rise buildings (GhaffarianHoseini et al., 2016). DSF system has two glazed surfaces with a central cavity. It can be a sealed box or open to air circulation; which affects the air temperature of the DSF system (Alberto et al., 2017). To conserve building energy through the DSF system, there are many researches carried out about the optimal design of DSF system and integrated with other systems such as PV system or blind system. Kim et al. compared building energy consumption between DSF system with interior or exterior blind system and a building where no passive technologies were applied. DSF system with the blind system could save total building energy up to 52% when compared to the base model (Kim et al., 2018). A. Alberto et al. conducted a parametric study of the DSF system regarding the thickness of the air gap. It

showed that transition from a 25 cm cavity to a 100 cm led to a decrease in the energy demand of up to 9.5% (Alberto et al., 2017). Kim et al. attached DSF system in a five-story residential building. It was found that the DSF system which had 90 cm air cavity could save 38% of heating and cooling energy of old residential buildings. Regarding the pay-back period, they suggested DSF system with 60 cm cavity was the best option (Kim et al., 2012). Luo et al. proposed a DSF system integrated with PV slat blinds. It could save building energy through the DSF system and generate electricity from the PV slat blind. They called their DSF "Photovoltaic blind double-skin façade (PVB-DSF)." It saved about 12% of energy in summer when compared to the conventional DSF system and saved 22.6% of energy in the summer season when compared to the conventional DSF system without shading devices (Luo et al., 2017). Souza et al. conducted an experimental study about temperature differences between outside air temperature, inside temperature, and temperature of the DSF system. This DSF system had a 100 mm air cavity. The result showed that the temperature of the DSF system was 25.6°C, inside temperature of the test cell was 23.6°C, when the outdoor air temperature was 23.1°C. It showed the DSF system captured the heat inside and had a positive effect on the inside temperature (Souza et al., 2018). Zomorodian and Tahsildoost applied the DSF system with external louver system to an office building to reduce building energy consumption in Teheran, Iran. The main result of this study was DSF system with external louver system could reduce the 14.8% of total building energy consumption compared to the single layer window model (Zomorodian and Tahsildoost, 2018). Silva et al. performed an experimental study to account for the variability of the tracer gas measurements and to investigate the influence of the shading device configuration on the head loss of the DSF system (Silva et al., 2015). Joe et al. proposed a DSF system for a residential building. They

compared the DSF system with curtain wall structure with an aluminum frame. DSF system could save 60% of cooling energy and 30% of heating energy when compared with the curtain wall structure (Joe et al., 2014). Chan et al. analyzed the energy performance of the conventional office building which installed DSF system in Hong Kong. They used the validated DSF model, and EnergyPlus simulation program was utilized to evaluate the energy performance with various window type, position, and layers. The main results were that the DSF system with a double reflective glazing as the outer glazing and a single clear glazing as the inner glazing could reduce the cooling energy consumption about 26% when compared with a single absorptive glazing (Chan et al., 2009). Gelesz and Reith found that DSF can reduce 9% to 12% of cooling energy in Central Europe when compared to triple glazing (Gelesz and Reith, 2015). Gratia and Herde conducted simulation study to analyze heating and cooling energy depending on installed direction of a DSF. Their results showed that the amount of decrease in energy was different based on the installed direction. Heating load is decreased regardless of installed direction of the DSF system. However, cooling load increased (Gratia and Herde, 2007a). Pak et al. conducted simulation study to develop a passive house with DSF system. The result was 19.1% of heating demands and 18.8% of cooling demands were reduced by installation of a DSF system to new residential house (Pak et al., 2018). He et al. discussed about window opening control of DSF system, and the results showed that the DSF system can save more energy than a double-glazing window in summer despite the DSF window opened or closed in China. The window opening control, which is ventilation control, could save more building energy (He et al., 2011). Most of the previous studies were focused on the DSF system itself or attached blind or PV system in the DSF system. Some researchers conducted experimental studies to understand the characteristics and inside conditions of the DSF system.

Compared to the previous studies found in literature, there are only a few studies conducted to analyze DSF systems installed in residential buildings, especially in high-rise apartment buildings. Yoon et al. analyzed the thermal performance of a DSF system in an apartment building. They showed heating energy savings of 39% in a cold climate (Yoon et al., 2018). Koh et al. conducted a CFD analysis of a DSF installed in an apartment building, which focused on the optimal design for the potential of passive heating (Koh et al., 2018). These two previous studies only looked at the DSF system installed in one floor, not multiple floors. Most of the previous studies did not consider the potential impact caused by different floor levels. They attempted to develop optimal controls only in one floor or space. Most of the previous studies mentioned the heating energy savings from the DSF system installation along with the window and/or damper controls. However, these studies looked at the performances in one floor. The focus of this study is to analyze the order of influence in thermal performance from different floor levels in installing a DSF system in high-rise apartment buildings.

4.3 Methods

This study aims to suggest installation of the DSF system to apartment unit as a retrofitting method. The typical retrofitting method is replacement of exterior window by high-performance window. However, the replacement of window means improving the U-value of the glazing. As mentioned before, balcony is extended into living room or other conditioned zone to make bigger living space. By enclosing balcony area, thermal buffer area is lost, and it increases the building energy consumption. However, DSF system has both high performance glazing and a thermal buffer area. Through the thermal buffer area, heating energy

consumption can be decreased more than typical retrofitting method. In this study, we compare the heating energy consumption by installing the DSF system in apartment units in different floor levels.

This study considered three cases as shown in Figure 4-2 to analyze building energy consumption especially heating energy consumption. Three case models developed to compare energy savings potentials. A 25-story apartment building is used to develop the Base-Case model. The Case-1 model represents a typical window retrofit which is replacement of existing balcony window as high performance window, and the Case-2 model is for the case with the DSF system installed in the Base-Case as a replacement of existing balcony window. The floor-to-floor height of apartment building is 2.5 meters. The seven-floor levels, 1st, 5th, 9th, 13th, 17th, 21st, and 25th, are analyzed to see the performance differences of the DSF in different floors.

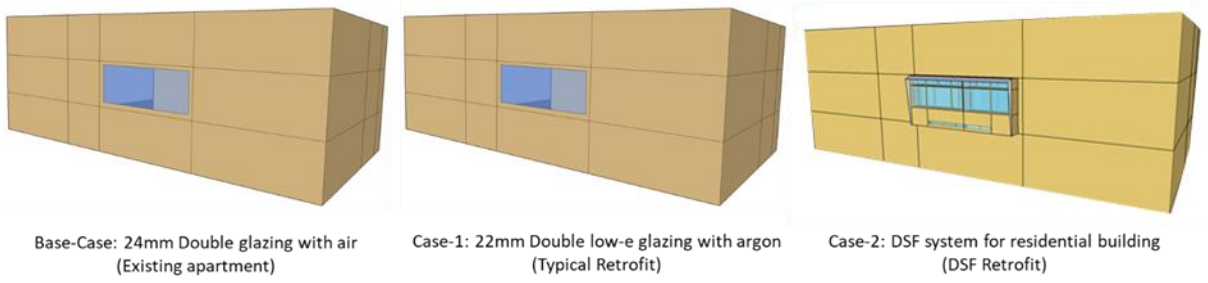

Figure 4-2: Three Case Simulation Geometry Models: Base-Case, Case-1 (Typical Window Retrofit), and Case-2 (DSF)

4.3.1 Description of the Proposed DSF System

Figure 4-3 shows the overall picture of the proposed DSF system. It consists of two layers, inner and outer. The outer layer includes fixed windows, operable windows, insulated

wall, and a damper for air circulation of outdoor A/C unit. The inner layer includes fixed windows, operable windows, outdoor A/C unit, and shelves. The DSF unit can capture heat as solar radiation comes into the DSF through the window. The heated air can be used by appropriate window opening controls, which can save heating energy in winter. DSF system plays a role as a thermal buffer area. The DSF system which is shown in the Figure 4-3 is currently being made for real, and for the window opening control to be considered in the future, the simulation model was created in the same structure as the actual DSF system. In this paper, we did not consider the Photovoltaic (PV) system. PV system will be considered in the future study.

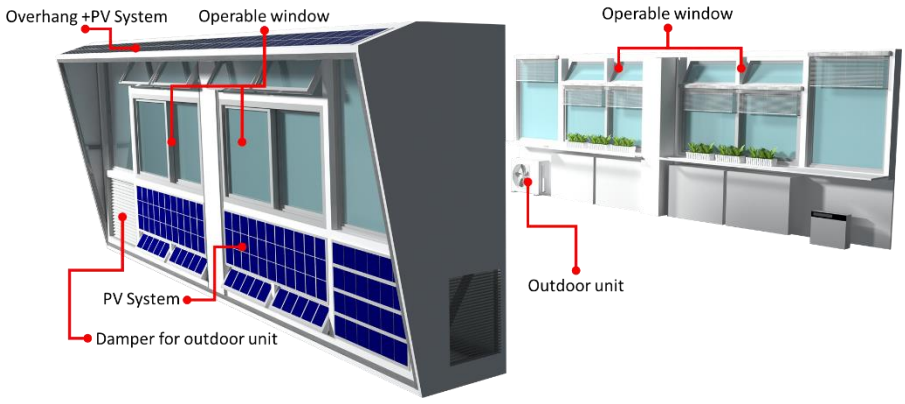

(a) Outer Layer (b) Inner Layer

Figure 4-3: Two layers of the proposed DSF system

4.3.2 Simulation Software

This study utilizes the EnergyPlus simulation program which Department of Energy (U.S. DOE) developed for energy performance evaluation. EnergyPlus is based on the heat balance method which is suggested by American Society of Heating, Refrigerating and Air-conditioning Engineers (ASHRAE). This program provides air flow network and radiant

heating system which is common heating system in South Korea. Air flow network is an important function to analyze double-skin façade system.

4.3.2.1 Air Flow Network

Air Flow Network (AFN) model in the EnergyPlus program can be used to simulate multi-zone airflows driven by wind and forced air distribution systems such as heating, ventilation and air-conditioning (HVAC) system (Walton, 1989). This study uses the airflow driven by wind only because the DSF system has no forced air distribution system. The input and output reference of EnergyPlus describes can-and-can't-do things by the AFN model. Here are the ones selected as applicable to the DSF system: air flow through cracks in exterior or inter-zone surfaces; natural ventilation such as air flow through open or partially open exterior windows and doors; zone level control of natural ventilation (all windows/doors in a zone that are defined with a component opening object have identical controls); individual surface control, such as a window, door, or glass-door of ventilation; inter-zone air flow; dependence of air flow on buoyancy effects and wind pressure; and dependence on window pressure on wind speed, wind direction, and surface orientation.

In order to conclude zone heating and cooling loads, the airflows interacting with other nodes are used as a part of node heat and moisture balances with the energy balance equation (Kim et al., 2018). The three sequential steps in the AFN model are 1) pressure and airflow calculations, 2) node temperature and humidity calculations, and 3) sensible and latent load calculations (Gu, 2007; USDOE, 2018).

Pressure and airflow calculations should be taken as the beginning step in the model. Various airflow components fabricate a network of airflow linking a set of nodes. Equation 4-

1 below is used for initialization of the pressure nodes that are required to solve node air pressure, which is the Newton's method:

$$\dot{m}_i = C_{i\rho} \frac{\Delta P_i}{\mu} \quad \text{Eq. 4-1)}$$

This initialization process interprets stack effect, which becomes a critical foundation of the airflows. Inlet and outlet of the air, the two nodes linked together in the AFN model demonstrates a close relationship between airflow and pressure. Bernoulli's equation defines the relationship from the pressure difference across each component (Equation 4-2) (Kim et al., 2018; USDOE, 2018):

$$\Delta P = (P_n + \frac{\rho V_n^2}{2}) - (P_m + \frac{\rho V_m^2}{2}) + \rho g(z_n - z_m) \quad \text{Eq. 4-2)}$$

4.3.2.2 Wind Speed

The basic Bernoulli's equation presented in Equation 4-2 omits the pressure difference caused by the wind. The equation 4-2 can be improved by rearranging terms and adding the wind pressure impacts as Equation 4-3 (Kim et al., 2018; USDOE, 2018).

$$\Delta P = P_{t,n} - P_{t,m} + P_s + P_w \quad \text{Eq. 4-3)}$$

Wind pressure also comes from the Bernoulli's equation, thus the pressure difference caused by the wind can be calculated in Equation 4-4.

$$P_w = C_p \rho \frac{V_{ref}^2}{2} \quad \text{Eq. 4-4)}$$

C_p plays a key role to conclude P_w. C_p could be drawn from the AFN model which considers two elements, the direction of building envelope and wind direction. This paper uses the surface average calculation method for calculating C_p.

The wind speed of the reference building is drawn from the measured meteorological wind speed. In order to estimate the reference wind speed, V_{ref} may be expressed as Equation 4-5 (Walton, 1989).

$$V_{ref} = V_{met}(\frac{\delta_{met}}{z_{met}})^{\alpha^{met}}(\frac{z}{\delta})^{\alpha} \quad \text{Eq. 4-5)}$$

Wind speed at local level is predicted by Equation 4-5. The local wind speed at the reference building should be taken into consideration of the fact that the wind speed in the weather file is different in that it is measured at a meteorological station location in an open field at the height of 10 m. To reflect differences of terrain and height of the reference building, the local wind speed is calculated for each surface modified from the meteorological wind speed. This modification is shown in Equation 4-6 (USDOE, 2019a).

$$\mathrm{U}_{\infty} = V_{met}(\frac{\delta_{met}}{z_{met}})^{\alpha^{met}}(\frac{z}{\delta})^{\alpha} \quad \text{Eq. 4-6)}$$

Where the subscript "met" is conditions at the meteorological site.

4.3.3 Simulation Modeling

The simulation model of the DSF system was calibrated with measured temperatures of DSF and sandwich panel. Figure 4-4 shows the model of the DSF system installed in the

center unit. Material properties are based on materials and construction name from a real drawing of an old apartment (MOLIT and KEA, 2017; USDOE, 2018). To describe real apartments, building materials are used based on the previous research which focused on the residential building (Yoon et al., 2018). Tables 4-1 and 4-2 show building material properties and construction sets (MOLIT and KEA, 2017; USDOE, 2018).

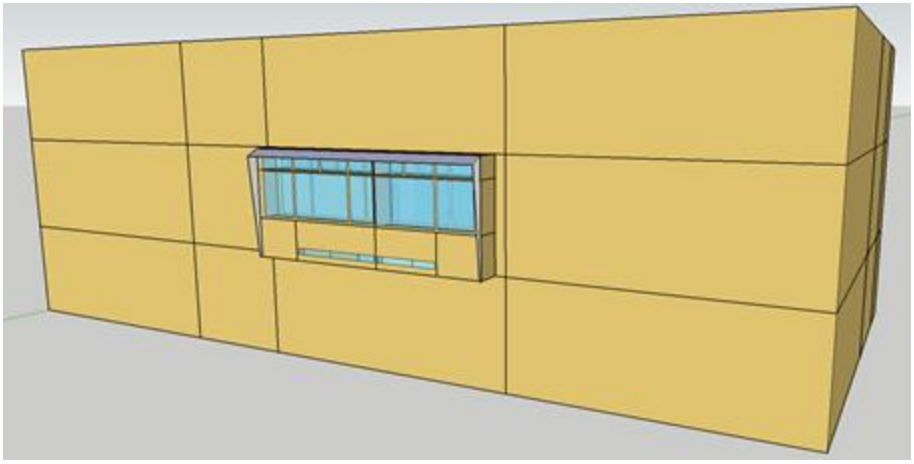

Figure 4-4: Simulation model of a typical apartment unit with DSF system installed

Table 4-1: Building material properties

Materials	Conductivity [W/m·K]	Density [kg/m^3]	Specific Heat [J/kg·K]
Insulation	0.031	43	1,210
Concrete	1.60	2,240	900
Gypsum board	0.18	800	1,090
Tile	1.30	1,920	1,260
Ceiling Finish	1.59	1,920	1,260
Floor Finish	0.27	640	1,210

Table 4-2: Construction set

Construction	Outer layer to inner layer (Thickness, mm)			
Exterior wall (S,W,E)	Concrete (200)	Insulation (70)	Gypsum board (9)	
Exterior wall (N)	Concrete (150)	Insulation (50)	Gypsum board (9)	
Interior wall	Gypsum board (9)	Concrete (120)	Gypsum board (9)	
Floor + roof	Ceiling finish (0.5)	Insulation (50)	Concrete (120)	Floor finish (0.5)
Construction for DSF	Gypsum board (9)	Insulation (50)	Gypsum board (9)	

Table 4-3 shows the properties of the window. For Base-Case, all windows have double glazing with air. For Case-1, south window had 22 mm double Low-E Glazing with argon, other windows located in north have double glazing with air, and all windows in the DSF system have double Low-E glazing with argon gas. The specifications of the window were obtained from a window manufacturing company. 24mm double glazing with air is made with 6mm clear glass, 12mm air, and 6mm clear glass. The 22mm double Low-E glazing with argon is made with 5mm clear glass, 12mm argon gas, and 5mm Low-E glass.

Table 4-3: Properties of window

Windows	U-value ($W/m^2 \cdot K$)	Solar Heat Gain Coefficient (SHGC)	Visible Transmittance (VT)
24mm double glazing with air	2.824	0.704	0.786
22mm double Low-E Glazing with argon	1.19	0.46	0.70

Table 4-4 shows the internal heat gains and heating and cooling set-points. These values are based on "Study on heating and cooling load standard per area for apartments in 2017" which was published by Korea Research Institute of Mechanical Facilities Industry (KRIMFI) (KRIMFI, 2017). Heating and internal heat gain schedules follow the report "Energy Technology Transfer and Diffusion" which was published by Korea Institute of Energy Research (KIER) (KIER, 2007). The radiant fraction of 0.7 and visible fraction of lights of 0.2 are from ASHRAE Standard 90.1-2004. Regarding the heating system, normally residential units including high-rise apartments use radiant floor heating system. This study used the "lowtemperatureradiant:Variableflow" function which is one of the HVAC systems available in EnergyPlus. The inside diameter of hydronic tubing for hot water coil of the radiant floor is 16mm and spacing between coils is 200mm (Lee et al., 2014).

Table 4-4: Internal heat gains and cooling and heating set-points

Internal heat gain	People	0.035 person/m^2 (2.6 persons/apartment unit)		
	Lights	10 W/m^2		
	Equipment	3.57 W/m^2 for room		
		1.61 W/m^2 for bathroom		
		3.90 W/m^2 for Livingroom		
Set-point	Floor heating (Nov.-Mar.)	Occupied (22˚C)	Weekday	00:00~09:00
				19:00~24:00
			Weekend	00:00~24:00
		Unoccupied (13˚C)	Weekday	09:00~19:00
	Hot water	60˚C		

4.3.4 Infiltration

To make the simulation modeling of the old-apartment unit, infiltration value should be known. Tests such as blower door test, is a good way to know the infiltration value. Therefore, for this study, we used infiltration value from previous experimental studies. There are some studies previously conducted on blower door test to measure infiltration rates in apartments. One of the tests shows representative infiltration results that can be referenced for this study. The apartment was built in 1996. The size of the apartment in the test was 79m^2 with effective leakage area of 2.95 cm^2/m^2 with the air leakage of 574 CMH50 or ACH of 3.16 (Won and Huh, 2002). However, we are not able to use this data directly because previous study does not describe the characteristics of the apartment unit. It is assumed that the apartment in previous study has similar condition as the case building in this study. This means that the east and west walls are faced other apartment units. Consequently, only south and north

walls and windows are exposed to outdoor conditions. If it were calculated based on ASHRAE Handbook of Fundamentals (i.e., 0.139 cm^2/m^2 for the exterior wall, 2.014 cm^2/m^2 for the interior wall, and 3.048 cm^2/m^2 for the windows), the calculated leakage is about 180.9 CMH50 or ACH of 1.0 (ASHRAE, 2009). This is a big difference compared to the measured value of 574 CMH50 or ACH of 3.16. To make the ACH of 3.16 for the case study model, the effective leakage area values are revised as 0.443 cm^2/m^2 for exterior wall, 6.423 cm^2/m^2 for interior wall, and 9.717 cm^2/m^2 for windows. As shown, the adjusted values are about three times higher than the effective leakage area values in ASHRAE Handbook of Fundamentals. When the revised effective leakage area values are applied to the experimental apartment of Won and Huh, the air leakage is calculated as 576.8 CMH50 or ACH of 3.17, which is very close to the measured value of 3.16. The revised effective leakage area values are used in this study. With these values, the ACH of the case building shows about 2.67. Figure 4-5 compares the ACHs of the three cases. The minimum value of ACH is about 2.50, medium value of ACH 2.67, and maximum value 2.82 in both Base-Case and Case-1. Case-1 ACH is not changed. In Case-2, the ACH values range from 1.90 to 2.15.

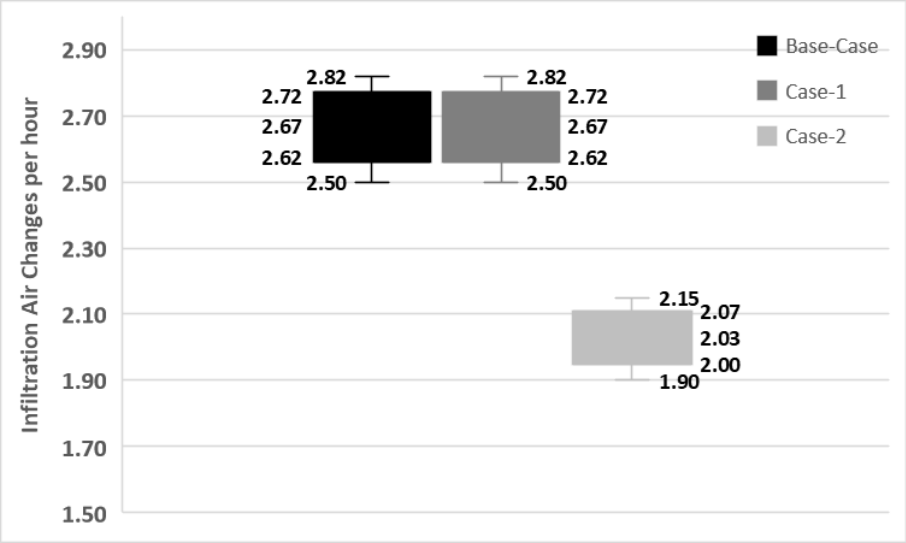

Figure 4-5: Infiltration ACH for three cases

4.4 Experimental Study

Before attaching the DSF system to the actual apartment unit, a mock-up test was conducted to understand the thermal performance of the DSF system. A mock-up test was set up in the City of Daejeon, South Korea. City of Daejeon is one of the biggest cities in South Korea. The location of Daejeon is shown in Figure 4-6. The latitude of Daejeon is 36º 21' N and the longitude is 127º 23' E. In order to validate the simulation model of this study, a mock-up simulation model was made as shown in Figure 4-7. The DSF system was installed onto a sandwich panel box as shown in Figure 4-8 (a). The weather data, such as temperature, relative humidity, and horizontal total solar radiation, and temperature and humidity of the DSF system and sandwich panel were recorded from August 17 to September 21, 2018 as shown in the Figure 4-8 (b). The temperature sensor used the T1 set sensor which is manufactured by 'T' company. The accuracy of the sensor is ± 0.5 ℃ and operation temperature of the sensor ranged

from -35 to 55℃ (Testo Ltd., 2019). The simulation model was validated with experimental data using temperature data.

Figure 4-6: Location of the Daejeon, South Korea

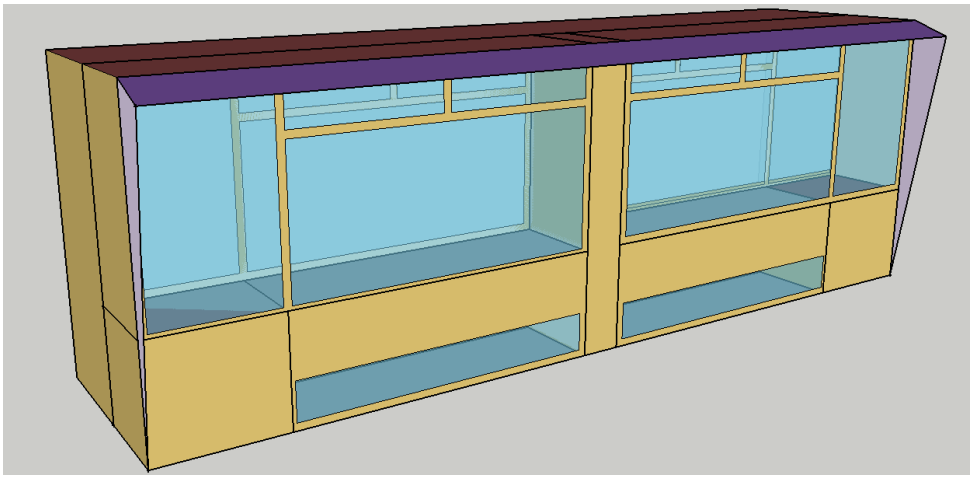

Figure 4-7: Simulation model of a Mock-up test

(a) Mock-up structure **(b) Sensor locations**

Figure 4-8: Mock-up set-up for experimental study

The Coefficient of Variation of the Root Mean Squared Error (CV(RMSE)) values for the dry-bulb temperature of the DSF system were 8.6% for DSF system and 8.8% for the panel box. These CV(RMSE) values are within the acceptable range for the hourly simulation.

Figures 4-9 and 4-10 show representative validated results. Two days were selected where all complete datasets are available. August 19 was the hottest day during the experiment and the time when outer window was opened during the whole day. August 25 was another hot day during the experiments, but on this day all the windows were closed. To validate simulation model, the temperatures of the DSF system and sandwich panel are compared and used to develop a statistical value of CV(RMSE). ASHRAE Guideline 14-2014 provides the tolerance ranges of the calibrated simulation models; i.e., CV(RMSE) of 15% when using monthly data and 30% when using hourly data for calibration (ASHRAE, 2014). The equations for CV(RMSE) are as follows:

$$\mathrm{RMSE}_{period} = \sqrt{\frac{\sum_{i=1}^{n}(y_{sim} - y_{mea})^2}{N}} \quad \text{Eq. 4-7)}$$

$$A_{period} = \frac{\sum_{period} M_{Interval}}{N_{Interval}} \quad \text{Eq. 4-8)}$$

$$\mathrm{Cv}\left(RMSE_{period}\right) = \frac{RMSE_{period}}{A_{period}} \times 100 \quad \text{Eq. 4-9)}$$

where,

y= monthly (or hourly) data

N= number of data

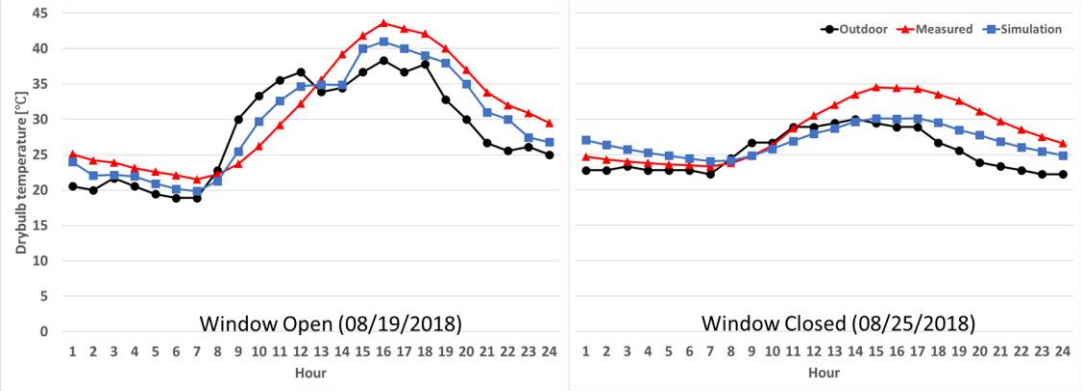

Figure 4-9: Comparison of temperatures: Outdoor temperature vs. DSF measured temperature vs. DSF simulation temperature

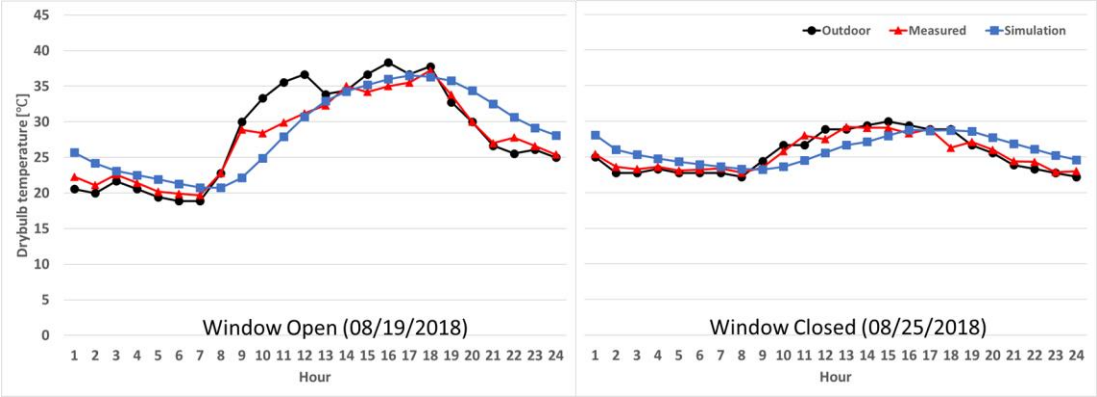

Figure 4-10: Comparison of temperatures: Outdoor temperature vs. Sandwich panel measured temperature vs. Sandwich panel simulation temperature

4.5 Results and Analysis

4.5.1 Outdoor Condition Analysis

The outdoor air temperature and wind speeds are compared to analyze the heating energy consumption of apartment in different floor levels during heating season. Both temperature and wind speeds adjacent to south wall areas are considered in this study since the DSF system is most likely installed in the south wall, considering typical construction of apartments in South Korea. Table 4-5 and Figure 4-11 show monthly and annual average outdoor air temperatures and wind speeds in different floors in a 25-story apartment building during heating season. The outside air temperature decreases as the floor level goes up. The outside air temperature differences between first floor and 25th floor is about 0.4°C in annual average. The wind speed adjacent to the 25th floor was 2.35 times higher than the first floor throughout the year. High wind speeds result in high convective heat transfer coefficient (U.S.DOE, 2019a). Both the outdoor air temperature and wind speeds are essential factors for the exterior convection heat transfer calculations (U.S.DOE, 2019a). As higher floor meets lower outdoor air temperature, it resulted in higher temperature differences between outdoor

air temperature and indoor air temperature in winter compared to the lower floors. Consequently, the higher floors experience more heating loads than lower floors. It is opposite in summer. The higher floors experience lower cooling loads compared to lower floors. The wind speeds also affect negatively for higher floors in heating season and positively in the cooling season. Considering the high heating dominant climate in Seoul, the heating loads reduction is more concerned than cooling loads reduction.

Table 4-5: Monthly average outdoor air temperature and wind speed in different floor levels during heating season

Monthly average outdoor air temperature [°C]						
	Nov	Dec	Jan	Feb	Mar	Average
25F	7.2	0.8	-2.5	-0.7	4.4	1.8
21F	7.2	0.9	-2.5	-0.7	4.5	1.9
17F	7.3	1.0	-2.4	-0.6	4.6	2.0
13F	7.4	1.0	-2.4	-0.5	4.6	2.0
9F	7.4	1.1	-2.3	-0.5	4.7	2.1
5F	7.5	1.2	-2.2	-0.4	4.7	2.2
1F	7.6	1.2	-2.2	-0.3	4.8	2.2
Monthly average wind speed [m/s]						
	Nov	Dec	Jan	Feb	Mar	Average
25F	3.8	2.9	3.6	4.9	3.5	3.74
21F	3.6	2.8	3.4	4.7	3.4	3.60
17F	3.5	2.7	3.3	4.5	3.2	3.43
13F	3.3	2.5	3.1	4.2	3.0	3.23
9F	3.0	2.3	2.8	3.9	2.8	2.97
5F	2.6	2.0	2.5	3.4	2.4	2.58
1F	1.6	1.2	1.5	2.1	1.5	1.59

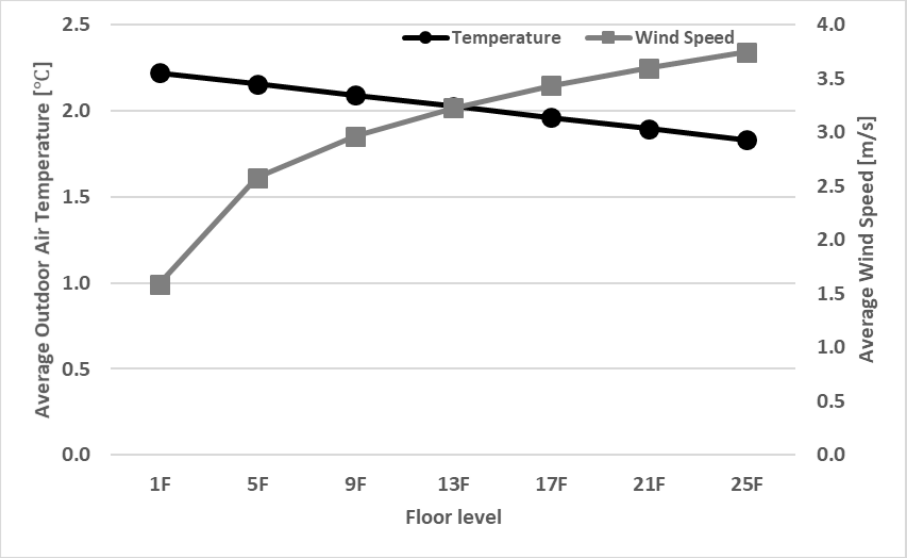

Figure 4-11: Annual average outdoor air temperature and wind speed in different floor levels during heating season

4.5.2 Heating Energy Consumption Analysis

The typical meteorological year weather file of Seoul, South Korea, is used for the simulation analysis. Figure 4-12 shows annual heating energy consumption of apartment in different floor levels for the three cases. There are seven representative floors, including 1F, 5F, 9F, 13F, 17F, 21F, and 25F. The Base-Case is a typical existing apartment unit, Case-1 a replacement of window which is typical retrofitting method, Case-2 the DSF system installed in Base-Case. A gas boiler is used to generate hot water for the radiant floor space heating. The fifth floor showed the least heating energy and the 25th floor the largest as expected. The first floor is directly connected to the ground, and its ceiling is the floor of the second floor. The constant ground temperature of 18 °C is used. The roof of the 25th floor is exposed to the outside. It increases the conduction heat transfer areas compared to other floors, which results in more heat loss. Additional infiltration can be expected. The 25th floor heating energy consumption is 19,765 kWh/year, which was 15.0% more than that of the first floor. The

ground was a positive effect on heating because the ground temperature is higher than outside air temperature in the winter. The ceiling of the 25th floor is faced directly outdoors. That is why the 25th floor used highest heating energy consumption. When exterior window is replaced with high-performance window (Case-1), the first floor shows the lowest heating energy of 16,251 kWh/year, and 25th floor shows the highest heating energy of 18,705 kWh/year. The 21st floor shows the highest heating energy savings of 5.7% compared to Base-Case. When DSF system is installed in the south wall, the fifth floor shows the lowest heating energy savings of 29.8%. The 21st floor has the highest heating energy savings of 30.0%. Table 4-6 shows the monthly heating energy consumption for all the cases in the heating season.

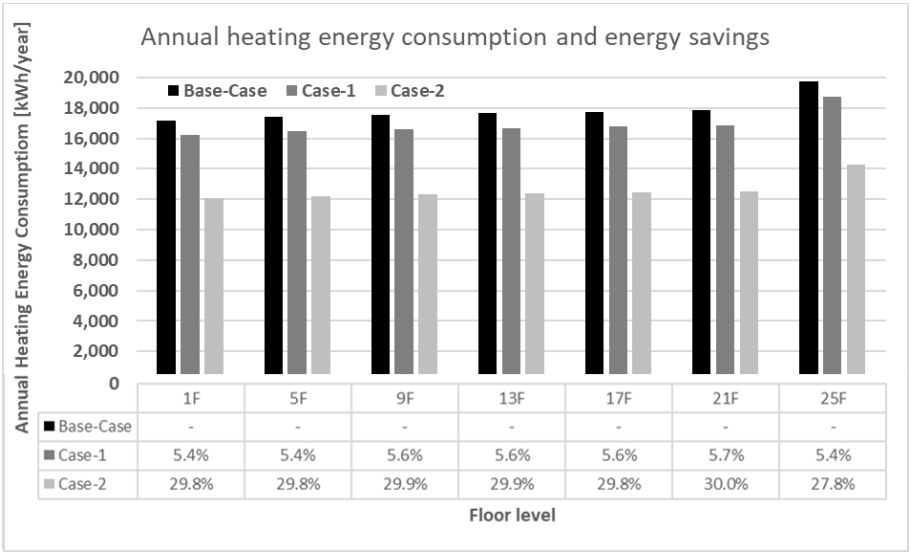

Figure 4-12: Annual heating energy consumption depending in different floor levels

Table 4-6: Monthly heating energy consumption in different floor levels

Gas consumption for the Base-Case [kWh/month]						
	Nov.	Dec.	Jan.	Feb.	Mar.	Total
25F	2,869	4,855	5,689	4,471	1,881	19,765
21F	2,534	4,410	5,175	4,065	1,698	17,882
17F	2,514	4,381	5,154	4,034	1,670	17,753
13F	2,485	4,364	5,125	4,004	1,675	17,653
9F	2,492	4,331	5,082	3,990	1,671	17,566
5F	2,420	4,325	5,060	3,965	1,636	17,406
1F	2,424	4,244	4,984	3,925	1,606	17,183
Gas consumption for the Case-1 [kWh/month]						
	Nov.	Dec.	Jan.	Feb.	Mar.	Total
25F	2,689	4,591	5,386	4,258	1,781	18,705
21F	2,401	4,145	4,892	3,828	1,596	16,862
17F	2,358	4,136	4,857	3,812	1,591	16,755
13F	2,357	4,106	4,857	3,789	1,556	16,666
9F	2,314	4,087	4,821	3,793	1,566	16,580
5F	2,294	4,077	4,806	3,749	1,543	16,468
1F	2,281	4,006	4,738	3,705	1,521	16,251
Gas consumption for the Case-2 [kWh/month]						
	Nov.	Dec.	Jan.	Feb.	Mar.	Total
25F	2,022	3,521	4,117	3,254	1,350	14,264
21F	1,727	3,101	3,662	2,848	1,177	12,516
17F	1,715	3,088	3,656	2,832	1,166	12,457
13F	1,701	3,071	3,632	2,814	1,160	12,377
9F	1,680	3,068	3,608	2,812	1,140	12,307
5F	1,678	3,022	3,584	2,795	1,143	12,222
1F	1,652	2,997	3,558	2,726	1,129	12,062

Figure 4-13 shows the temperature differences between outdoor, inside of the DSF system, and room thermostat in a representative day, January 10, which includes typical winter weather conditions. The black dash line shows heating setpoint temperature, the red line air temperature of DSF system, and the blue line outdoor dry-bulb temperature. The shaded area represents the temperature differences between the air temperature of the DSF system and outdoor dry-bulb temperature. In winter, the inside of the DSF system air temperature shows 21 ~ 32℃ higher than the outdoor air temperature. Outdoor air temperature ranges from -11.8 to -5.6℃. The window in south wall of Base-Case is directly exposed to the external environment. However, Case-2 has a thermal buffer area by DSF system, which results in lower heating energy use compared to Base-Case and Case-1. An optimal window opening control, which will be implemented in future studies, has potential to further reduce heating energy consumption.

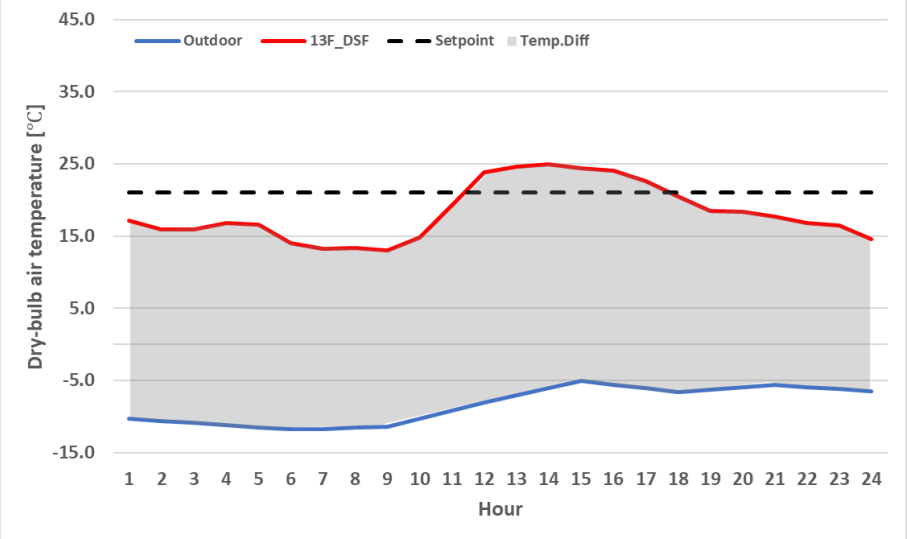

Figure 4-13: Comparison of temperatures in January 10

Figure 4-14 shows the inside face temperature of the south wall and window of the first and 25th floor, respectively, with and without DSF system in heating season. The bars represent the south wall inside face temperature, and the lines represent the south window inside face temperature. With the DSF system, wall inside face temperature increases from 0.6 to 1.0 ℃ in the first floor, 0.5 to 1.1 ℃ in the 25th floor. The south window inside face temperature increases from 1.8 to 4.2 ℃ in the first floor and 2.0 to 4.4℃ in the 25th floor. Therefore, it can be seen that the heating energy is reduced by installing the DSF system. When comparing the first floor and the 25th floor, it can be seen that the 25th floor has a lower wall inside face air temperature about 0.2 ~ 0.7 ℃ and lower south window inside face temperature about 0.4 ~ 0.7℃ than the first floor. Therefore, heating energy increases as the floor level increases. As described in Table 4-5 and Figure 4-11, since the outdoor air temperature is decreased with increased floor levels as well as wind speed increases, it affects the inside face temperature of the first floor is higher than 25th floor.

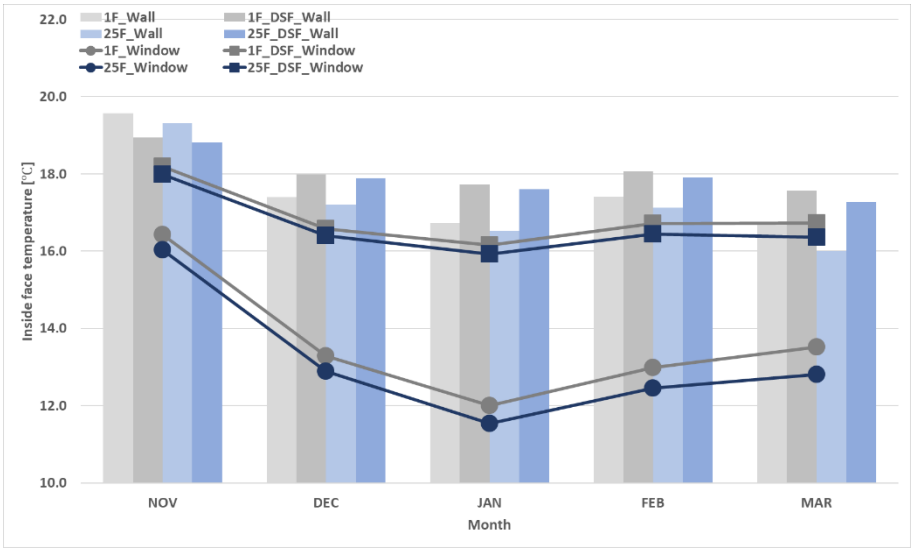

Figure 4-14: South wall and window inside face temperature in heating season

Figure 4-15 shows the annual heat loss through windows. The window heat loss pattem shows that as the number of floors increases, the window heat loss increases. The highest window heat loss is about 3,392 kWh/year in the 25th floor and the lowest window heat loss about 3,145 kWh/year in the first floor in Base-Case. In Case-1, the first floor has lowest window heat loss of 2,331 kWh/year and 25th floor the highest window heat loss of 2,494 kWh/year. Case-2 shows the lowest window heat loss of 1,940 kWh/year in the first floor and the highest window heat loss of 2,075 kWh/year in the 25th floor.

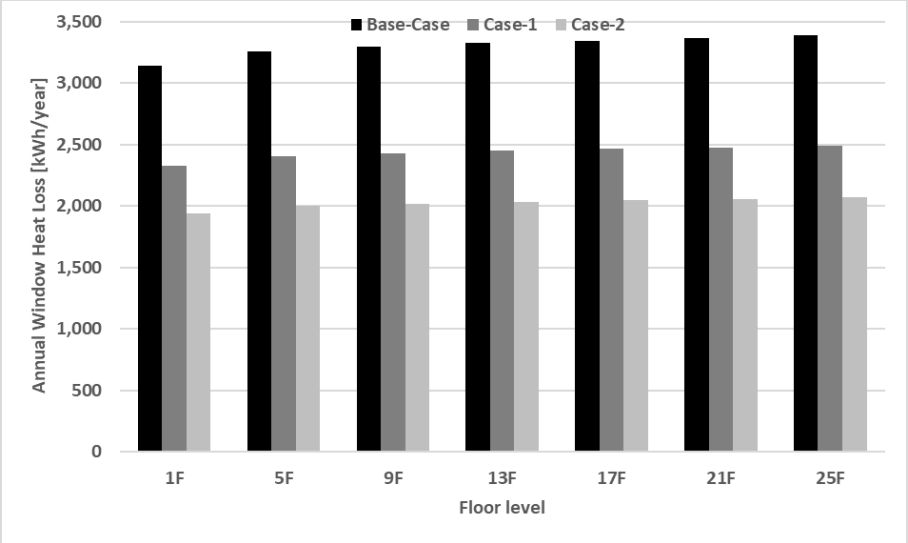

Figure 4-15: Window heat loss in heating season for three cases

Figure 4-16 shows the annual heat loss through the walls. The wall conduction heat loss is calculated by sum of heat loss from walls, floor, and ceiling. The pattern of the heat loss through the wall is increased with increased floor levels. However, the first floor is higher wall heat loss than others. The roof of the 25th floor is faced outdoors directly. The east and west wall of the case building are faced other apartment units, only south and north wall are faced outdoors. That is why the amount of increased wall heat loss is not significant. The first floor

shows the highest conduction heat loss savings of 9.5% and the 25th floor the lowest conduction heat loss savings of 3.7% by the installation of the DSF system.

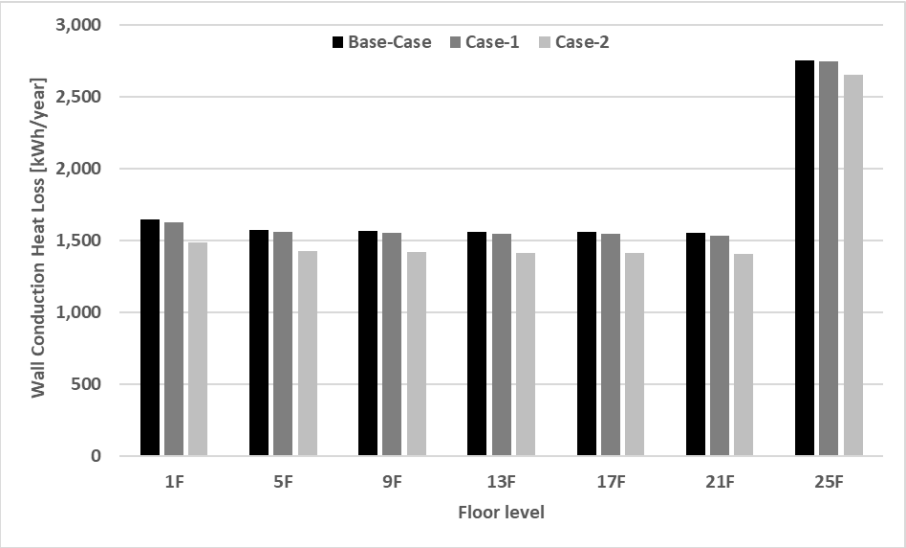

Figure 4-16: Wall conduction heat loss in heating season for three cases

As discussed earlier, the ACH of the case building is about the 2.7. The ACH of 2.7 is high and has large impact on heating energy consumption. Figure 4-17 shows the infiltration heat loss in different floor levels. The infiltration heat loss is increased as the floor level increases. The lowest infiltration heat loss of the Base-Case is 12,243 kWh/year in the first floor, and highest infiltration heat loss of the Base-Case is about 12,553 kWh/year in the 25th floor. Case-1 and Case-2 also have similar patterns. By installation of the DSF system, fifth floor shows the lowest infiltration heat loss savings of 23.4% and the 25th floor the highest infiltration heat loss savings of 23.7% compared to Base-Case.

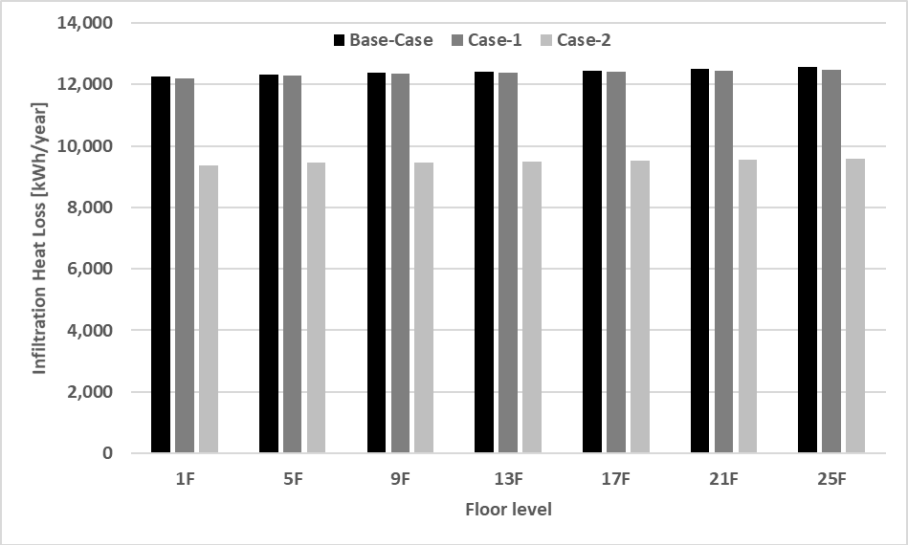

Figure 4-17: Infiltration heat loss in heating season for three cases

4.6 Conclusion

This paper presented a double-skin façade (DSF) system, which can be used as a replacement of balcony for the retrofitting of old apartment units. As an energy-efficient system, a DSF was proposed to replace existing windows in apartments to save thermal energy. A DSF system energy model was developed and calibrated to measured data gathered from a real-scale DSF system physical structure. The main goal was to analyze the energy savings potential in different floor levels of multi-story apartment buildings. In heating, the first-floor apartment unit consumed the least heating energy and the 25th floor the most. The outside air temperature differences between the first floor and the 25th floor was about 0.4 °C. The wind speed in the 25th floor was 2.35 times faster than the first floor in average during the year. It was a negative effect on heating energy savings. Comparing between Base-Case and Case-2, there was maximum of 30.0% heating energy savings in the 21st floor.

If the DSF system is installed to apartment unit in cold climate condition, which means heating dominated areas, then DSF system can make more heating energy savings due to thermal buffer area and higher air temperature inside DSF system than outside air temperature.

For further studies, a guideline of the optimal control of DSF system will be developed for different floor levels based on the heating and cooling energy consumption patterns and outdoor conditions. I will do cost analysis and calculate payback period as installation of the DSF system is a proposed retrofitting method. This study only considered heating energy consumption, however in the near future, we will consider the whole energy consumption for optimal control of DSF system. Also, in the near future, the proposed DSF system will be installed in a real apartment unit to gather real performance data to confirm the energy performances and to confirm the building characteristics such as infiltration value to make more accurate simulation model. The measured performance data will be used to calibrate the DSF system simulation model. Through this process, optimal specifications of DSF system will be developed to achieve maximum energy efficiency.

Chapter 5 HEATING ENERGY SAVINGS POTENTIAL FROM RETROFITTING OLD APARTMENTS WITH AN ADVANCED DOUBLE-SKIN FAÇADE SYSTEM IN COLD CLIMATE

Chapter 4 expressed how much building energy can be saved by installation of the DSF system in different floor level. In this chapter, I will describe how building energy is saved by installation of the DSF system. Three case models were developed: Base-Case with existing apartment, Case-1 with typical retrofitting, and Case-2 with the proposed DSF system. The EnergyPlus simulation program was used to develop simulation models for a floor radiant heating system. A typical gas boiler was selected for low-temperature radiant system modeling. The air flow network method was used to model the proposed DSF system. Five heating months, i.e., November to March, and one representative day, i.e., January 24, were selected for detailed analysis.

5.1 Introduction

Buildings generate about 23% of the total CO_2 generation in South Korea. Embedded energy used for producing and transporting subsidiary building materials and construction is estimated to reach approximately 38% of the entire CO_2 generation (Seo and Lee, 2016). Many studies have been conducted to conserve energy in buildings. New policies have also been developed to improve building energy efficiency, e.g., improved insulation, starting with the South Korean energy conservation policy in the 1980s (Oliver et al., 2001). These policies

have been enforced on both new and existing buildings. For existing buildings, performance improvement is mostly conducted through retrofitting processes.

This paper presents the results of simulation modeling studies for a double-skin façade (DSF) system applied in apartments to improve energy performance and focuses on 20- to 30-year-old apartments which comprise more than 65% of the total retrofitting rate of residential buildings. Figure 5-1 shows the pre- and post-installation of the DSF system in an apartment complex in South Korea. Figure 5-1(a) is the façade of an existing apartment building where air conditioning (A/C) condensing units are installed arbitrarily. Figure 5-1(b) is a rendering of the future façade of the apartment after the DSF installation.

(a) (b)

Figure 5-1: Pre- and Post-installation of a DSF system
(a) Existing apartment; (b) rendering with DSF installation

This paper uses a new and advanced DSF system as a balcony window replacement to improve the thermal performance of apartments, aiming to determine the applicability of the DSF system in apartments by analyzing energy performance. The main subject of this paper,

therefore, is to study the potential of the system for heating energy savings. Since the city of Seoul is a heating-dominant area, heat loss parameters are analyzed, and energy savings achieved from installing the DSF system are discussed. Three cases are developed for comparative analyses: The Base-Case is an apartment unit built 20 to 30 years ago with typical construction at that time. Case-1 is the same apartment unit as Base-Case with a typical retrofit of windows. Case-2 is an apartment unit with the DSF system installed. All three cases have the same traditional floor radiant heating system, which uses hot water supplied from an individual boiler.

The scope of this paper is classified into two aspects.

First, the energy consumption of boilers by the installation of the DSF system is compared to analyze the annual heating energy consumption according to the thermal performance of the DSF system and characteristics of boiler part load ratio (PLR).

Second, this paper also calculates simply payback period considering manufacturing, transportation, and installation cost. The detailed cost analysis will be performed in the future with suggestions such as reduction of manufacturing, transportation, and installation cost and suggest subsidies to reduce the payback period, which is one of the disadvantages of the DSF system.

One of the novelties of this paper is to know how the installation of a DSF system can reduce building energy consumption not only for the system itself but also for the radiant heating system. This paper also analyzes floor temperature, boiler gas energy consumption, and PLR of the boiler to understand the how the boiler works after the installation of the DSF system and to propose the optimal boiler capacity to further reduce heating energy consumption in the future.

5.2 Literature Review

5.2.1 Apartment Retrofitting

The South Korean government is strengthening its policies to reduce energy consumption through retrofitting in existing apartments. Windows need to have double Low-E glass or triple glazing. The heat transmission coefficient (U-value) should be 3.0 W/(m^2·K) instead of 3.84 W/(m^2·K) (Song and Choi, 2012). The majority of studies focus on the technical viewpoint, such as improvement of the insulation of exterior walls and exterior windows, improvement of infiltration, and replacement with high-efficiency equipment (Song and Choi, 2012). However, residents do not prefer replacement with high-efficiency equipment, and reinforcement of exterior walls as these entail lengthy remodeling time and discomfort or inconvenience during the replacement period. The retrofitting rate of residential buildings in South Korea is 12.7% for buildings not more than 10 years old, 12.5% for those 10 to 19 years old, 20.6% for those 20 to 29 years old, and 44.8% for those over 30 years old (Lim et al., 2017).

The replacement of windows is a method frequently applied to residential buildings, especially apartments because the construction period is relatively short. Reports suggested that buildings facing southwest with clear glazing windows had the highest energy savings of 12.3% in the cooling season (Chan and Chow, 2010). Raeissi and Taheri investigated the optimum dimensions of overhangs to increase energy savings in A/C systems in Iran (Raeissi and Taheri, 1998). By using the appropriate size, cooling loads was reported to have been reduced by about 12.7% during the summer season. Meanwhile, there was an insignificant increase of 0.6% in winter heating demand.

5.2.2 Double-Skin Façade System

Kim et al. analyzed the thermal and daylighting effects of a DSF system with interior and exterior blinds. The results demonstrated that the DSF model could save up to 40% for heating, 2% for cooling, and 5% in total loads compared to the base model that had no blinds or controls (Kim et al., 2018). Qahtan investigated the effectiveness of a DSF system in controlling heat gain under the direct solar radiation of the west orientation in the tropics in Malaysia. The results confirmed that the DSF system effectively controlled the heat gain as reflected in the difference between outdoor, indoor, and surface temperatures. However, the DSF system increased cooling requirements because of the penetration of tropical direct solar radiation (Qahtan, 2019). Chan et al. discussed the energy performance of a DSF system applied to a conventional office building in Hong Kong. The validated DSF model was then utilized to evaluate energy performance with various configurations, such as window type, position, and layers. The results indicated that a DSF system with a single clear window as an inner side and a double reflective window as an outer side could generate annual cooling energy savings of about 26% compared to a single-skin façade system with a single absorptive window (Chan et al., 2009).

Meanwhile, a variety of DSF models were selected for an office building in Tehran, using dynamic simulation programs. The results showed that the total energy consumption of the box-type DSF model with an external louver shading was reduced by 14.8% compared to the single-layer window model (Zomorodian and Tahsildoost, 2018). Gelesz and Reith evaluated the energy and comfort performance of the DSF system and compared it to double- and triple-glazed, single-skin façades for an office in Central Europe. Results revealed that the DSF system saved 7% in cooling energy compared to the double-glazed model. The DSF

system also performed better than the triple-glazed model while maintaining the same level of thermal comfort (Gelesz and Reith, 2015). Alberto et al. analyzed the DSF system using Design Builder and EnergyPlus, taking advantage of the computational fluid dynamics (CFD) module, to gain better insight into building performance, air flow path, air cavity depth, openings area, and type of glazing. They found that the most critical factor that determines the efficiency of the DSF system was air flow path, while the most efficient geometry was the multi-story DSF system that reduced about 30% of heating, ventilating, and air-conditioning (HVAC) energy demands (Alberto et al., 2017).

5.3 Simulation Software

EnergyPlus simulation program is selected because it is one of the suitable simulation tools to make the DSF system and radiant floor heating system considered in this paper. The EnergyPlus simulation program uses the pressure balance equation to compute the air flow network (AFN) model. Besides, it uses conduction transfer functions (CTFs) to calculate multiple layer conduction heat transfer in radiant floor heating systems.

5.3.1 Air Flow Network

An AFN model in the EnergyPlus simulation program was developed using the pressure balance equation, as expressed in Equation 5-1 (Dutton et al, 2008; U.S.DOE, 2019a). The inlet and outlet of the components connecting the two zones are at relatively different heights and in relatively different positions from the nodes representing the volume of the zones. The analysis of air flow using the components of each zone was based on Bernoulli's equation (U.S.DOE, 2019a).

$$\Delta p = \left(p_n + \frac{\rho {V_n}^2}{2}\right) - \left(p_m + \frac{\rho {V_m}^2}{2}\right) + \rho g(z_n - z_m) + p_w, \quad \text{Eq. 5-1)}$$

where Δp is the total pressure difference between nodes n and m (Pa); p_n and p_m are the inlet and outlet static pressures (Pa); V_n and V_m are the inlet and outlet air flow velocities (m/s); ρ is the air density (kg/m^3); g is the acceleration due to gravity (9.81 m/s2); z_n and z_m are the inlet and outlet elevation (m); and p_w is the wind surface pressure relative to static pressure in the undisturbed flow (Pa).

In Equation 5-2, p_s represents the stacking effect. If a wind pressure term is added to the two consecutive zones, i.e., node 1 and node 2, the pressure difference of all successive nodes can be expressed as Equation 5-2 and follows traditional flow direction indications. With a positive value, the flow is from node 1 to node 2; in case of a negative value, it is from node 2 to node 1 (U.S.DOE, 2019a).

$$\Delta p = p_1 - p_2 + p_s + p_w \quad \text{Eq. 5-2)}$$

where p_s is the pressure difference due to density and height differences (Pa).

By using the AFN model which can calculate air flow for multi-zones, the natural ventilation of the DSF system can be analyzed. In previous studies, the EnergyPlus simulation program was utilized to analyze the energy performance of DSF systems, stacking effect, and natural ventilation characteristics of DSF (Winkelmann, 2011; U.S.DOE, 2019b).

5.3.2 Radiant Floor Heating System

When the development of a radiant floor heating system model is perceived as completely separate from an energy analysis program, it diminishes the capabilities of the

simulation itself; hence, the program is unable to enhance or extend adequately (Strand and Pedersen, 2002). Heat transfer mechanisms through multilayered slabs and heat sources play a key role in the radiant floor heating system in EnergyPlus. To calculate the surface and zone temperature in given time intervals, EnergyPlus uses the heat balance method of each surface within the conditioned zone by considering the internal heat gain and loss caused by the radiation and convection between interior surfaces (Raftery et al., 2011). With the updated zone temperature, the heating zone load is determined on a time horizon, which can be used to determine the heating system response to meet the zone heating requirement. EnergyPlus provides several types of radiant heating systems, such as low and high-temperature radiant systems with two types of flows, i.e., variable flow and constant flow. Typical residential buildings in South Korea are equipped with the low-temperature radiant floor heating system that uses hot fluid circulated through tubes within the floor slab in variable volumes. This paper uses the low-temperature radiant system with the variable flow option. Figure 5-2 demonstrates the radiant floor heating system applied to the conditioned zone in this paper. The system capacity of the corresponding zone floor is chosen based on the load calculation sizing with the design day. The low-temperature radiant system with the flow option is a combination of mixing valves, a pump, and the radiant heating panel that includes heat source as shown in Figure 5-2.

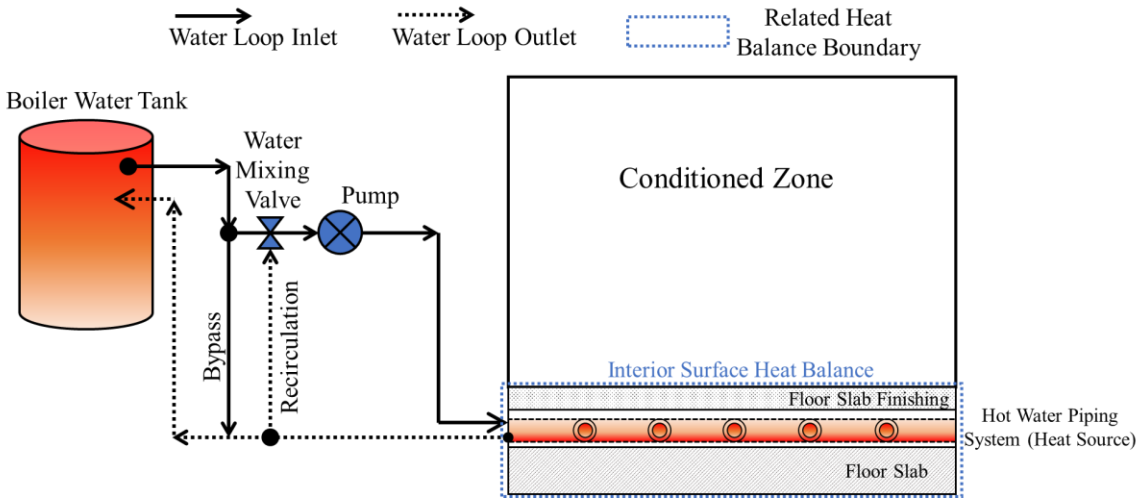

Figure 5-2: Radiant system component details

The CTFs is employed to compute multiple layer conduction heat transfer in EnergyPlus. There are two typical methods for calculating CTFs: the Laplace transform method and the state space method. Although both methods are suitable for the CTFs calculation in an accurate manner, the current version of EnergyPlus uses the state space method to compute the CTFs (U.S.DOE, 2019a). With the heat transfer solver, the interior floor surface heat balance can be calculated as

$$q''[\text{surface heat balance}] = \sum_{r=1}^{M} X_r T_{\text{i},t-r+1} - \sum_{r=1}^{M} Y_r T_{\text{o},t-r+1} + \sum_{r=1}^{s} F_r q''_{\text{i},t-r} + \sum_{r=1}^{M} W_r q_{\text{source},t-r+1} \quad \text{Eq. 5-3)}$$

where $q''[\text{surface heat balance}]$ is the interior floor surface heat balance (W/m^2), s is the number of order of CTFs; Both M and r are a finite number defined by order of CTFs; X, Y, F, and W are the conduction heat transfer functions which are constant; T is the temperature as a function of position and time (℃); o is the outside of the building element; i is the inside

of the building element; t is the current time step (h); $q''_{(i,t-r)}$ is the heat flux at a certain layer and time (W/m^2), which equals $-k\frac{\partial T(x,t)}{\partial x}$; x is the position, k is the thermal conductivity (W/(m·K)); and $q_{source,t-r+1}$ is the internal heat source of each calculation time, which is provided by the radiation system to keep the surface heat balance (W).

The surface heat balance on the left-hand side of Equation 5-3 considers several zone energy balance terms, including incident solar energy throughout exterior windows, radiation heat transfer from internal heat sources, such as lighting and electrical equipment, and radiation and convection between the floor surface and the surrounding surfaces and the air within the conditioned zone. In terms of temperature and heat flux calculation in heat transfer analysis, transient one-dimensional heat conduction through a homogeneous layer with constant thermal properties is considered in this calculation. The transient one-dimensional equation is typically coupled with Fourier's law of conduction at any location and time to temperature.

A heat source term on the right-hand side of Equation 5-3 considers heat exchange analysis for a hydronic system. In this calculation, the effectiveness-number of transfer unit (effectiveness-NTU) method is used with several assumptions, such as the constant water tubing length. Using the effectiveness-NTU heat exchanger algorithm, the energy balance rate relationship between the heat source and the water temperature is applied to each calculation step in order to estimate end energy use in the heating system. Hot water circulating in the closed loop in the radiant floor heating system indicates the amount of heat used for heating. Based on the heat balance method which the EnergyPlus simulation program used, heat is supplied to the floor piping system by the amount of heat calculated (U.S.DOE, 2019a). Radiant floor heating systems, unlike the conventional HVAC systems, reach the room set point temperature by the surface temperature rather than by the air supplied. Certain floor

surface temperatures are required to reach room set temperatures (U.S.DOE, 2019a). More details on load and energy calculation of the radiant heating system can be referred to in Ref. (U.S.DOE, 2019a).

Experimental validation of the low-temperature radiant heat transfer accuracy in EnergyPlus was conducted in a model residence that has a radiant cooling and heating system by comparing measured data with predicted ones (Chantrasrisalai et al., 2003). The other validation of the radiant system in EnergyPlus was made by comparing experimental measurements and test results using the Building Energy Simulation Test (BESTEST) suite (Raftery et al, 2011; Henninger et al, 2004).

5.3.3 Passive Heating

Windows are controlled open or close to bringing warm air from the DSF system module to the indoor area to achieve passive thermal heating. It is essential to optimally control the window to save as much heating energy as possible. Figure 5-3 depicts a window opening algorithm for the heating season. Figure 5-4 (a) shows the window opening conditions while Figure 5-4 (b) the air nodes in EnergyPlus. In the EnergyPlus program, the vertical and horizontal window openings in AFN are used for airflow connected zones in multiple linkages. Horizontal openings in the DSF system are used for surfaces between individual DSF zones to consider the air pressure and temperature differences even though the actual DSF system is one zone. Vertical openings in the DSF system are used for the interior window between the zone and the middle of the DSF system for passive heating. Table 5-1 lists the input values for the AFN used in this paper. Since the values in Table 5-1 cannot be obtained from actual

experiments, the values presented in the previous studies and the EnergyPlus simulation input and output reference were used (Kim et al, 2018; Dutton et al, 2008; U.S.DOE, 2019b).

In order to consider the ventilation between the DSF system and the interior zone through internal windows of the DSF, it was assumed that the interior window could be controlled. If the air temperature of the DSF system is lower than the indoor air temperature, both the outer and inner windows are closed. Discharge coefficient values Cd for the vertical and horizontal opening are set to 0.65 and 0.2, respectively, directly obtained from Ref. (Kim et al, 2018). The infrared transparent (IRT) surface function in EnergyPlus is used to consider the impacts of radiation, conduction, and convection in the DSF system. A "Full interior and exterior method" is used to consider direct and diffuse solar radiation factors through exterior and interior windows of the DSF (Kim et al, 2018; Dutton et al, 2008).

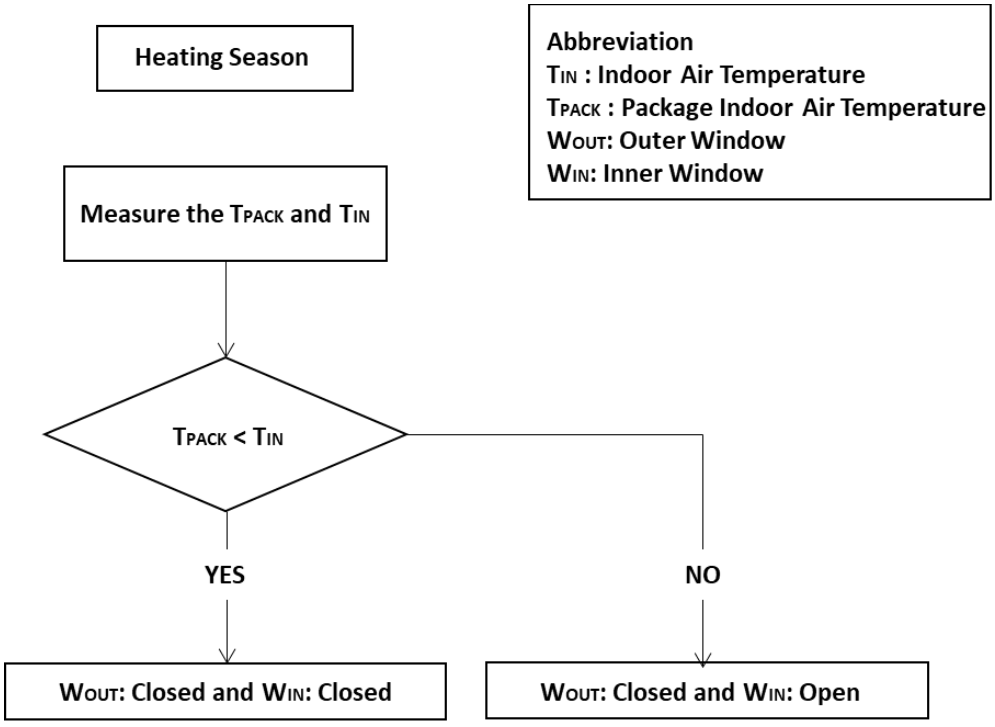

Figure 5-3: Windows control algorithm of proposed DSF system in winter

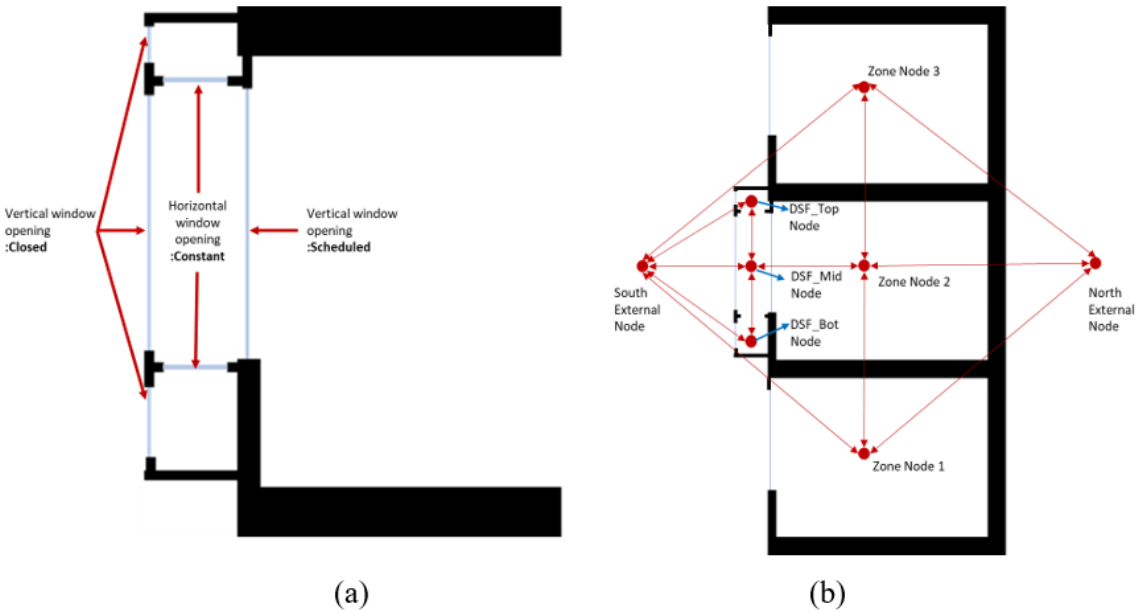

Figure 5-4: Window opening conditions and air-nodes connection of the DSF system

(a) DSF system opening conditions; (b) air nodes for simulation model

Table 5-1: Coefficient values of the DSF flow element (Kim et al, 2018; Dutton et al, 2008; U.S.DOE, 2019b)

Parameter		Value
Vertical opening	Air mass flow coefficient when opening is closed	0.001 (kg/s·m)
	Air mass flow exponent when opening is closed	0.667 (Dimensionless)
	Discharge coefficient	0.65 (Dimensionless)
Horizontal opening	Air mass flow coefficient when opening is closed	0.001 (kg/s·m)
	Air mass flow exponent when opening is closed	0.667 (Dimensionless)
	Discharge coefficient	0.2 (Dimensionless)
Opening/Crack factor		0.5 (Dimensionless)
Minimum venting open factor		0.3 (Dimensionless)

5.3.4 Thermal Characteristics of DSF System

Optical properties, thermal properties, the effect of buffer area, and the convection on each glass surface are important factors considered in the theoretical analysis of the DSF system with multi-layers. Depending on the condition of the external environment, the optical properties that occur in the DSF system include absorption, reflection, and transmission of direct/diffuse/reflective solar radiations (Gratia and Herde, 2004; Gratia and Herde, 2007a). The thermal properties of each surface are affected by the interfacial long-wave radiation of the buffer area in the DSF system and the convective heat transfer of the inner and outer surfaces. The effect on air flow can be caused by upper and lower ventilation damper conditions and the temperature in the buffer area. The characteristics of the DSF system can be represented in a two-dimensional form. Figure 5-5 illustrates the air flow and heat transfer in the DSF system. The optical properties of each surface and the buffer area reflect the passage of direct and diffuse solar radiations through Glass #1 from the outside. The solar radiation that passes through Glass #1 is the direct solar radiation. The process of reflection and absorption is repeated and finally flows into the room through Glass #2. It is necessary to adopt a theoretical analysis method that can mathematically verify the environment of the above physical phenomena. Although simulation modeling technologies can provide valuable results to analyze various physical phenomena, it is necessary to analyze unsteady state heat conduction, radiation, and convection heat transfer. Moreover, the high operation speed is required to cope with various parameter configurations. Accordingly, complex heat transfer analyses can be conducted by using EnergyPlus on the complex physical phenomena of the DSF system, such as solar radiation and temperatures of indoor, outdoor, and buffer areas (Kim and Park, 2010).

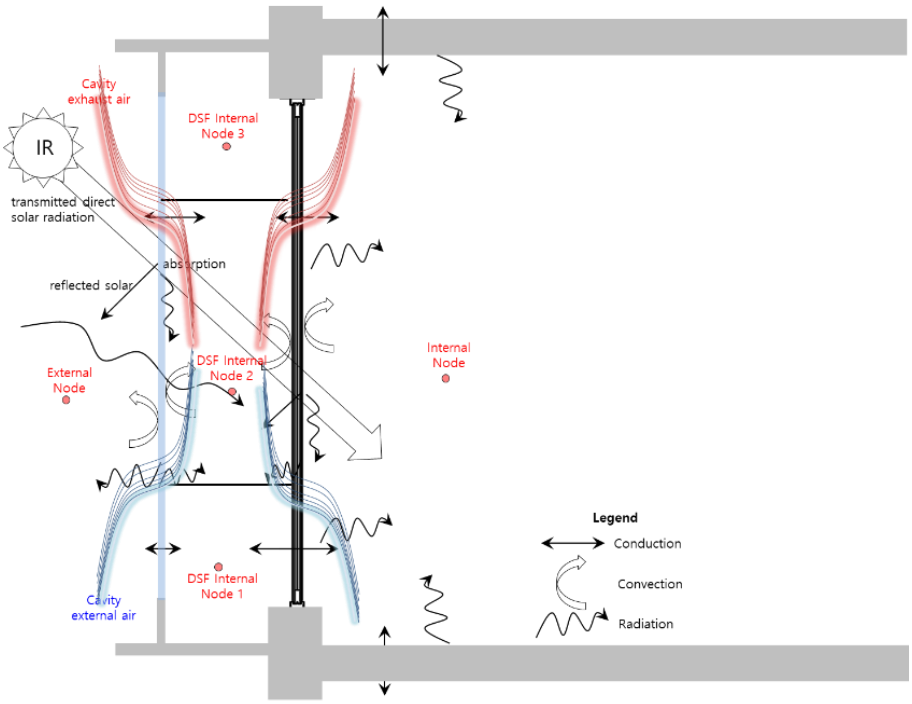

Figure 5-5: Air flow and heat transfer in DSF system

5.4 Simulation Model

5.4.1 Proposed DSF System

Figure 5-6 illustrates the outer and inner layer compositions of the proposed DSF system. The system has operable windows and insulated walls in the outer layer which includes a damper for the outdoor unit, photovoltaic (PV) systems, fixed/operable windows, and the overhang. The inner layer includes the outdoor unit, fixed and operable windows, and shelves. The depth of the DSF system is 700 mm. The DSF system can be used for retrofitting apartment units to improve energy efficiency. It would be interesting to see how much heating energy could be saved from retrofitting the existing balcony with the DSF system.

The radiant heating system which is mainly used in apartment buildings in South Korea consumes gas energy. As previously mentioned, this paper aims to reduce the heating energy

of residential buildings through the installation of a DSF system. Accordingly, PV systems that generate electrical energy are excluded. Future studies on annual energy savings will be conducted to explore electricity energy generated by the PV system.

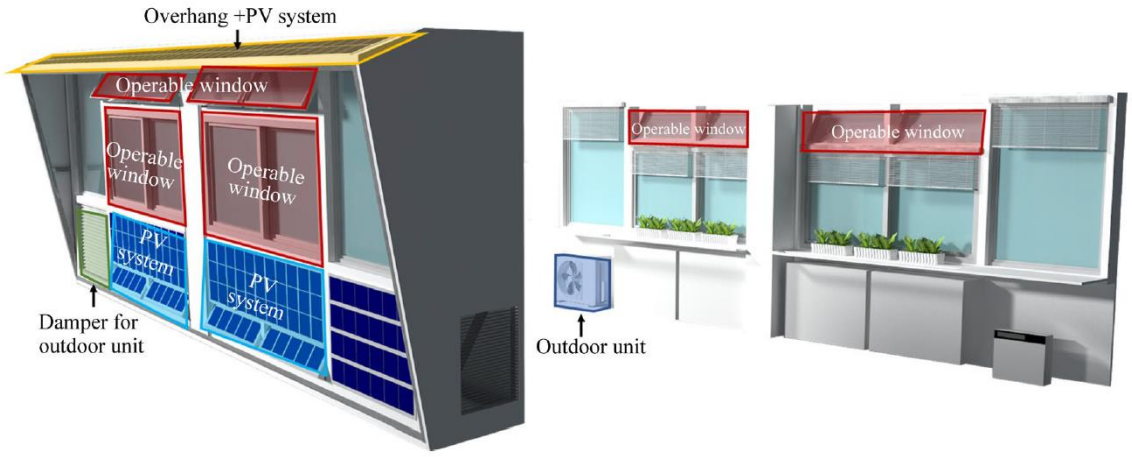

Figure 5-6: Composition of proposed DSF system

5.4.2 Simulation Cases

The construction specifications of a typical existing apartment, i.e., 20 years old, were used to create the details of the case study models. Figure 5-7 provides a drawing of an old apartment built in December 1999 in Seoul, South Korea. The 2016 Population and Housing Census, an annual report published by Statistics Korea, reported that the average size of high-rise apartment units is 80.4 m^2 for units built before 1979, 65.6 m^2 for those built between 1980 and 1989, and 70.0 m^2 for those constructed between 1990 and 1999 (Statistic Korea, 2017). The floor plan used in this paper is a common high-rise apartment building unit with a size of 75 m^2. The apartment balcony space was initially used as an auxiliary living space, i.e., unconditioned zone, for residents and for other functions, such as ventilation and lighting.

Nonetheless, it retained the form of a semi-outdoor space typical of the 1960s when the first apartments were built (Kim and Oh, 2012). In December 2005, balcony expansion was officially permitted. Apartment owners removed the inner balcony windows and extended the area as part of the living room space, thus increasing both the total conditioned space and the apartment resale value (Kim and Oh, 2012). As a result, the previous buffer area of the balcony disappeared, which meant an increase in energy consumption both in summer and in winter. The proposed DSF system is intended to be a replacement for the remaining outer wall/window of the balcony to eventually bring back the thermal buffer area and increase energy savings.

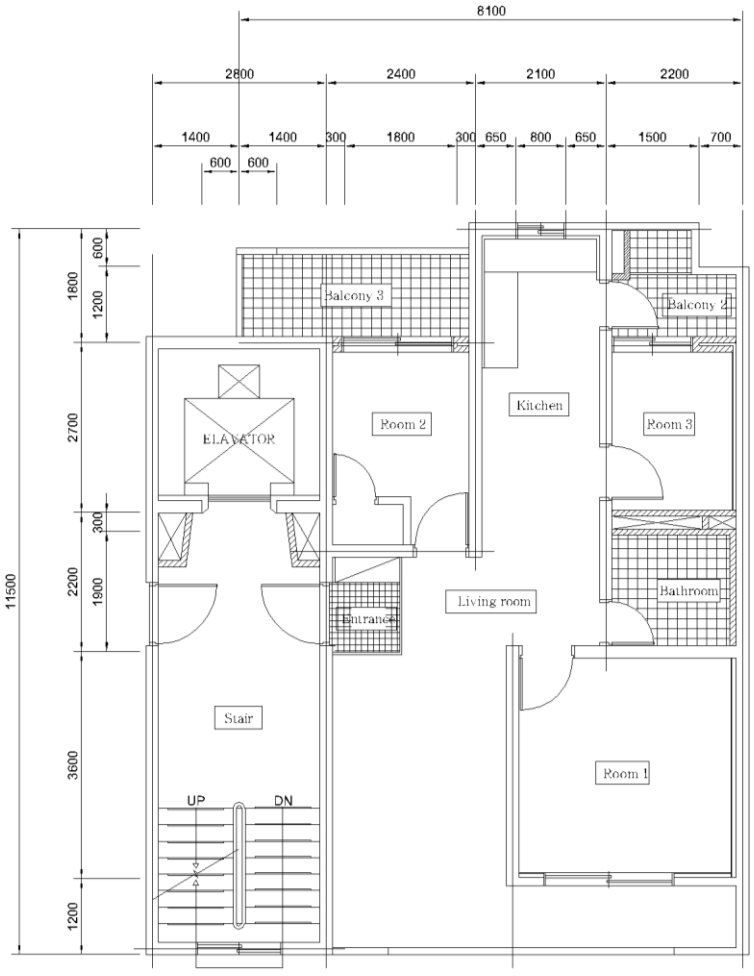

Figure 5-7: Typical floor plan of high-rise apartments

Figure 5-8 presents the geometry models of the three cases. The Base-Case model is an apartment with an enclosed balcony. Two cases were then developed to determine the effect of different retrofitting methods. The simulation model has three floors and three units per floor. The central unit located in the middle of the second floor was used for analysis. The Case-1 model, i.e., typical remodeling, includes a balcony window replaced with a new glazing type, which is a typical retrofitting method for energy savings. The Case-2 model includes the DSF system, as well as the window opening control, which is the proposed retrofitting method in this paper. Window opening control is not optional but required for the DSF system to save the heating energy consumption of the residential building, and it is already confirmed (Yoon et al., 2018). That is the reason for not considering the DSF system without window opening control in this paper.

Most apartments have separate heating and cooling systems in South Korea. Space heating is provided by a floor radiant heating system while space cooling is provided by a stand-alone A/C system. Both heating and cooling systems have individual on/off control. As previously mentioned, this paper focuses only on the heating system, considering the heating-dominant climate of Seoul, South Korea. A gas boiler is installed in residential buildings for space heating, in general. The air temperature of the DSF system is compared with the indoor air temperature to control windows for free heating in winter.

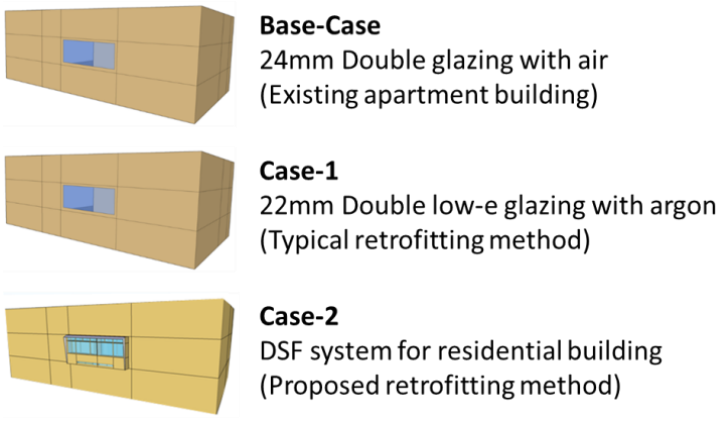

Figure 5-8: Simulation geometry models of Base-Case, Case-1 (typical window retrofit), and Case-2 (DSF)

5.4.3 Description of the Simulation Modeling

A weather file for Seoul, South Korea was used for the simulation. The latitude and longitude of the Seoul are 37°33' N and 126°58' E. The city of Seoul has four seasons with hot/humid summer and cold/dry winter. Outdoor air temperature ranges from –11.8 to 32.7 ℃. The heating energy analysis focused on the heating season from November to March during which the outdoor air temperature ranged from −11.8 to 16.6 ℃.

Figure 5-9 presents a simulation model of Case-2, which is the proposed retrofitting method. This simulation model was validated in Ref. (Yoon et al., 2019).

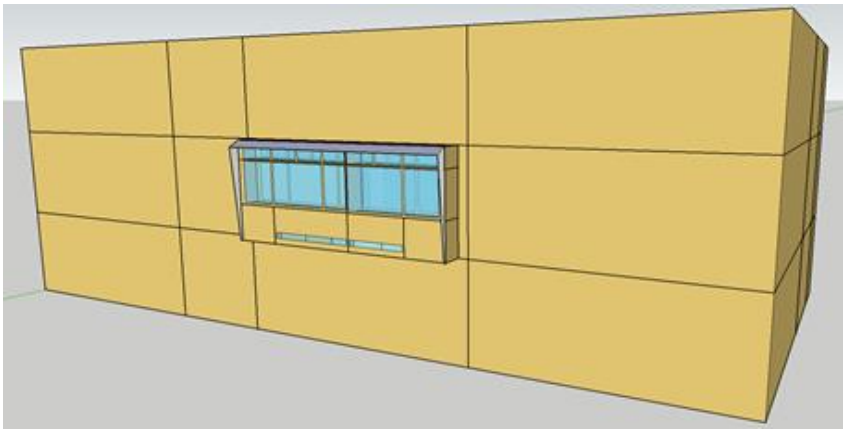

Figure 5-9: Simulation model of Case-2

Tables 5-2 and 5-3 outline the properties of building materials and construction sets of the building and the DSF system (Yoon et al., 2019; MOLIT and KEA, 2017; U.S.DOE, 2019). Case apartment constructions and materials were all based on the drawing of the apartment building in Figure 5-7.

Table 5-2: Building material properties

Materials	Conductivity ($W \cdot m^{-1} \cdot K^{-1}$)	Specific heat ($J \cdot kg^{-1} \cdot K^{-1}$)	Density ($kg \cdot m^{-3}$)
Insulation	0.03	1210	43
Concrete	1.60	900	2240
Gypsum board	0.18	1090	800
Ceiling finish	1.59	1260	1920
Floor finish	0.27	1210	640

Table 5-3: Construction set

Construction	Outer layer to inner layer (Thickness/mm)			
Exterior wall	Concrete (200)	Insulation (70)	Gypsum board (9)	
Interior wall	Gypsum board (9)	Concrete (120)	Gypsum board (9)	
Floor	Ceiling finish (0.5)	Insulation (50)	Concrete (120)	Floor finish (0.5)
Ceiling	Floor finish (0.5)	Concrete (120)	Insulation (50)	Ceiling finish (0.5)
Construction for DSF	Gypsum board (9)	Insulation (50)	Gypsum board (9)	

Table 5-4 shows the properties of the windows such as U-value, Solar Heat Gain Coefficient (SHGC), and Visible Transmittance (VT). For Base-Case, all windows installed in the apartment building were double glazed with air. Double Low-E windows with argon gas were used for Case-1 (i.e., the typical retrofitting method that entails replacement of the balcony window). Case-2 had exterior windows replaced with the DSF system that consisted of double Low-E windows with argon gas. Interior windows for the DSF system were double glazed with air. The specifications of the windows were obtained from a window manufacturing company. The 24-mm double-glazed window consisted of 6 mm clear glass, 12 mm air gap, and 6 mm clear glass. The 22 mm double Low-E glazed window consisted of 5 mm clear glass, 12 mm argon gas gap, and 5 mm Low-E glass.

Table 5-4: Properties of windows

Windows	U-value/($W \cdot m^{-2} \cdot K^{-1}$)	SHGC	VT
24 mm double glazed	2.824	0.704	0.786
22 mm double Low-E glazed	1.190	0.460	0.700

5.4.4 Internal Loads

Table 5-5 shows internal heat gain and heating set points. These values were based on the Study on Heating and Cooling Load Standard per Area for Apartments in 2017, published by the Korea Research Institute of Mechanical Facilities Industry (KRIMFI) (KRIMFI, 2017). Heating and internal heat gain schedules were based on the report Energy Technology Transfer and Diffusion 2007 (KIER, 2007).

Yoon et al. calculated the infiltration value of an apartment building installed with a DSF system by using the infiltration value of apartment buildings and effective leakage area values in the ASHRAE Handbook of Fundamentals (Yoon et al., 2019; ASHRAE, 2009). The air change per hour (ACH) of Base-Case and Case-1 was 2.82, while the ACH of Case-2 was 2.15 (Yoon et al., 2019).

Table 5-5: Internal heat gain and cooling and heating setpoints

<table>
<tr><td rowspan="5">Internal heat gain</td><td>People</td><td colspan="3">0.035 person/m^2 (2.6 persons/apartment)</td></tr>
<tr><td>Light power density</td><td colspan="3">10 W/m^2</td></tr>
<tr><td rowspan="3">Equipment power density</td><td colspan="3">3.57 W/m^2 for room</td></tr>
<tr><td colspan="3">1.61 W/m^2 for bathroom</td></tr>
<tr><td colspan="3">3.90 W/m^2 for living room</td></tr>
<tr><td rowspan="5">Setpoint</td><td rowspan="4">Floor heating (November to March)</td><td rowspan="3">Occupied (21 ℃)</td><td rowspan="2">Weekday</td><td>00:00~09:00</td></tr>
<tr><td>19:00~24:00</td></tr>
<tr><td>Weekend</td><td>00:00~24:00</td></tr>
<tr><td>Unoccupied (13 ℃)</td><td>Weekday</td><td>09:00~19:00</td></tr>
<tr><td>Hot water</td><td colspan="3">60 ℃</td></tr>
</table>

5.4.5 Gas Boiler Heating System

For the heating system, the low temperature radiant: Variable flow function was used in EnergyPlus. This function is a water-based radiant system. Energy is either supplied or removed through the surface, such as walls or floor (U.S.DOE, 2019b). A gas boiler which had a thermal efficiency of 80% and produced hot water with a temperature of 60 ℃ was used as a radiant floor heating system. The inside diameter of hydronic tubing for the hot water coil of the radiant floor was 16mm. The spacing between coils was 200mm (Lee et al., 2014). The length of each heating coil located inside the floor was calculated by considering each zone size and the spacing of coils. As tabulated in Table 5-5, the heating setpoint temperature was 21 ℃ during the occupied hours and 13 ℃ during the unoccupied hours. The set temperature of hot water was fixed at 60 ℃ (Yu et al., 2015). Figure 5-10 illustrates the typical efficiency and coefficients for non-electric and non-condensing boilers used in this paper (U.S.DOE, 2019b). Equation 5-4 is the boiler efficiency equation (U.S.DOE, 2019a). Boiler efficiency

ranged from 68.4% at a PLR of 10% to 80.9% at a PLR of 100%. The a, b, and c are the PLR coefficients.

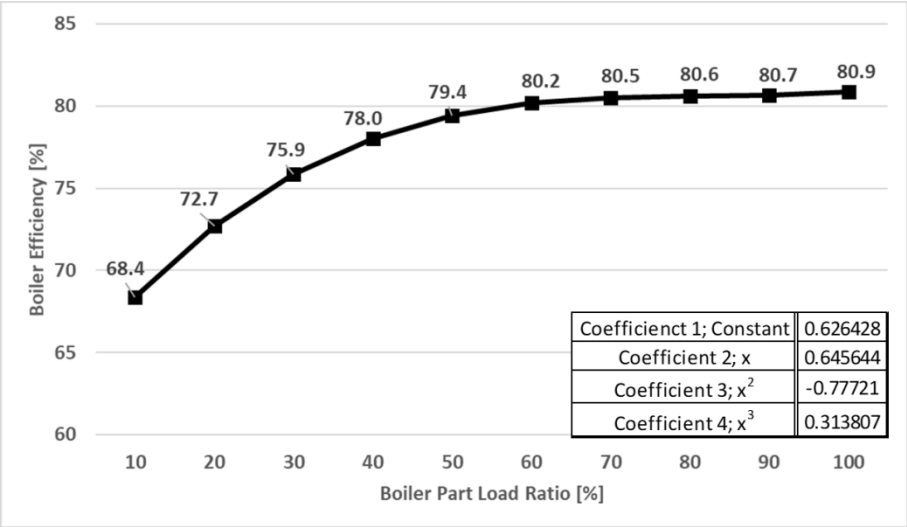

Figure 5-10: Boiler efficiency and values

$$\text{Boiler Efficiency} = a + b(\text{PLR}) + c(\text{PLR})^2 + d(\text{PLR})^3 \qquad \text{Eq. 5-4)}$$

5.5 Analysis

5.5.1 Gas Consumption on January 24

January 24 is the date selected as the winter representative day to analyze hourly boiler gas consumption for space heating. January 24 has the typical heating loads during the winter, because of this, January 24 also was used for the winter representative day in Ref. (Lee et al., 2019). The boiler size was 18 kW for all cases. Figure 5-11 presents the PLR of the boiler for each case. The distribution of PLR during boiler operation was 0–86% in Base-Case, 0–84% for Case-1, and 0–65% for Case-2. This distribution meant that Case-2 had less heating load

than the other cases. Notably, in all three cases, the boiler was repeatedly turned on and off during the boiler operation time, in which the zone radiant HVAC heating rate changed accordingly (see Figure 5-12). The radiant HVAC heating rate is the heating rate of the low-temperature radiant system. The heating rate is calculated by considering the zone conditions and the control of the low-temperature radiant system. The radiant floor heating system heats the floor via radiant heat instead of heating the indoor air directly. The room temperature was set at 21 °C. The boiler was turned on when room temperature reached 20.5 °C and turned off when it reached 21.5 °C.

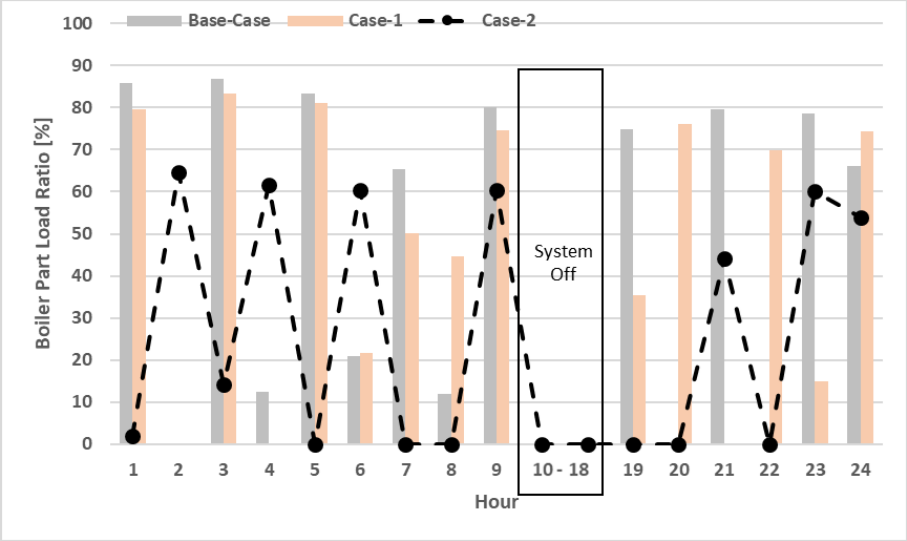

Figure 5-11: Comparison of PLRs of boiler for three cases on January 24

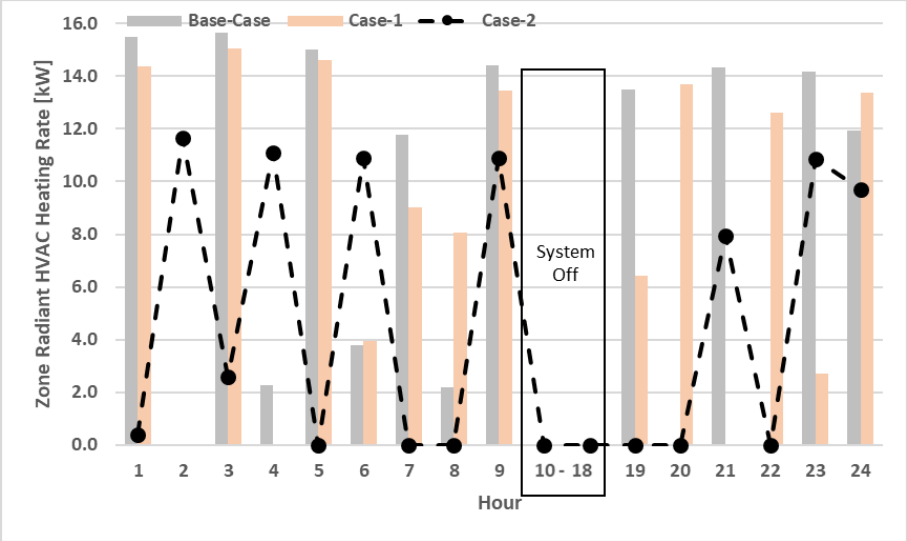

Figure 5-12: Comparison of zone radiant heating rate for three cases on January 24

Figure 5-13 displays the temperature changes in indoor air and radiant floor surface during the day. The floor was heated by the hot water coming from the boiler. The floor surface temperature was increased so that the indoor air temperature reached the heating setpoint temperatures. Accordingly, the floor surface was heated up to 34 ℃ by the boiler supply water that had a temperature of 60 ℃. This paper compared floor surface temperature with a previous experimental study to confirm the range of the floor surface temperature. Cho et al., conducted an experimental study on the application of low-temperature radiant floor heating system which this paper used (Cho et al., 2019). They used hot water of 50 ℃ for radiant floor heating system, and maximum floor surface temperature was 37.8 ℃ which meant the surface floor temperature in this paper was in a reasonable temperature range. In the unoccupied hours between 9 AM and 7 PM, floor surface temperature gradually decreased since there was no hot water supply. Meanwhile, indoor air temperature gradually increased after 2 PM due to solar radiation coming into space through the glazing during the daytime.

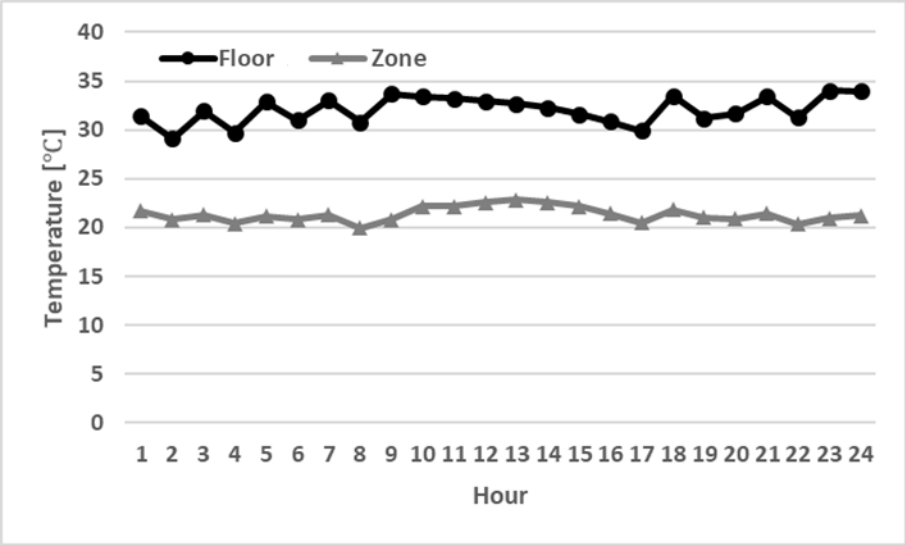

Figure 5-13: Floor surface temperature and indoor air temperature in Base-Case on January 24

Figure 5-14 compares boiler gas consumption in three cases. The gas consumption rate reached up to 24 kWh for Base-Case, 23 kWh for Case-1, and 18 kWh for Case-2. Case-2 had the least gas consumption rate. Between 7 PM and 8 PM, no heating energy was used in Case-2 due to the heat generated in the DSF area during the day.

All three cases had the same gas consumption pattern as the PLR pattern. The boiler efficiency used in this paper can explain why gas consumption pattern and PLR pattern are similar. There was a difference of about 3% in boiler efficiency from 40% to 100% for each PLR sections described in Figure 5-10, which is not a big difference. Besides, in Figure 5-11, it can be seen that the boilers in the three cases operate over 40% of the PLR except for a few hours. As a result, the PLR pattern is similar to the gas consumption pattern.

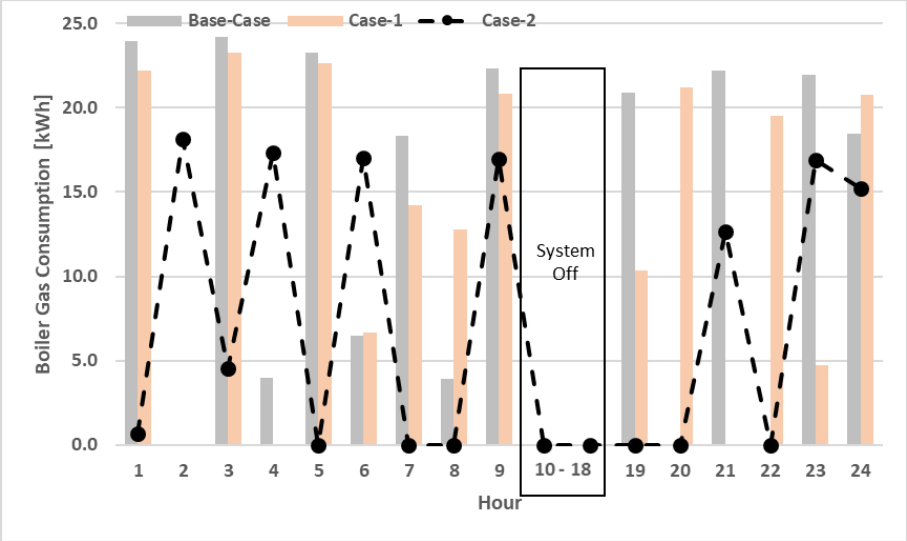

Figure 5-14: Comparison of hourly boiler gas consumption on January 24

As shown in Figure 5-7, 90% of the south wall is covered with windows. A large amount of heat loss is expected through the window area during the wintertime, thus increasing the heating load. Figure 5-15 illustrates the window heat loss of each case. The respective maximum and minimum heat losses through the window area were 1.11 and 0.62 kWh for Base-Case, 0.64 and 0.24 for Case-1, and 0.40 and 0.07 kWh for Case-2. Notably, window heat loss decreased significantly in Case-2 due to the improved U-value of the window, the air cavity of the DSF system, and reduced infiltration.

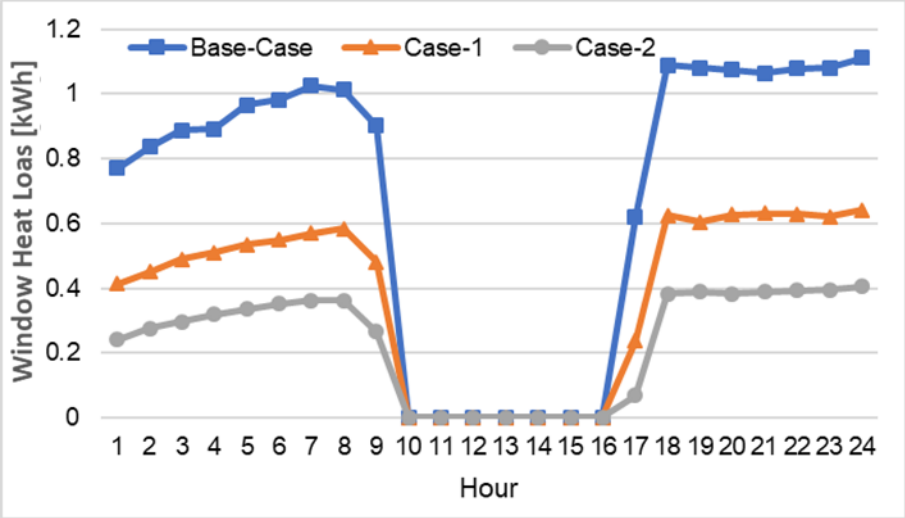

Figure 5-15: Window heat loss for the three cases on January 24

Figure 5-16 shows that the outdoor air temperature ranged from –6.5 to –3.2 ℃ while the DSF inside air temperature ranged from 15.0 to 24.4 ℃ on January 24. Case-2 had a thermal buffer from the DSF system, which significantly reduced delta T in the heat loss calculation, ranging from 21.5 ℃ to a maximum of 37.6 ℃. This thermal buffer resulted in substantial heating energy savings in winter.

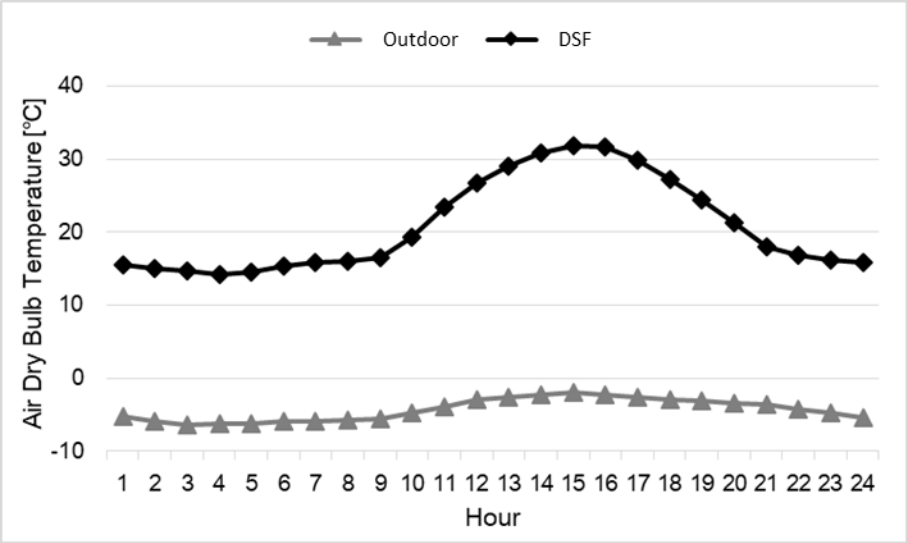

Figure 5-16: Outdoor and DSF inside air temperature on January 24

5.5.2 Total Heating Energy Consumption and Savings

Figure 5-17 presents the daily window heat loss for each case in the winter months, i.e., November to March. The daily heat loss value excluded heat loss occurred from 9 AM until 7 PM since the boiler did not typically operate during the daytime when there were no occupants. The window heat loss ranged from 2.79 to 18.30 kWh/day for Base-Case, 0.46 to 10.23 kWh/day for Case-1, and 0.66 to 6.24 kWh/day for Case-2. As expected, window heat loss of Case-1 was 45% less than that of Base-Case due to high-performance windows replacement. The window heat loss of Case-2 was more substantial than that of Base-Case: 66% less compared to Base-Case, which was due to improved window performance, reduced infiltration, and the thermal buffer area that the DSF system created. This considerable heat loss reduction decreased boiler gas consumption in Case-2.

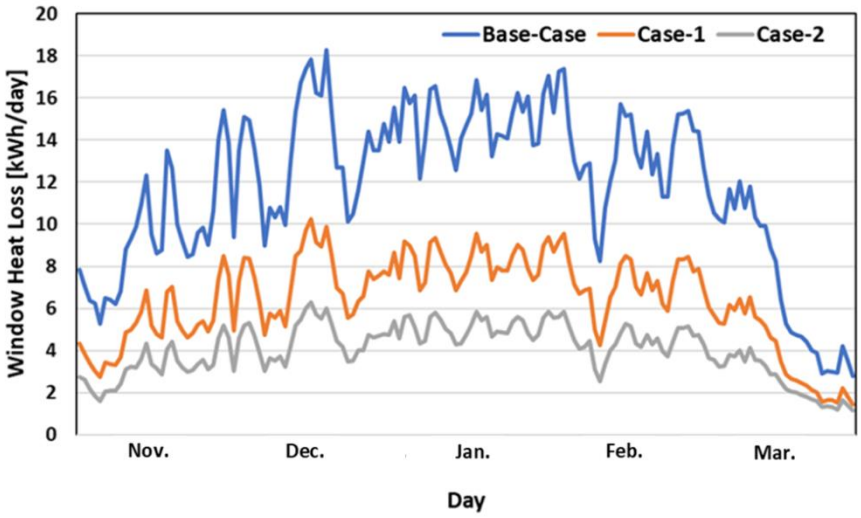

Figure 5-17: Daily window heat loss in three cases during occupied hours (7 PM to 9 AM)

Figure 5-18 provides the annual heat loss summary for the three main heat loss areas, i.e., window, wall, and infiltration, of the three cases during the heating season. Case-2 had the least heat loss of 2.04 MWh/year in the window area, which is about 39% less than the heat loss in Base-Case. There was not much difference between the heat loss through the wall in the three cases due to minor changes in or modifications of the wall areas. Notably, 90% of the south wall is covered by windows, resulting in minimal heat loss differences. Heat loss through infiltration had a significant impact on the heating energy in winter (see Figure 5-18). The infiltration heat loss was nearly four times higher than the window heat loss and nine times higher than the wall heat loss. Case-2 had a significant heat loss reduction in infiltration, i.e., 24% reduction, compared to Base-Case. The ACHs were about 2.6~2.8 in both Base-Case and Case-1 and about 1.9~2.1 in Case-2 (Yoon et al., 2019). Case-2 had a DSF system that significantly prevented infiltration due to its double-layer construction and improved air tightness.

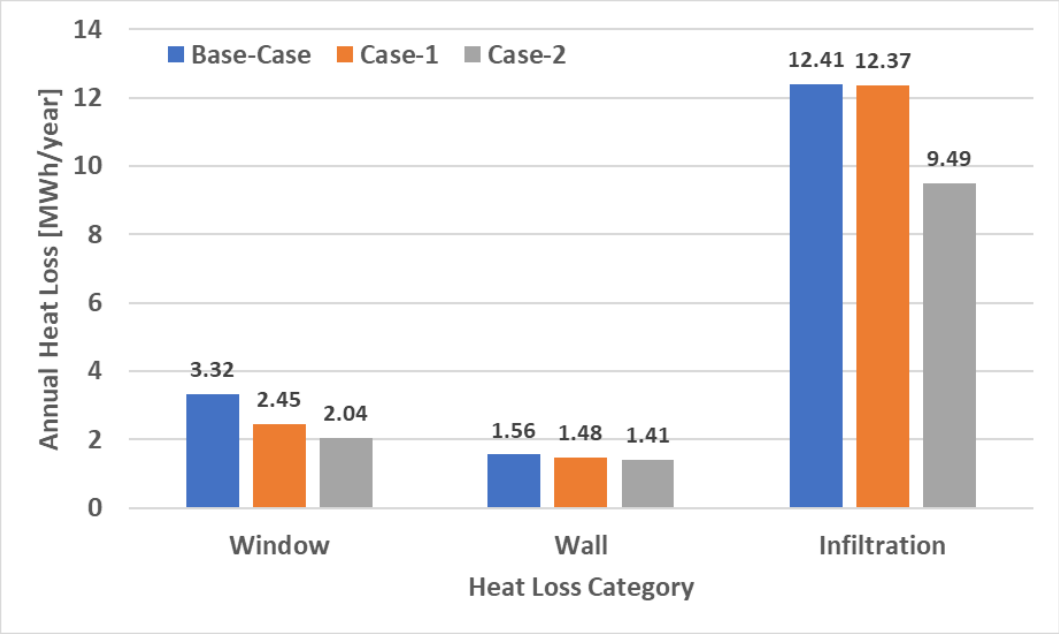

Figure 5-18: Annual window, wall, and infiltration heat loss in heating season for three cases

Figure 5-19 shows the monthly gas consumption of the three cases during the heating months. As expected, all cases had the highest boiler gas consumption in January and the lowest in March. The gas consumption was about 5.1 MWh/month in Base-Case, 4.9 MWh/month in Case-1, and 3.3 MWh/month in Case-2 in January. Annual heating energy savings in Case-2 were 38.8% compared to Base-Case and 35.2% compared to Case-1.

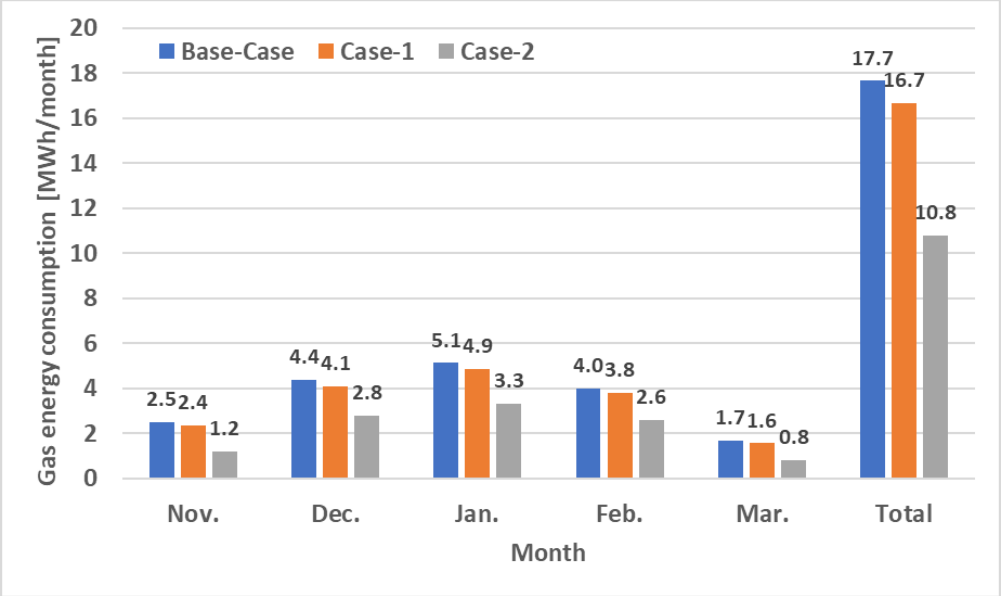

Figure 5-19: Comparison of monthly boiler gas consumption

5.6 Discussion

This paper compared heating energy consumption by the installation of the DSF system using a validated EnergyPlus simulation model. Three case models were developed, Base-Case, i.e., existing apartment, Case-1, i.e., typical remodeling/retrofitting with high-performance double-glazed windows, and Case-2, i.e., proposed remodeling/retrofitting with DSF system.

After the installation of the DSF system, the boiler works in the low PLR section. The less PLR of the boiler means that the boiler efficiency will also be decreased depending on the boiler efficiency.

If boiler capacity decreases, the boiler works in the high PLR section, which means that the boiler efficiency will be higher, and the heating energy consumption would then be further reduced. It shows that there is an opportunity to reduce the more heating energy consumption by the installation of the DSF system, which means that the heating energy consumption can

be reduced by not only the installation of the DSF system itself but also a smaller boiler capacity than before.

Heat losses are one of the main factors to explain the heating energy saving by the installation of the DSF system because of the internal heat gains, internal heat gain schedules, type of heating system, and heating set-point are the same in all cases. Window and wall heat losses can be reduced because the DSF system works as a thermal buffer, and south windows and walls are not adjacent outside directly but the DSF system. Due to the high-insulated wall, high-performance window, and the captured air of the DSF system, the range of the air temperature inside the DSF is from 21.5 to 37.6 ℃ which is higher than the outdoor temperature (–11.8 to 16.6 ℃).

Because of the higher temperature than the outside air temperature, the temperature differences between indoor and outdoor air temperatures are reduced by the installation of the DSF system. Small temperature differences have less effect on heat transfer, which accounts for the reduction in window and wall heat losses. Besides, the low U-value window also reduces window heat loss.

The old apartment building which is the target building of this paper has poor-insulated walls, low-performance windows, and high infiltration values because of poor construction code at that time it was built. By the installation of the DSF system, the south side of the apartment unit has an additional space and a double-layered construction, with 700mm air, high-insulated exterior wall, and high-performance exterior windows, which not only decreases the window and wall heat loss but also decreases the infiltration heat loss.

By the installation of the DSF system, the south side surface of the building has an additional space and a sturdy construction, which reduced the infiltration value of the target apartment unit. Therefore, the infiltration heat loss is reduced.

These analyses indicate that 38.8% of gas energy consumption for space heating can be saved. In addition, if a DSF system is installed in a new building, not for retrofitting, the boiler capacity can be reduced by about 30% due to the low PLR of the boiler by reduced the heating load after installation of the DSF system.

5.7 Conclusion

This paper proposed a DSF system as a balcony replacement for 20- to 30-year-old apartments in South Korea. It explained how heating energy consumption can be saved by the installation of the DSF system.

The DSF system will be installed in a real building in the near future to calibrate the simulation model and confirm the energy performance of the DSF system. One of the disadvantages of the DSF system is the payback period. The estimated cost of the DSF system, including production, transportation, installation, and labor cost, is about $24,500, and the payback period is more than 30 years. Notably, this estimation only considers energy saving costs. Attempts will consequently be made to find subsidies and to minimize the production and transportation costs to reduce the payback period. In the future, a cost analysis will be conducted for providing suggestions to achieve a reasonable payback period.

Chapter 6 ANALYSIS OF LIFE CYCLE COST AND CARBON EMISSION REDUCTION OF DOUBLE SKIN FAÇADE SYSTEM APPLIED TO OLD HIGH-RISE APARTMENTS IN SOUTH KOREA

In this chapter, I will describe payback period and carbon dioxide emission reduction by installation of the double-skin façade (DSF) system. Three case models were developed: Case 1 with existing apartment, Case 2 with proposed DSF system without window control, and Case 3 with proposed DSF system and window control. The EnergyPlus simulation program was used to develop simulation models and simulation model is calibrated with actual data. Life cycle cost analysis was performed based on the cost provided by the manufacturer company and utility company and simulation results.

6.1 Introduction

According to the International Energy Agency's analysis of global carbon dioxide (CO_2) emissions, CO_2 emissions from fossil fuel combustion increased by 60% in 2017 compared to 1990 (IEA, 2019). CO_2 is a greenhouse gas that will stay in the atmosphere for more than 10 years, so a solution to reduce greenhouse gas emissions is urgently needed (Terenoire et al., 2019). To this end, the Paris Agreement, agreed in the 21st United Nations Framework Convention on Climate Change (UNFCCC) in 2015, aims to reduce greenhouse gas emissions by 37% compared to normal business as usual (BAU) emissions (UNFCCC, 2015). 95% of fossil fuels, the main source of CO_2 emissions, are imported from abroad, and according to 2015 statistics, 17% of the country's total energy consumption is used in buildings

(KEEI, 2016). Therefore, national-level solutions for building energy savings should be prepared to reduce CO_2 emissions, one of the main causes of greenhouse gas growth (Sung and Faith, 2019).

Many efforts are being made to save energy and to strengthen building insulation standards to solve greenhouse gas emissions, but most of the policies are focused on new buildings. More than 47.7% of residential buildings are more than 20 years old, up 440,000 from 7.97 million in 2017 (46.5%) (Statistics Office, 2019). Therefore, policies on the construction of new buildings are important, but many measures are needed to cope with old buildings that have already been built.

Low-rise buildings and self-reliant buildings have a large skin area, making them more suitable for the introduction of renewable energy. This means that there are more options to choose from to save energy than high-rise buildings. However, it is noteworthy that Korea's land mass is 100,000 square kilometers, ranking 107^{th} in the world and the 28th largest population in the world, with more than 51.7 million inhabitants (KOSIS, 2020). Simply put, Korea's population density is high. South Korea has a population density of $527/km^2$ and is the 24^{th} highest in the world (KOSIS, 2020). More important than average population density is population density in large cities.

The population is concentrated in six major cities around Seoul, the capital of Korea, and Seoul, which has the highest population density, has the sixth highest population density in the world with $16,700/km^2$ (Market Statistics, 2007). The problem of population density in Korea is a serious problem. The high population density led to a residential type that everyone could live in, with high-rise apartments the most formed in the form of housing. In fact, 61.4%

of residential buildings are high-rise apartments, and more than 10 million high-rise apartments in Korea (National Statistical Office, 2019).

The application of renewable energy is quite difficult because the skin area of high-rise buildings is limited, and the building roof is a common space. It is also difficult to replace heating, ventilation, and air-conditioning (HVAC) due to the use of a central system. Therefore, most of the renovation methods of high-rise apartments are limited to window replacement. According to the review of the green remodeling project supported by the Korean government, about 10,000 cases were window replacement, while only 146 cases were added to insulation or the HVAC system (Lim et al., 2017).

However, the building insulation standards of high-rise apartments that are more than 20 years old are not as strict as they are now, so there was a limit to simply replacing external windows to save energy. Therefore, this work aims to propose a double-skin facade (DSF) system that reinforces wall insulation performance and window effectiveness as a retrofit method and to conduct life cycle cost analysis (LCCA) to evaluate the suitability of DSF systems. Relevant previous studies are introduced next.

6.2 Literature review

Yoon et al. evaluated the thermal performance of a DSF system installed in a high-rise apartment at different floor levels in the heating-dominant climate regions. They found that the first-floor apartment unit consumes the least heating energy and that the 25th floor consumes the most (Yoon et al., 2019). Kim et al. investigated the thermal effects of the DSF system with interior and exterior blinds. Results indicated that the DSF model can save up to 40%, 2%, and 5% for heating, cooling, and total loads when compared to the cases without blinds or controls.

Also, the DSF system and the exterior blind models could reduce the building cooling, heating loads, and lighting energy consumption by around 27 and 52% respectively (Kim et al., 2018).

Chan et al. analyzed that a double-skin façade system with single clear glazing can provide an annual saving of around 26% in building cooling energy compared to a conventional single-skin façade system with single clear glazing (Chan et al., 2009). Joe et al. measured an actual behavior of a multi-story DSF system in South Korea. The DSF building resulted in 15.8% and 7.2% reduction in heating and cooling energy consumption respectively compared to the single skin facade (Joe et al., 2013).

Gratia and Herde examined three cases to find the most efficient position of shading devices in a DSF system. They claimed that the DSF system could reduce cooling energy consumption by up to 23.2% per day, depending on the location and color of the blind and control method of the DSF system (Gratia and Herde, 2007b). Spastri et al. found that the energy consumption of DSF system with the dynamic environmental control system can be reduced by 4.00% on the hottest days and 4.00% on the coldest days (Spastri et al., 2015). Moon et al. examined optimum control strategies for the DSF system to maintain an energy-efficient indoor thermal environment. Novel ANN model was utilized to achieve the control strategies for the operation of ventilation of a DSF system and a building cooling system (Moon et al., 2014b).

Moon et al. analyzed several thermal control strategies to control the DSF buildings in summer. Compared to other algorithms, the Fuzzy Logic-based control algorithm for the cooling system improved building energy efficiency up to 49.4% (Moon et al., 2018). Choi et al. measured the behavior of a multi-story DSF system during the heating season in an office

building. They estimated that noteworthy energy saving was possible if multi-story DSF system is integrated with the HVAC system as a preheating space (Choi et al., 2017).

Moon et al. proposed an effective thermal control method for buildings with DSF systems. They developed four rule-based control logic and ANN-based control logic to control the cooling and DSF system (Moon et al., 2014a). Seo et al. argued that a DSF building can reduce 10.5% cooling energy compared to a non-DSF building with the same HVAC system. Also, they analyzed 4.5% additional savings when using the ANN-based control method (Seo et al., 2019).

Ghaffarianhoseini et al. analyzed the advantages and challenges of the DSF system. They argued that the key drawback of the DSF system is its high initial costs in comparison with the single facade system (GhaffarianHoseini et al., 2016). Hay and Ostertag argued that the DSF system has a potential to reduce annual cooling energy consumption by 9.2%. Also, the return period for the initial investment cost of the DSF system was found to be 8.2 years (Hay and Ostertag, 2018). Pomponi et al. analyzed life cycle cost assessment study to analyze DSF refurbishment strategies against an up-to-standard single skin alternative. They used 128 cases of DSF configurations, and 98% of the DSF configurations had a better life cycle energy performance than the single skin alternative. Additionally, nearly 83% of the DSF cases showed a better life cycle cost performance than the single skin facade (Pomponi et al., 2015).

Previous studies have shown that DSF systems form heat buffers that contribute to reduced energy consumption. Furthermore, it is shown that additional energy savings are possible through window control and optimal design of DSF systems. However, most previous studies have conducted analyses in terms of energy consumption in the absence of studies on payback periods. Reducing payback and energy consumption are also important to make more

effective modifications to the DSF system. Therefore, this study ultimately seeks to calculate the realistic payback period by considering subsidies, expected energy savings, installation costs and transportation costs provided in Korea to evaluate the adequacy of the DSF system proposed in this study.

6.3 Methods

The method of this study is divided into three parts. The first part is to evaluate energy savings by installing a DSF system in a high-rise apartment. The second part is the reduction of CO_2 emissions by installation of the DSF system, and the third part is the LCCA of the DSF system. The EnergyPlus simulation program version 9.0 is used for the calculations of energy savings, CO_2 emissions, and life cycle costs.

6.3.1 Simulation condition

To simulate an old apartment building, the Department of Energy (DOE) Ref Pre-1980 Template representing apartments from the past, among the templates provided by EnergyPlus related to residential buildings, was used. The template provides information of buildings built in the 1980s. The types and properties of the building material in the DOE Ref Pre-1980 Template and materials for DSF system are as in Table 6-1. CRC and OSB stand for cellulose fiber reinforced board and oriented strand board, respectively.

Table 6-1: Building material information

Material	Conductivity (W/m·K)	Density (kg/m^3)	Specific heat (J/kg·K)
Wood siding	0.11	544	1,210
Insulation	0.049	265	836
Gypsum board	0.16	785	830
Metal decking	45	7,680	418
Roof insulation	0.049	265	836
Roof membrane	0.16	1,121	1,460
CRC	0.24	32	920
OSB	0.13	600	1,460
Skytech insulation	0.032	135	750
Low-e insulation	0.0135	16	1,865
PF board	0.02	520	1,200

Tables 6-2 and 6-3 refer to construction of the old high-rise apartment building and the DSF system with the order of building materials in Table 6-1. The numbers in the parenthesis refer to the thickness of each building material. The thermal transmittance of the exterior wall was 1.011 W/m^2·K. For the DSF system, the thermal transmittance of the side wall was 0.324 W/m^2·K, 0.176 W/m^2·K for the southern wall, and 0.456 W/m^2·K for the roof and the floor. Table 6-4 shows the windows applied to this paper, which represents old apartments with window with a thermal transmittance of 5.84 W/m^2·K and 22 mm double layer Low-E window charged with argon gas that was applied to the DSF system.

Table 6-2: Construction of the old high-rise apartment building

Construction	Exterior to interior thickness in mm		
Exterior wall	Wood siding (10)	Insulation (33)	Gypsum board (12.7)
Interior wall	Gypsum board (19)	Air space	Gypsum board (19)
Floor and ceiling	Acoustic Tile (19)	Ceiling air space	Concrete (100)

Table 6-3: Construction of the DSF system

Construction	Exterior to interior thickness in mm				
Side wall	CRC board (6)	OSB (11.5)	Skytech insulation (13)	Low-e insulation (200)	Skytech insulation (30)
Floor and roof	CRC board (6)	OSB (11.5)	Skytech insulation (13)		Low-e insulation (60)
South wall	CRC board (6)	OSB (11.5)	Skytech insulation (13)		PF board (100)

Table 6-4: Window properties

Windows	U-value ($W/m^2 \cdot K$)	Solar Heat Gain Coefficient (SHGC)
DOE Ref Pre-1980 Window (Old high-rise apartment building)	5.84	0.54
22-mm double Low-E Glazing with Argon (DSF system)	0.96	0.347

Table 6-5 shows the internal heat gain and the heating and cooling set temperatures. The internal heat gain and heating and cooling set temperatures were based on the study on heating and cooling load standard per area for apartments, published by the Korea Research Institute of Mechanical Facilities Industry (KRIMFI, 2017). For the air infiltration value, an air infiltration experiment was conducted with an actual blower door test to input the median values of the experiment results. The heating temperature was set at 20℃ and the cooling temperature at 26℃.

Table 6-5: Internal heat gain and heating and cooling set points

Internal heat gain	People	0.035 person/m^2	
	Lights	10 W/m^2	
	Equipment	3.90 W/m^2	
Infiltration		1 Air Change Per Hour (old high-rise apartment building) 0.25 Air Change Per Hour (room with attached DSF system) 0.2 Air Change Per Hour (DSF system)	
Set point	Heating (November to March)	20 ℃	0:00~24:00
	Cooling (May to October)	26 ℃	00:00~24:00

The DSF system suggested in this study has photovoltaic (PV) panels at overhangs and the southern wall of the DSF system, as shown in Figure 6-1.

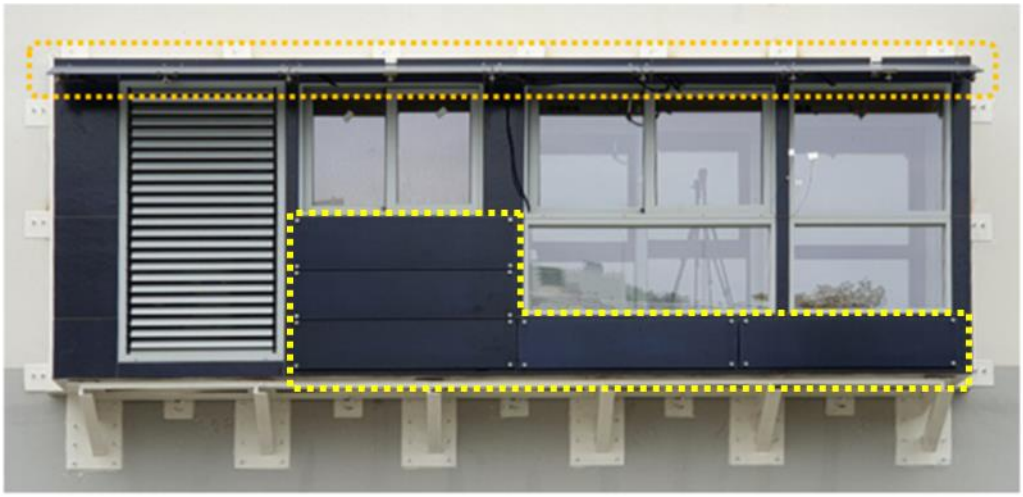

Figure 6-1: Location of the installation of the PV panels

Table 6-6 shows the size of the PV panels installed on the overhangs and southern wall of the DSF system. There are a total of seven different PV panel sizes, with four PV panels

installed on each of the overhang and the southern wall. The area of the PV panels installed on the overhang is 2.537 m^2, and the area of the PV panels installed on the southern wall is 2.41 m^2. All the PV panels used are from company C, and the efficiency of the PV panels installed for this study, based on the company's catalog, is 11.6%.

Table 6-6: The size and number of installed PV panels

Location	PV length (mm)	PV height (mm)	EA	Area (m^2)	Total installed area (m^2)
Overhang	1,674	461	1	0.772	2.537
	1,436	461	1	0.662	
	1,342	461	1	0.619	
	1,051	461	1	0.485	
Wall	1,633	389	1	0.635	2.410
	1,633	369	1	0.603	
	1,588	369	2	1.172	

The program utilized for PV electricity generation analysis is the System Advisor Model (SAM), a program provided by the National Renewable Energy Laboratory (NREL) of the United States. The amount of PV electricity generation could be analyzed based on the user's meteorological data, if the user has meteorological data with the filename extension of Comma-Separated Values (CSV). An analysis was conducted by utilizing the PVWatts functions built into the SAM program since only the size of the current PV panels, PV efficiency, and the details of the PV cell testing for the amount of electricity generated in the laboratory were available.

The electricity generation of the PV panels installed on the overhang and on the wall was analyzed separately. The default value of 96% was used for inverter efficiency.

6.3.2 Calibration

6.3.2.1 Experimental study

To improve the reliability of the simulation results, it is necessary to verify the simulation model. Therefore, an experimental study was conducted for this verification.

To collect actual measurement data, an actual measurement experiment was conducted from October 1, 2019 to January 15, 2020 on a test building located at Sejong-si in South Korea. Figure 6-2 shows a view of the building utilized for the actual measurements. The building is comprised of a total of three stories, with same floor plans on each floor. To minimize external conditions, the measurement experiments were conducted in the two test rooms located on the 2nd floor. The heating, ventilation, and air conditioning (HVAC) system installed for the experimental study was a stand-type heat pump (HP) system manufactured by company C.

Figure 6-2: The view of the building for actual measurement experiment

6.3.2.2 Calibration method

The Measurement and Verification (M&V) Standard calibrates the simulation model and judges the accuracy of the calibrated simulation through a comparison with actual measurement values. ASHRAE Guideline 14-2014, International Performance Measurement and Verification Protocol (IPMVP), and Federal Energy Management Program (FEMP) are representative M&V guides and indicators for determining the accuracy of the simulation model by Normalized Mean Bias Error (NMBE) and Coefficient of Variation of the Root Mean Square Error (CV(RMSE)). Smaller absolute values of the two error indicators indicate better calibration of the simulation model. Table 6-7 denotes the tolerance range of each of the M&V guides (ASHRAE, 2014; IPMVP, 2002; FEMP, 2015). The tolerance range of the error indicators vary according to the calibration unit, and, if the calibration is done with monthly unit data, the permitted error rate value is different for each of the guides. However, if calibration is done with hourly unit data, the error rate is $\pm$10% for NMBE and 30% for CV(RMSE), equal for all of the three indicators. This study conducted calibration by utilizing hourly unit data, and the standard of error indicator utilized was $\pm$10% for NMBE and 30% for CV(RMSE) for all three indicators. Equations 6-1 to 6-4 were used to calculate NMBE and CV(RMSE).

Table 6-7: Tolerance range in calibrating simulation model

Calibration Unit	Error Indicator	Tolerance range		
		ASHRAE Guideline 14-2014	IPMVP	FEMP
Monthly	NMBE	±5%	±20%	±5%
	CV(RMSE)	15%	5%	15%
Hourly	NMBE	±10%		
	CV(RMSE)	30%		

$$NMBE(\%) = \frac{\sum_{period}(S-M)_{interval}}{\sum_{period} M_{interval}} \times 100 \quad \text{Eq. 6-1)}$$

$$RMSE_{period} = \frac{\sqrt{\sum (S-M)^2_{interval}}}{N_{interval}} \quad \text{Eq. 6-2)}$$

$$A_{period} = \frac{\sum_{period} M_{interval}}{N_{interval}} \quad \text{Eq. 6-3)}$$

$$CV\left(RMSE_{period}\right)(\%) = \frac{RMSE_{period}}{A_{period}} \times 100 \quad \text{Eq. 6-4)}$$

where,

S : Energy consumption calculated through simulation

M : Energy consumption measured in actual measurement

$N_{Interval}$: Number of measured data

A_{period} : Average energy consumption during measurement period

6.3.2.3 Calibration results

Figures 6-3 and 6-4 show the simulation model calibration results based on the hourly measurement data from this study. The periods of electricity consumption data were from November 4, 2019 to November 11, 2019 and from December 1, 2019 to January 15, 2020 for

the actual measurement data that had been collected from October 1, 2019 to January 15, 2020. However, actual measurement data for approximately 3 weeks was utilized in the calibration after excluding periods during which electricity consumption data collection was problematic due to external factors, such as a power outage during the measurement. Company C did not provide performance data and conditions for the HP system utilized in the experiment, except for the rated cooling and heating capacity. Therefore, the default efficiency curve provided by the EnergyPlus program was utilized for the efficiency curve of the HP system. The CV(RMSE) for the simulation results compared to the data of actual measurement of the electricity consumption of the HP system was 26.8% for CV(RMSE) and 3.9% for NMBE in Case 1 and 22.7% and 5.9%, respectively, for Case 2. Both simulations satisfied ±10% for NMBE and 30% for CV(RMSE), the allowed standard of hourly error indicator, showing that the accuracy of the calibrated simulation model of this study had been secured.

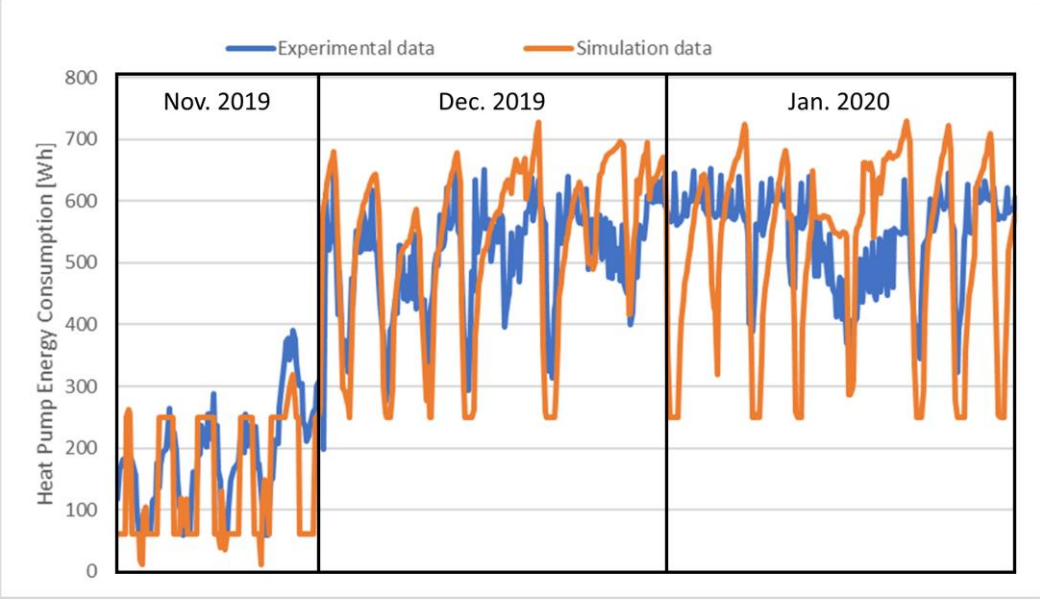

Figure 6-3: Calibration results (Base model)

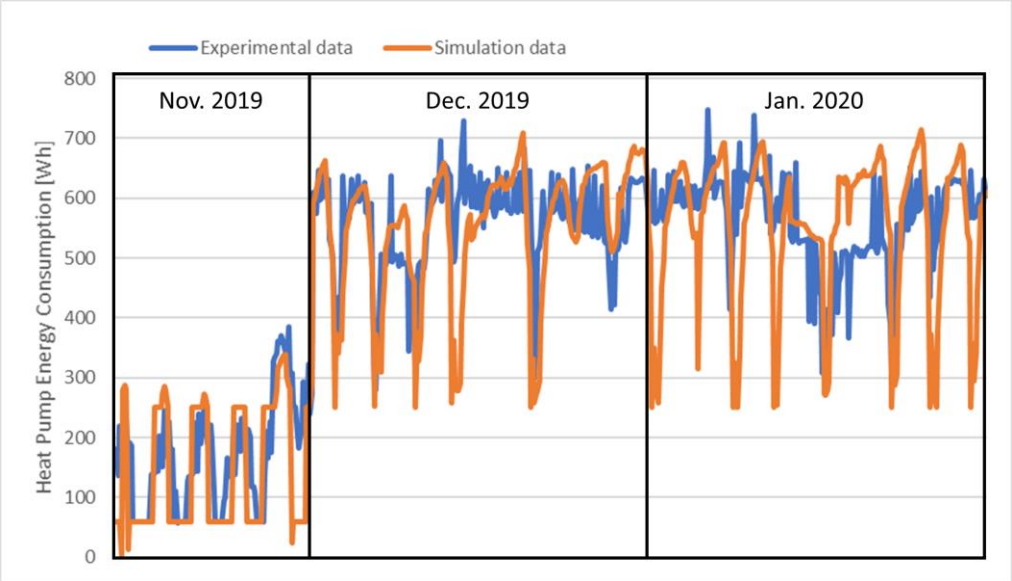

Figure 6-4: Calibration results (with DSF system installed)

6.4 Energy consumption analysis

6.4.1 Simulation cases

- Case 1: Old apartment without DSF system (Base model)
- Case 2: Old apartment with DSF system (without window control)
- Case 3: Old apartment with DSF system (with window control)

Case 1 changed the input values of a calibrated simulation model without a DSF system to the conditions of an old high-rise apartment building. Case 2 is attached to the calibrated DSF system without window control to Case 1. The impact of the DSF system on the energy saving in the building could be verified by comparing Cases 1 and 2.

In Case 3, DSF window control logic was added to the simulation model of Case 2, and the comparison of Case 2 without window opening and closing control with Case 3 will verify the additional saving that can be achieved in energy consumption.

6.4.2 Representative day analysis

6.4.2.1 Comparison of energy consumption on summer representative day

Figure 6-5 contains a graph representing the cooling energy consumed by the HP system in the each of the cases on the summer representative day. Case 1 consumed 125 Wh to 1,273 Wh, Case 2 149 Wh to 476 Wh, and Case 3 147 Wh to 475 Wh of the cooling energy. Between 6 PM and 7 AM – the time of use in residential buildings – Case 2 showed a saving of 45.0% in cooling energy compared to Case 1, and Case 3 showed a 46.7% saving in cooling energy compared to Case 1. Furthermore, during the non-use hours between 8 AM to 5 PM, Case 2 saved 54.7% in cooling energy consumption and Case 3 saved 55.4% in cooling energy consumption, compared to Case 1.

For lighting, all three cases showed lighting energy consumption between a minimum of 0 Wh and a maximum of 323 Wh since lighting was turned on according to the input schedule.

Figure 6-6 contains a graph showing total energy consumption on cooling, heating, and lighting on the summer representative day. Since heating was not required during summer, no heating energy was used. Case 1 consumed 14.4 kWh/day for cooling and 2.2 kWh/day for lighting and consumed a total of 16.3 kWh/day during the summer representative day; Case 2 consumed a total of 9.2 kWh/day, which is 44.6% less than Case 1; and Case 3 consumed a total of 9.1 kWh/day, which is 45.2% less than Case 1.

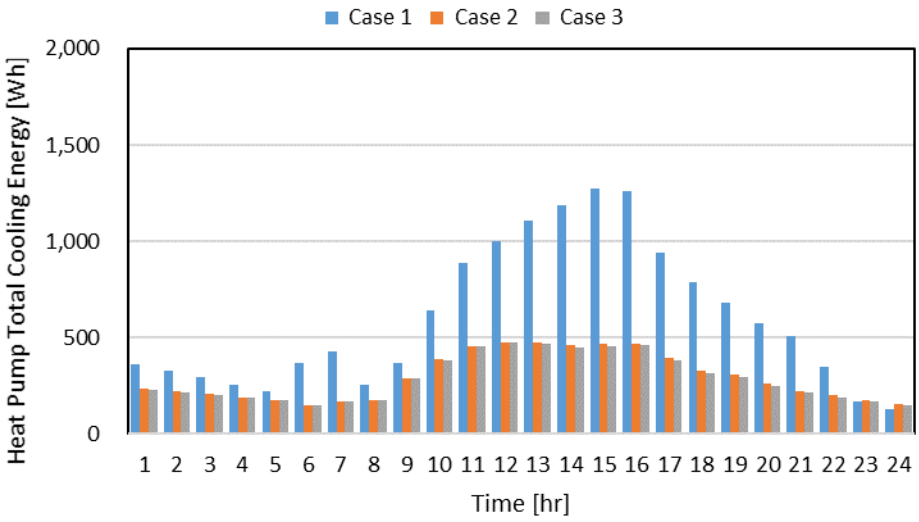

Figure 6-5: Heat Pump cooling energy consumption on summer representative day

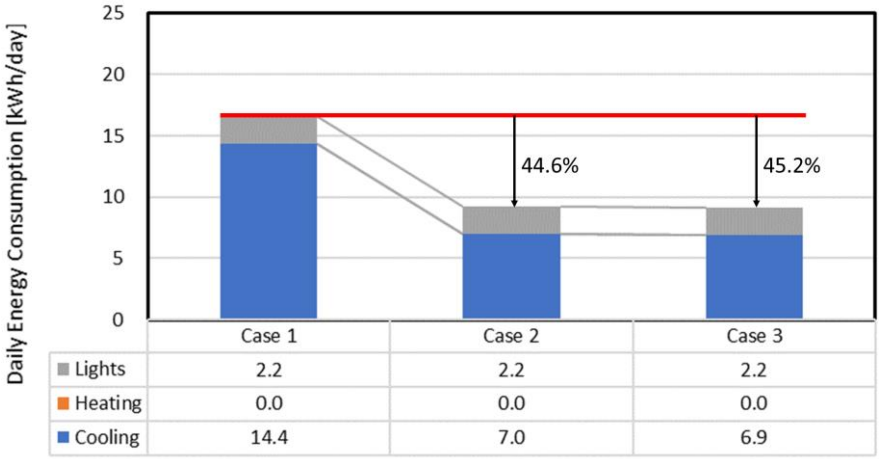

Figure 6-6: Total energy consumption on summer representative day

6.4.2.2 Comparison of energy consumption on winter representative day

Figure 6-7 contains a graph showing heating energy consumption of the HP system for each of the cases on winter representative day. Case 1 consumed 464 Wh to 1,155 Wh, Case 2 397 Wh to 668 Wh, and Case 3 250 Wh to 660 Wh of the heating energy. Case 2 saved 41.2% in heating energy compared to Case 1 between 6 PM to 7 AM – the time of use in residential

buildings – and Case 3 saved 41.6% compared to Case 1. In addition, between 8 AM and 5 PM – the non-use time in the building – Case 2 saved 33.0% in heating energy and Case 3 36.1%, compared to Case 1. Since a schedule equal to summer representative day was used, all three cases showed a minimum of 0 Wh to a maximum of 323 Wh for lighting energy consumption.

Figure 6-8 contains a graph showing total energy consumption on cooling, heating, and lighting during the winter representative day. Since cooling was not required during the winter, no cooling energy was used. Case 1 consumed 19.1 kWh/day for heating and 2.2 kWh/day for lighting, a total of 21.3 kWh/day during the winter representative day. Case 2 consumed a total of 14.0 kWh/day, which is 34.3% less than Case 1; and Case 3 consumed a total of 13.7 kWh/day, which is 35.7% less than Case 1.

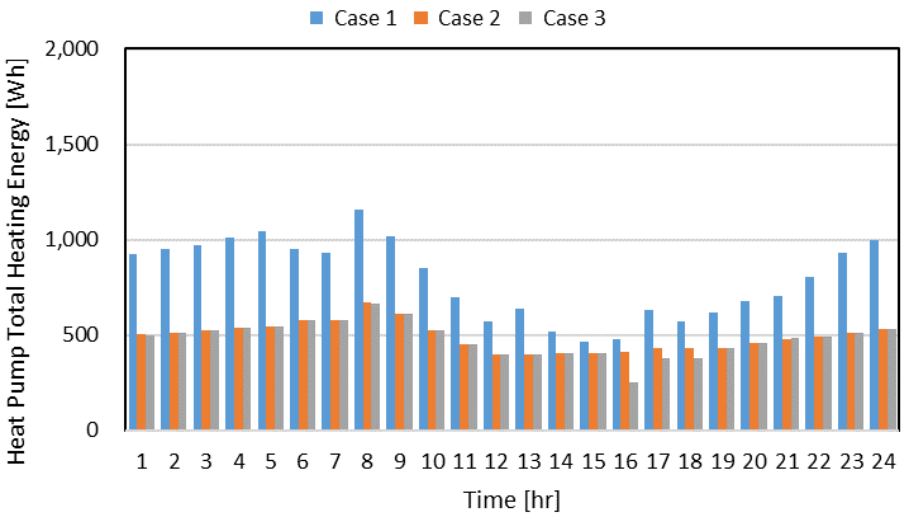

Figure 6-7: Heat Pump heating energy consumption on winter representative day

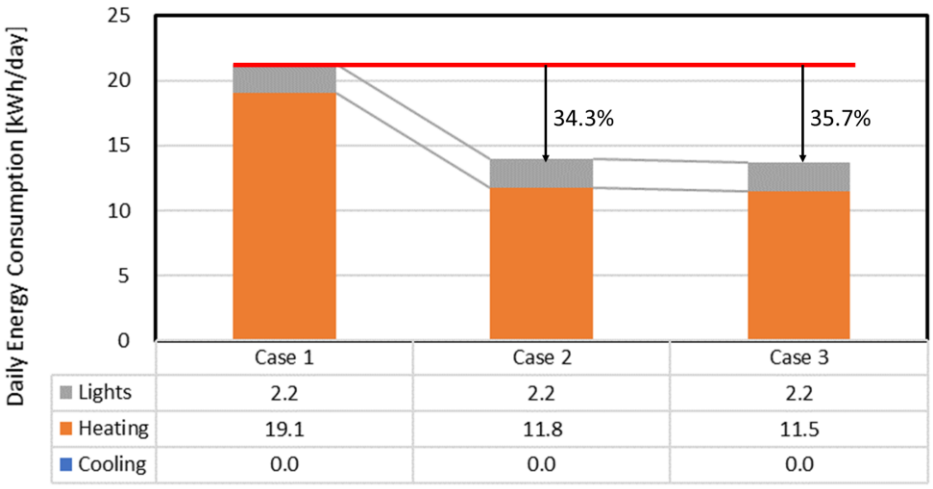

Figure 6-8: Total energy consumption on winter representative day

6.4.3 Window control logic

The window control logic in Figure 6-9 was applied to EnergyPlus to open and close the window. On the summer season, the exterior windows of the DSF system are controlled when the indoor air temperature is 26℃ or higher, the outdoor air temperature is 24℃ or higher, and the inside air temperature of the DSF system is 5℃ higher than the outdoor air temperature. However, the heating and cooling were on 24 hours a day in the summer representative day for this paper, so that there was no time when the indoor air temperature was 26℃ or higher. Therefore, exterior windows of the DSF system are opened to circulate the heated air in the DSF system with outdoor air only when the outdoor air temperature is 24℃ or higher and the inside air temperature of the DSF system is 5℃ or more higher than the outdoor air temperature.

Figure 6-10 shows the inside air temperature of the DSF system, the outdoor air dry-bulb temperature, and the window control schedule of the DSF system on summer representative day. For the window control schedule, 0 is closed and 100 is opened. When window is closed, the heat accumulates in the DSF system so the indoor air temperature of the

DSF system increases steadily during the day. When the window is opened, the inside air temperature of the DSF system mixes with the outdoor air, following the temperature pattem of the outdoor air.

Figure 6-11 represents the window control schedule, outdoor air dry-bulb temperature, and inside air temperature pattern of the DSF system on winter representative day. As the windows open, the inside air temperature of the DSF system is lowered by mixing with the indoor temperature of 20℃ or lower. Therefore, it was verified that the input window control was working accurately.

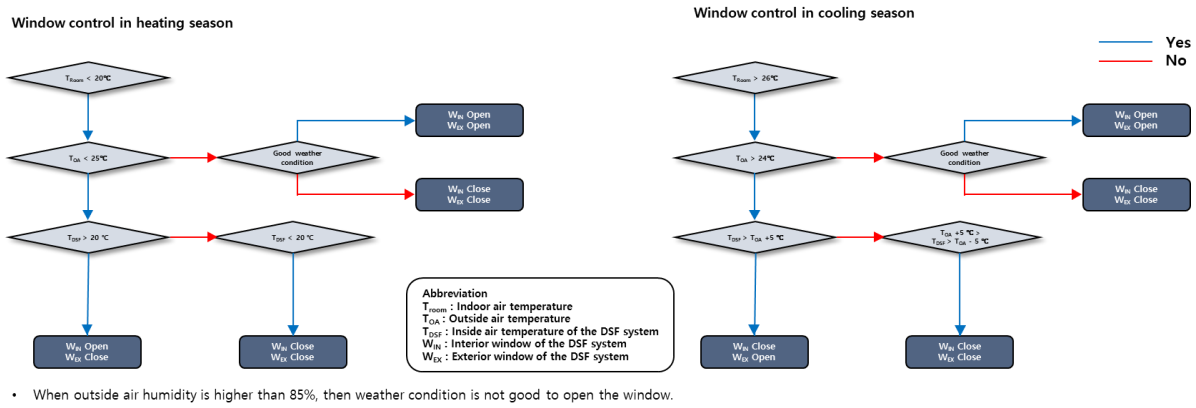

Figure 6-9: Window control logic for the heating and cooling periods

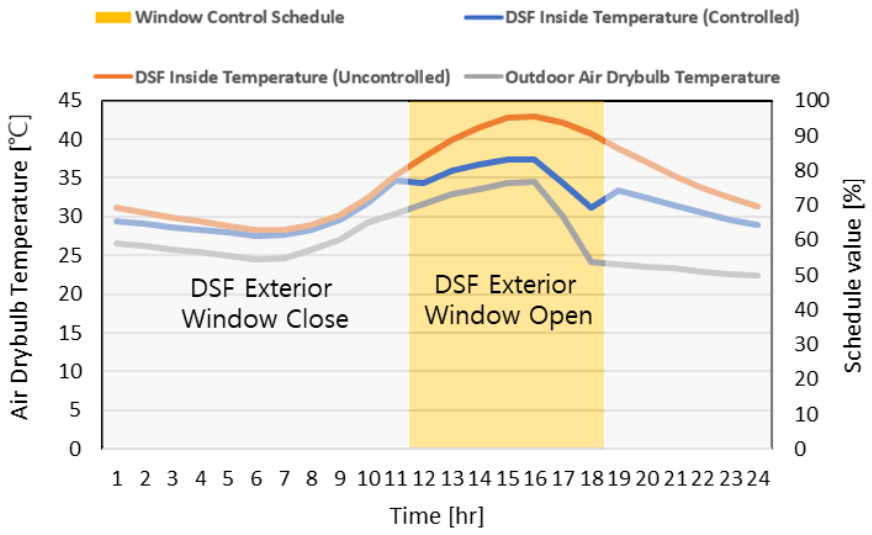

Figure 6-10: DSF window control schedule and temperature patterns on summer representative day

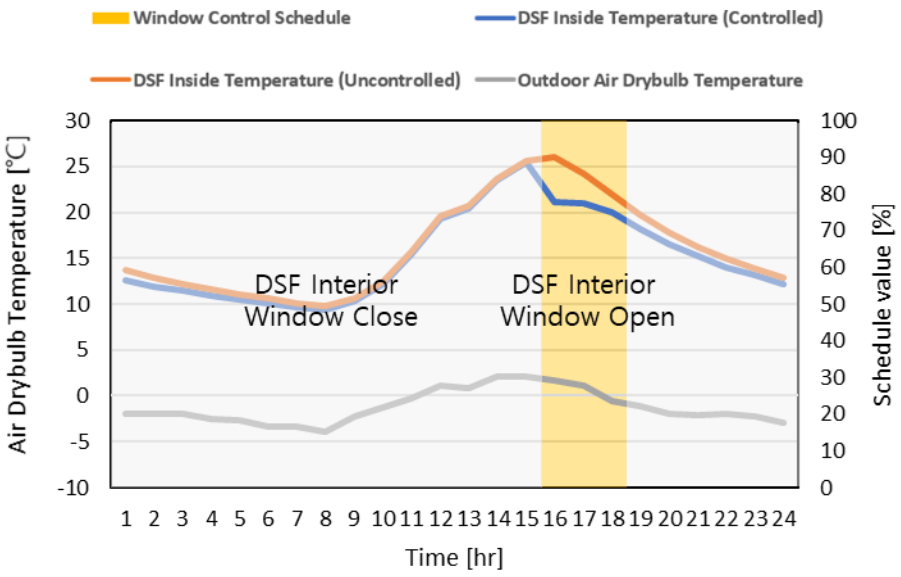

Figure 6-11: DSF window control schedule and temperature patterns on winter representative day

6.4.4 Analysis of total annual energy consumption

Figure 6-12 shows the saving in energy consumption for cooling, heating, and lighting through window control in the DSF system. A saving of 60.1% could be achieved in the energy

required for cooling annually through the installation of a DSF system, and a comparison of Case 2 and Case 3 shows that window control could add an additional saving of 2.4%. Therefore, a comparison of Cases 1 and 3 shows an annual saving of up to 61.6% in cooling energy, and a saving of 37.5% is possible in the heating energy through the DSF system. A comparison of Cases 2 and 3 show that an additional 0.4% of the heating energy used for the HP system could be saved through window control. A comparison of Case 1 and Case 3 shows that up to 37.7% of annual heating energy could be saved. Since there is no lighting control, the indoor lighting consumed 1,105 kWh/year, regardless of which case. Therefore, a maximum of 33.7% in annual cooling, heating, and lighting energy could ultimately be saved annually.

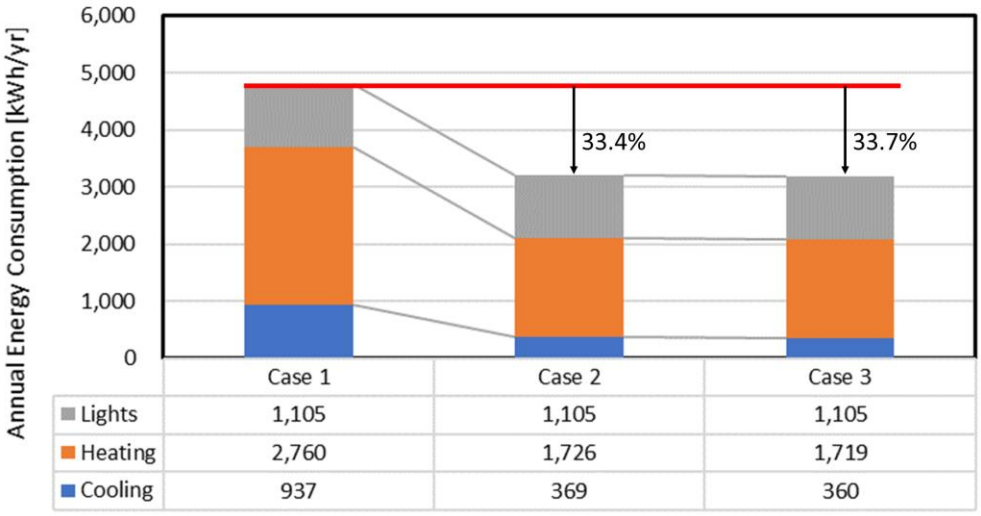

	Case 1	Case 2	Case 3
Lights	1,105	1,105	1,105
Heating	2,760	1,726	1,719
Cooling	937	369	360

Figure 6-12: Energy consumption saving for each factor

Figure 6-13 shows the monthly electrical energy generated by the installed PV system. The PV panels on the overhangs, tilted at 20 degrees, generate significant amounts of electricity during the summer, and the PV panels on the walls generate less electricity during

the summer with the high solar altitude angle. The annual electricity generation by the PV panels on the southern wall is 190.7 kWh/year, and the PV panels on the overhang produce 309.6 kWh/year. The PV panels installed on the overhang produce 62.4% more electrical energy than the PV panels installed on the wall.

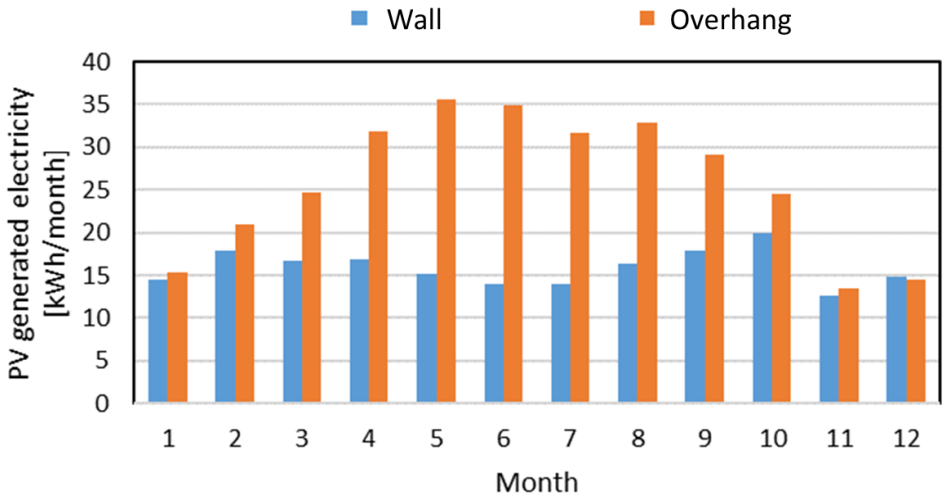

Figure 6-13: Electric energy generated by the PV system

Assuming that all of the electrical energy generated by the PV panels is used for cooling, heating, or lighting, up to 44.1% of annual cooling, heating, and lighting energy consumption could be saved, as shown in Figure 6-14. When considering cooling and heating energy consumption directly impacted by the installation of the DSF system, up to 57.3% of the cooling and heating energy consumption could be saved annually.

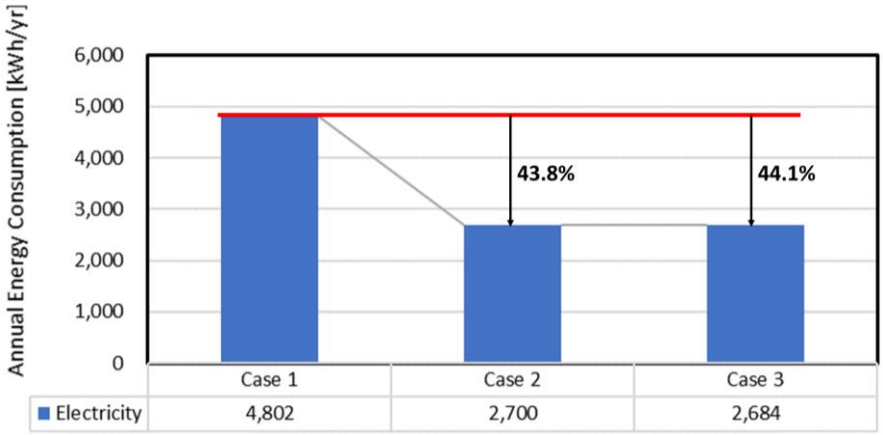

Figure 6-14: Annual energy consumption saved with electrical energy generated by PV system

6.5 Analysis of carbon dioxide emission

The Intergovernmental Panel on Climate Change (IPCC) provides formulas for calculating CO_2 emissions (Hyun et al., 2014). To calculate the CO_2 emission, the TOE (ton of oil equivalent) must first be calculated, using Equation 6-5.

The TOE is the energy generated when one ton of crude oil is combusted, and 1 TOE equals 1 kcal. The amount of fuel is the total amount of fuel used, and the oil conversion coefficient according to actual caloric value is recommended by the IPCC. Table 6-8 refers to the amount of net heating value and the oil conversion coefficient of the fuel used in this study, according to the energy calorie conversion from the Framework Act on Energy. Table 6-9 refers to the CO_2 emission coefficient (Lee et al., 2015).

TC (ton of carbon)/TOE – the carbon emission coefficient in Equation 6-6 – is the carbon intensity and signifies the carbon content of the fuel. The TC calculated by Equation 6-6 is utilized to calculate TCO_2 through Equation 6-7 (Hyun et al., 2014).

$$\text{TOE} = \text{The amount of fuel} \times \text{Net heating value} / 10^7 \text{ kcal} \quad \text{Eq. 6-5)}$$

Table 6-8: Net heating value and oil conversion coefficient

Fuel	Unit	Net heating value		Oil conversion coefficient
		Kcal	MJ	
Electricity	kWh	2,300	9.6	0.230

Table 6-9: Carbon dioxide emission coefficient

Fuel	Carbon emission coefficient		Carbon dioxide emission coefficient
	kg C/GC	TC/TOE	TCO_2/MWh
Electricity	-	-	0.4585

$$TC = TOE \times TC/TOE \times \text{burning rate} \quad \text{Eq. 6-6)}$$

$$TCO_2 = TC \times 44(CO_2 \text{ molecular weight}) / 12 \text{ (Carbon atomic rate)} \quad \text{Eq. 6-7)}$$

However, in the case of electricity Power is calculated based on the CO_2 generated from the fuel used to produce electricity, not the CO_2 emitted from electricity. Since the calculation is based on the CO_2 emitted from the fuel used, there is no official CO_2 emission coefficient for the electricity yet. In South Korea, the Korea Power Exchange (KPX) recommends the use of 0.4585 TCO_2/MWh as the CO_2 emission coefficient developed by considering hydroelectric power generation, nuclear energy generation, and thermal power generation (Lee et al., 2015). Therefore, 0.4585 TCO_2/MWh, as the CO_2 emission coefficient, is multiplied by the amount of electric energy used to calculate TCO_2.

Figure 6-15 refers to the CO_2 emissions for each case. Case 1 emitted 2.20 TCO_2, Case 2 1.24 TCO_2, and Case 3 1.23 TCO_2 annually. As for the reduction rate, Case 2 emits 0.96 TCO_2 less CO_2 annually than Case 1, which is a reduction rate of 43.8%, and Case 3 emits 0.97 TCO_2 less annually than Case 1, which is a reduction rate of 44.1%. This is equal to the amount of electrical energy saved when all the electrical energy generated by the PV system is used.

The reason is that cooling and heating system in the analysis consumes electrical energy. Therefore, since the only source of energy is electricity, the rate of electric energy saved and the reduction rate of CO_2 are equal.

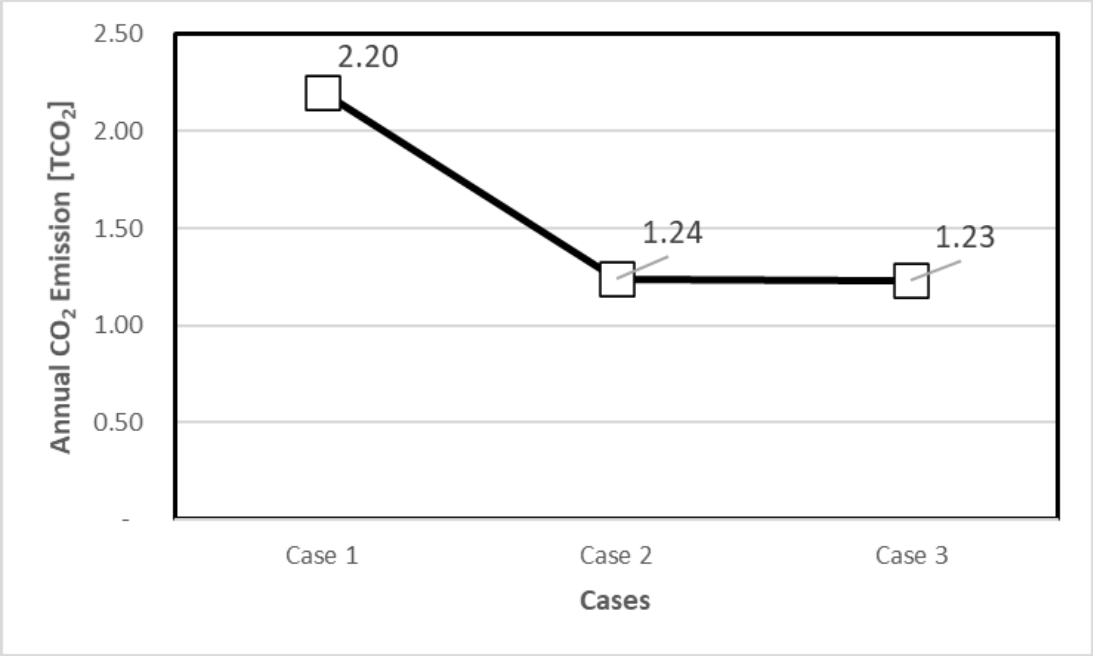

Figure 6-15: Annual CO_2 emission in each case

6.6 Life cycle cost analysis

As mentioned above, to suggest installing the DSF system in a retrofitted method, a short payback period is as important as saving energy. For the LCCA, three main categories were created (initial cost, maintenance cost, and cost savings), as shown in Figure 6-16.

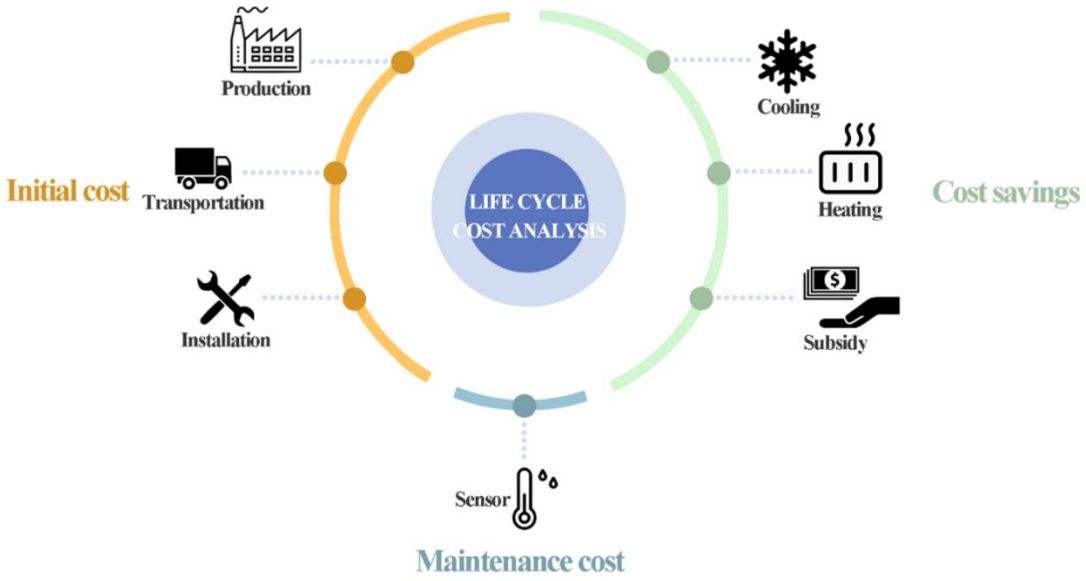

Figure 6-16: Factors considered for life cycle cost analysis

Equation 6-8 is used to analyze the life cycle cost. To analyze the life cycle cost, first the initial cost and then the maintenance cost were calculated. The LCCA is calculated by calculating the amount initial recovered after installation and the calculation of the annual saving in electrical energy cost through the amount of electricity energy saved annually.

$$\text{Payback period} = C_{in} + C_m – C_r - C_e \quad \text{Eq. 6-8)}$$

Where, C_{in} is initial cost ($), C_m is maintenance cost ($), C_r is the amount recovered in initial stage ($), and C_e is electric cost savings ($).

6.6.1 Initial cost

Equation 6-9 is used to calculate initial cost and Equation 6-10 to calculate production cost. Production cost is the sum of the cost of building the DSF structure, the cost of the windows, and the cost of the PV panels.

$$C_{in} = C_{pro}+C_{tr}+C_i \quad \text{Eq. 6-9)}$$

Where, C_{pro} is the production cost ($), C_{tr} is the transportation cost ($), and C_i is the installation cost

$$C_{pro} = C_{st}+C_{win}+C_{PV} \quad \text{Eq. 6-10)}$$

Where, C_{st} is the production cost for DSF structure, C_{win} is the cost for windows, and C_{PV} is the cost for PV panels.

The factors included in the production cost for the DSF structure are material and labor costs for building the DSF system, and each of the amounts refers to the amount is provided by the manufacturer company. The currency exchange rate used to convert the amount to US dollars was 1,200 won/$. The amount was rounded to whole dollars. As shown in Table 6-10, the total cost for building and installing the DSF system was $12,091. The cost of building the DSF system includes the components for building the walls, the frames of the DSF system, and the factors required for the window control. Therefore, it includes the cost of the materials to build the DSF system, the electric operator device for window control, and the cost of the internal and external windows of the DSF system. The cost of the PV system refers to the cost the PV panels.

To calculate the transportation and installation costs, Equation 6-11 was utilized.

$$C_{tr} = C_{eq} + C_l \quad \text{Eq. 6-11)}$$

Where, C_{eq} is transport equipment cost ($) and C_l is labor cost for the installation of the DSF system ($)

The transport equipment cost refers to the cost of the equipment rental to transport and install the DSF system, and the labor cost refers to the labor cost for DSF system installation.

Table 6-10: The cost of building and installing the DSF system

Type	Amount ($)
DSF system construction	7,008
Cost for the windows	1,250
PV system cost	2,250
Transport and lifting equipment	1,083
Labor cost	500
Total	12,091

6.6.2 Amount of initial recovery

The initially recovered is the amount of the cost recovered in the first year after the DSF installation. It was assumed that the installation of the DSF system eliminates the necessity to replace the windows – the typical retrofitting method. Thus, the cost of replacing windows was included in the amount of initial recovery. The amount provided by a company specializing in windows as cost of replacing exterior windows.

Equation 6-12 shows the amount that could be recovered in the first year of DSF installation. The cost of replacing windows refers to the cost of replacing windows (typical

retrofitting method), which was made unnecessary by the DSF system installation. Up to 80% of the cost of installing PV panels could be recovered as a subsidy. Although PV subsidies are not always supported, some cities provide steady support. The PV subsidy provided by Seoul Metropolitan City provides $1 per watt up to 500W of installed capacity of PV system, and another 60 cents per watt between 501W and 1,000W. Apart from this installation capacity, each house receives $45 for installing a PV system (Seoul Energy, 2020). The total capacity of the PV system is 656W, with 500W eligible for receiving $1 per W, and the remaining 156W eligible for receiving 60 cents per W. $594 could be received for the PV capacity and with the $45 subsidy for houses with PV systems, bring the total subsidy to $639. Table 6-11 shows the amount of initial recovery.

Equation 6-12 was used to calculate the initially recovered amount.

$$C_r = C_{re} + C_s \quad \text{Eq. 6-12)}$$

Where, C_{re} is the replacement cost of the typical retrofitting ($) and C_s is the amount of subsidy for installing the PV system ($)

Table 6-11: The amount of initial recovery

Type	Amount ($)
Typical cost of window replacement	5,148
PV subsidy	639
Total	5,787

6.6.3 Maintenance cost

The maintenance cost involves the cost of the server management controlling the DSF system. The cost of the server that manages the internal data of the DSF system, the external

environmental data, and internal building data collected for window control and provide information to residents is $66 annually. This information regarding the cost was sourced from an actual company that manages building data.

6.6.4 Payback period calculation

Of the $12,091 – the initial investment for the DSF system installation as seen in Table 6-10 – $5,787 is recovered immediately as the initial recovery amount shown in Table 6-11. The remainder of the initial investment, $6,304 after the initial recovery had been subtracted, plus the annual operational cost of $66 annually, is the amount that will establish the payback period.

The electricity costs saved through the installation of the DSF system, window control, and the amount of electricity generated by the PV system were elements to calculate the amount saved every year. To calculate the cost of electrical energy consumption, it is necessary to know how much electrical energy is used every month. The Korea Electric Power Corporation (KEPCO) has different fees for electricity in the summer season and the other seasons, and the charge is differentiated into three types, according to the amount of electrical energy consumed. Table 6-12 shows the electricity charge table provided by KEPCO which was converted to US dollars for this paper, with the currency exchange rate of 1,200 won per dollar. (KEPCO, 2021).

Table 6-12: Electricity charge

Summer (July 1 ~ August 31)			
Section		Demand charge ($/household)	Energy Charge ($/kWh)
1	1~300 kWh	0.76	0.08
2	301~450 kWh	1.33	0.16
3	450 kWh	6.08	0.23
Other seasons (January 1 ~ June 30 and September 1 ~ December 31)			
Section		Demand charge ($/household)	Energy Charge ($/kWh)
1	1~200 kWh	0.76	0.08
2	201~400 kWh	1.33	0.16
3	400 kWh	6.08	0.23

Figure 6-17 shows the electrical energy charge with the demand charge and energy charge shown in Table 6-12, based on the monthly electrical energy consumption for each case. The electricity bill is $965 for Case 1, $450 for Case 2, and $448 for Case 3, annually. Therefore, $517 could be saved in electricity bill annually with the DSF system and window control.

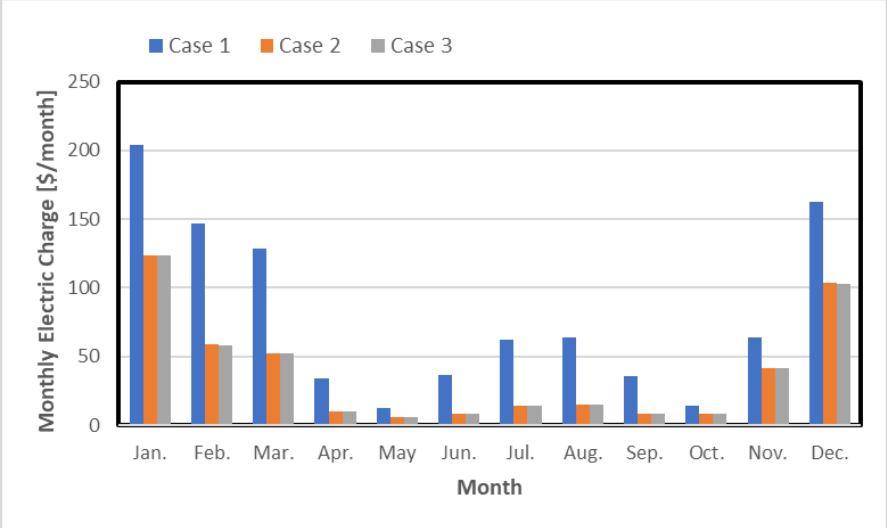

Figure 6-17: Monthly electricity charge for each case

Figure 6-18 shows the payback period for the DSF system, calculated by considering the aforementioned initial investment, initially recovered amount, operational costs, and reduced electricity charge. As mentioned before, $5,787 of the $12,091, the initial investment, could be seen as initial recovery. Of the remaining $6,304 – the amount remaining after deducting the initial recovery – $517 could be saved annually in electricity costs. However, the amount of $66 paid for operation costs must be deducted, leaving $451 as the amount that could be recovered every year to calculate the payback period. In the graph in Figure 6-18, 0 refers to the initial investment has been paid back, and the amount decreases sharply in the first year due to the initial recovery. Thereafter, $451 is recovered every year, meaning that the total amount of the investment could be recovered within 15 years of the DSF system installation. Therefore, the payback period for the DSF system proposed by this study is 15 years.

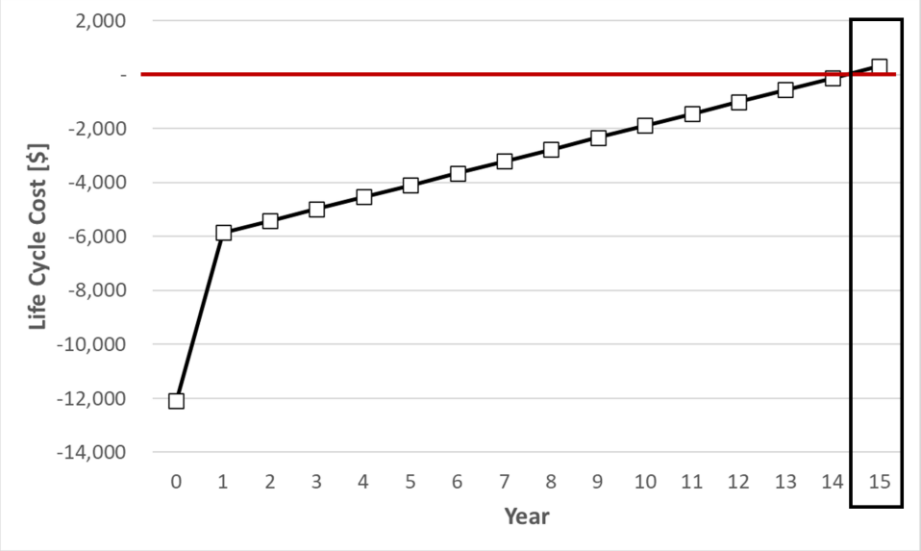

Figure 6-18: Life cycle cost analysis

6.7 Discussions

The payback period of 15 years is not a short time. Therefore, this chapter describes the factors that are not directly related to the payback period, but can reduce the payback period. Although the type and size of projects that support renovation by location are different, subsidies for the renovation of apartments support loan interest rather than a direct renovation. In addition, subsidies are normally provided for the renovation of the entire apartment complex rather than individual apartment units. For this reason, it does not apply to this study because this study is focused on apartment units, not the entire apartment complex. Thus, although there is no direct impact on the payback period, the increase in real estate value is an expected effect from retrofitting.

As an example, in June 2018, the Seoul Metropolitan Government designated seven apartments as pilot complexes. Figure 6-19 shows that apartment prices in selected retrofit apartment complexes are rising significantly compared to the past (MOLIT, 2021). The axis X of Figure 6-19 shows the name of the apartment in the test apartment complex as an abbreviation. In the six months before the designation of the test complex, apartment prices differed by apartment complexes, but rose up to 17%, at least 4% and an average of 11%. After the designation of the test complex, the price of apartments rose up to 51%, the lowest 7%, and the average 24%.

Of course, a single apartment complex, not a whole apartment complex, may not contribute to a surge in apartment prices. Also, it is difficult to predict the actual increase because the prices of apartments vary significantly. It is impossible to predict the real estate growth rate. However, as shown in Figure 19, apartment prices rose significantly a month after the designation of the test complex in June. Reconstruction seems to have affected apartment

prices. It is not predictable how much the payback period will be shortened, but rising real estate prices are expected to have a positive impact on the payback period calculated above.

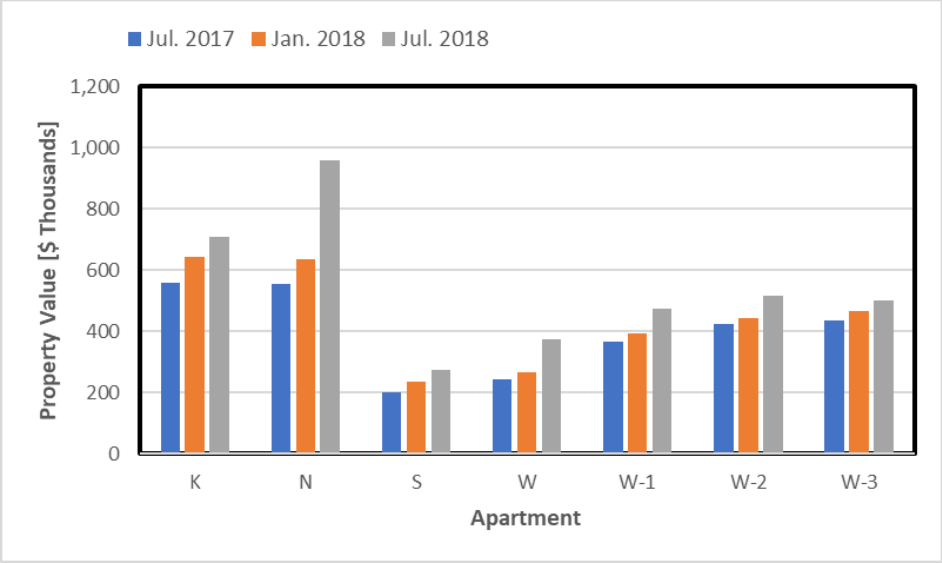

Figure 6-19: Price changes of the apartments designated as testing complex

6.8 Conclusion

In this study, life cycle costs were analyzed for the DSF system installed in old apartments in South Korea, which saves energy and reduces greenhouse gas emissions.

Results show that the DSF system saved 33.4% of heating, cooling, and lighting energy consumption, and saved 33.7% if the internal temperature of the DSF system is properly adjusted through the opening and closing windows. It can also save up to 44.1% of energy consumption by fully utilizing the electricity generated by PV panels installed in DSF systems.

In the case of greenhouse gas emissions, analysis was conducted by CO_2 emissions, which account for a large proportion of greenhouse gas emissions. The calibrated simulation

model used only electricity with a reduction in CO_2 emissions equal to the rate of energy consumption reduction, which shows the CO_2 emissions reduction of 44.1%.

For the life cycle cost analysis, the prices were provided by the actual companies; i.e. the cost of establishing and installing DSF systems such as transportation and lifting. The most plausible subsidy is the PV system installation grant. Considering the reduced electricity bill due to the installation of DSF systems, the payback period is calculated to be 15 years.

However, if the government subsidizes the retrofitting costs and/or the real estate prices rise due to the retrofitting, the payback period is likely to be shortened substantially.

Although this study assumes that the annual energy savings are the same, further analysis will be made in consideration of changes in energy use due to climate change and energy cost increases. Furthermore, the payback period for applying the DSF system to all apartment complex, not a single apartment unit, will be calculated.

Chapter 7 CONCLUSION AND FUTURE STUDIES

7.1 Conclusion

Energy efficiency improvement is absolutely necessary to solve the problem of fossil fuel depletion and global warming that the world faces. Buildings make up a large part of their energy use. This study proposes a DSF system as a retrofit method to reduce the energy use in old high-rise apartments over 20 years old. The region subject to analysis is South Korea, where high-rise apartment complexes are popular due to the high population density.

This paper consists of three research papers. Each paper evaluates whether the DSF system is an appropriate retrofit method for old high-rise apartment buildings, taking into account the energy savings and carbon dioxide emissions from the installation of the DSF system along with the analysis of life cycle costs. The summary of each research paper is as follows.

The goal of the first research paper is to analyze the potential for heating energy savings in different floors of high-rise apartment buildings. For analysis, simulation models of high-rise apartments are developed as shown in Figure 7-1, and a DSF system is installed for analysis every four floors. The main results of the first research paper are as follows.

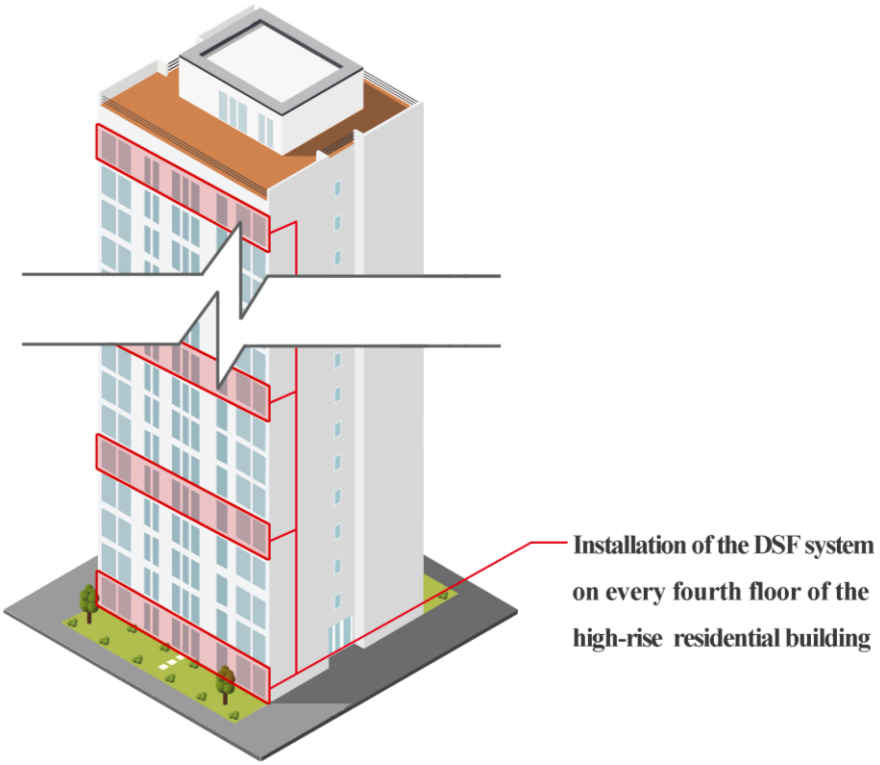

Figure 7-1: Location of the installation of the DSF system

- The 5th floor consumed the least amount of heating energy and the 25th floor the most. The amount of heating energy consumption of the 25th floor is 19,765 kWh annually, 15.0% more than the heating energy consumption of the 1st floor. Since the ground temperature is higher than the outdoor air temperature in the winter, the ground temperature affects the heating energy savings positively. Since the roof of the 25th floor is exposed to the external environment, it has a wider area touching the external environment compared to other floors. Therefore, the 25th floor consumes the most energy.
- In Case 1 where the exterior windows are replaced by high-performance windows, the 1st floor consumed 16,251 kWh annually, which is the highest amount of heating energy. The 21st floor showed the highest heating energy savings of 5.7% compared to

base case. If the DSF system were to be installed on the southern wall, the heating energy savings on the 5th floor is the lowest as 29.8%. The 21st floor showed the highest heating energy savings of 30.0%.

The second research paper aims to compare and analyze the annual heating energy consumption according to the thermal performance of the DSF system and the part load ratio (PLR) characteristics of the gas boiler.

- The PLR distribution of the boiler during the period in which the boiler is activated during the winter representative days was 0-86% in the Base-Case, 0-84% in Case-1, and 0-65% in Case-2. The maximum PLR value of Case-2 is smaller than that of other cases, which means that the heating load of Case-2 is lower than that of other cases because the same boiler capacity is installed in all cases.
- The boilers are repeatedly turned on and off according to the zone radiant HVAC heating rate during the operating hours of all three cases. The radiant floor heating system heats the space through the radiant heat of the floor surface rather than heating the indoor air directly. The internal heating set-point temperature is 21 ℃, with the boiler turned on when the indoor temperature is lower than 20.5 ℃and turned off at 21.5 ℃.
- The gas consumption rate for heating on winter representative days is 24 kWh at maximum in case of the Base-Case, 23 kWh in Case-1, and 18 kWh in Case-2. The gas consumption rate of Case-2 is the lowest. During the period from 7 PM to 8 PM, the internal heat of the DSF system accumulated during the day affects heating load reduction positively that no gas is consumed for heating during this period for Case-2.

- Also, the comparison of the PLR pattern and gas consumption pattern of Case-2 with those of Base-Case and Case-1 shows a delay of one hour. This is because the DSF serves as a thermal buffer, causing a thermal delay that delays the PLR pattern and gas consumption rate pattern of the boilers in Base-Case and Case-1 by 1 hour.
- All three cases show gas consumption patterns similar to the PLR patterns of the boiler. This could be explained by the boiler efficiency curve used in the research. The efficiency curve of the boiler changes the boiler efficiency by the boiler's PLR. The boiler efficiency curve applied in this research verified 3% change of boiler efficiency with the boiler's PLR increasing from 40% to 100%. In other words, since there is no great difference in the boiler efficiency according to the changes of the boiler's PLR, the PLR pattern of the boiler is similar to the gas consumption pattern.
- Figure 7-2 shows comparison of the annual gas consumption in three cases. Annual gas consumption is 17.7 MWh annually for the Base-Case, 16.7 MWh for Case-1, and 10.8 MWh for Case-2. Case-2 shows annual gas consumption that is lower by 38.8% compared to Base-Case and consumes 35.2% less gas annually compared to Case-1.

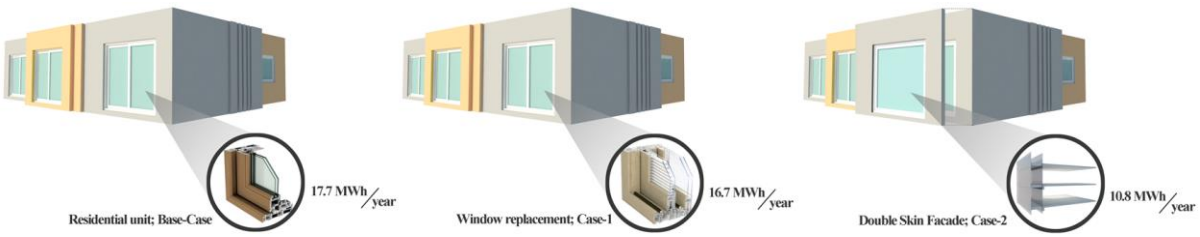

Figure 7-2: Comparison of the annual gas consumption in three cases

The key objective of the third research paper is to calculate the carbon dioxide emission as relates to energy consumption. Furthermore, life cycle cost analysis is conducted by

considering the initial cost and maintenance cost provided by a manufacturer company and building data managing company, electricity bill, and subsidy for installation of the PV system. The results of the third research paper are as follows.

- To calculate the initial cost, the costs of building, transportation, and installing the DSF system are considered, which are calculated based on the estimates of a company specializing in the system. An initial cost of $12,091 is calculated. The server management cost for the automatic control of the DSF system is $66 annually.
- In case of the initially recovered costs, since the DSF system installation is an alternative to the replacement of exterior windows as a typical retrofitting method, the saved cost of window replacement, and the subsidies for the PV system attached to the DSF system add up to the initially recovered cost of $5,787.
- The electricity bill saved from the energy savings by the application of the DSF system is calculated to be $517 annually, with the payback period from DSF system installation being 15 years.
- The price increase of apartment complexes with retrofit projects show that retrofitting has had positive impacts on the values of the apartments. Although it would not be possible to definitely state the increase of apartment prices from retrofitting by a specific amount or a specific percentage since the prices of apartments differ according to the sizes and the locations, it seems that retrofitting will have positive impacts on the increase of property value. Therefore, it is estimated that the payback period will be dramatically shortened from 15 years according to the estimated increase of property value.

7.2 Future Studies

This study proposes an advanced DSF system as a retrofit method to save energy in old, high-rise apartment buildings. The energy conservation and carbon dioxide emission reduction of the DSF system are verified, with the payback period calculated to be 15 years.

The future studies of this study are as follows.

1) Confined Region

The analysis of this study is limited to the climates in South Korean. In the future, analysis on different climates such as hot and humid regions and coastal regions will be carried out. Through such additional analyses, energy savings obtained by the DSF system installed in different climates will be analyzed, with appropriate optimal window opening control of the DSF system suggested according to different climates. Also, the subsidies for retrofitting provided by the region or nation of analysis will be identified to calculate the payback period when the DSF system proposed by this research is installed in different regions or nations.

2) Confined Building Type

A DSF system is used as a retrofit method for an old high-rise apartment building in this study. Buildings anticipated to save great amounts of energy through the DSF system are buildings exposed greatly to external environments including sunlight due to large window area. Since windows are inferior in terms of thermal performance to walls, buildings with large exterior window areas have lower thermal performance compared to buildings with large exterior wall areas. The high-rise apartment buildings analyzed in this study usually have large living room windows or balcony windows. That is why energy consumption can be saved by

the installation of the DSF system which can be contributed improvement of the thermal performance of the exterior wall and window. Therefore, calculation of energy savings and payback period by applying the DSF system to office buildings with curtain-wall structure or other building types in addition to high-rise apartment buildings will be pursued. Also, analysis on the appropriateness of single-story DSF system as suggested in this study and the multi-story DSF system will be conducted as well.

3) Limitation of the Experimental Study

This study conducted experimental study on a testing building to collect and analyze experiment data. The simulation model was calibrated through collected data. However, the test building has been built 2010s. So, I changed the input values of a calibrated simulation model to the conditions of an old high-rise apartment building. For more meticulous analysis and assessment of the DSF system's thermal performance, experimental study on an actual old high-rise apartment building is needed.

4) Climate Change

LCCA was carried out in this study with the assumption that an equal amount of energy is saved every year, but future studies are needed to analyze energy savings considering the fluctuating energy consumption caused by global warming. More realistic LCCA based on this analysis is needed.

5) Expansion to Apartment Complex

This study applied the DSF system as a retrofitting method on a single apartment unit. In retrofitting old apartment buildings in South Korea, multiple retrofitting methods (e.g., reinforcement of exterior insulation of walls, replacement of windows, replacement of lightings installed on the communal space of apartment complexes) are implemented simultaneously on the overall apartment complex rather than on each of the apartment units.

Therefore, if the DSF system is installed to the entire apartment complex rather than one apartment unit, other subsidies (e.g., interest rate support) can be expected in addition to the subsidy for the installation of the PV system which is applied in this study. Also, it can be expected to save the production cost, transportation cost, and installation cost due to mass production and installation of the DSF system. Considering these factors, it is necessary to calculate the payback period when installing the DSF system in the apartment complex.

REFERENCES

Alberto, A., Ramos, N.M.M., and Almeida, R.M.S.F. 2017. Parametric study of double skin facades performance in mild climate countries. Journal of Building Engineering, 12, 87-98.

American Society of Heating, Refrigerating and Air-Conditioning Engineers (ASHRAE). 2009. ASHRAE Handbook of Fundamentals. American Society of Heating, Ventilating, and Air Conditioning Engineers, Atlanta, Georgia.

American Society of Heating, Refrigerating and Air-Conditioning Engineers (ASHRAE). 2014. ASHRAE Guideline 14-2014, Section 5.3.3.3.10.

Arumagi, E. and Kalamees, T. 2014. Analysis of energy economic renovation for historic wooden apartment buildings in cold climates. Applied Energy, 115, 540-548.

Augenbroe, G., Brown, J., Heo, T.S., Kim, S.G., Li, Z., McManus, S., and Zhao, F. 2008. Lessons from an advanced building simulation course, third national conference of IBPSA-USA Berkeley, California.

City Mayors Statistics. 2007. The largest cities in the world by land area, population and density. Available: http://www.citymayors.com/statistics/largest-cities-density-125.html

Chan, A.L.S. and Chow, T.T. 2010. Investigation on energy performance and energy payback period of application of balcony for residential apartment in Hong Kong. Energy and Buildings, 42, 2400-2405.

Chan, A.L.S., Chow, T.T., Fong, K.F., and Lin, Z. 2009. Investigation on energy performance of double skin facade in Hong Kong, Energy and Buildings, 41, 1135-1142.

Chang, H. 2006. The East Asian Development Experience: The Miracle, the Crisis, and the Future. Zed Books.

Chantrasrisalai, C., Ghatti, V., Fisher, D.E., and Scheatzle, D.G. 2003.Experimental validation of the EnergyPlus low-temperature radiant simulation. American Society of Heating, Refrigerating and Air-conditioning Engineers (ASHRAE) Transactions, 109, 614–623.

Chin, K.I. and Yoon, J.H. 2010. Movable BIPV Shading Device Design for Apartment Building Balcony, Journal of the Korean Solar Energy Society, 30, 85-92.

Chin, K.I., Yoon, J.H., and Kim H.J. 2010. Window PV system design for apartment balcony

and evaluation of energy output, Conference of Korean Institute of Architectural Sustainable Environment and Building Systems, South Korea.

Cho, J., Park, B., and Lim, T. 2019. Experimental and numerical study on the application of low-temperature radiant floor heating system with capillary tube: thermal performance analysis. Applied Thermal Engineering, 163: 114360.

Choi, W., Joe, J., Kwak, Y., and Huh, J.H. 2017. Operation and control strategies for multi-storey double skin facades during the heating season. Energy and Buildings, 49, 454-465.

Dallo, G., Galante, A., and Pasetti, G. 2012. A methodology for evaluating the potential energy savings of retrofitting residential building stocks. Sustainable Cities and Society, 4, 12-21.

Dutton, S., Shao, L., and Riffat, S. 2008. Validation and parametric analysis of EnergyPlus: air flow network Model using contam. In: Third National Conference of International Building Performance Simulation Association (IBPSA-USA) (Simbuild 2008). Berkeley, California, USA, 124–131.

Federal Energy Management Program (FEMP). 2015. M&V Guidelines: Measurement and Verification for Performance-Based Contracts Version 4.0, Section 4.5.3.

Gelesz, A. and Reith, A. 2015. Climate-based performance evaluation of double skin facades by building energy modelling in Central Europe. Proceeding of Conference for 6th international buildings physics conference, 78, 555-560.

GhaffarianHoseini, A., GhaffarianHoseini, A., Berardi, U., Tookey, J., Li, D.H.W., and Kariminia, S. 2016. Exploring the advantages and challenges of double-skin facades (DSFs). Renewable and sustainable Energy, 60, 1052-1065.

Gratia, E. and Herde, A.D. 2004. Optimal operation of a south double-skin façade. Energy and Buildings, 36, 41–60.

Gratia, E. and Herde, A.D. 2007a. Are energy consumptions decreased with the addition of a double - skin?. Energy and Buildings, 39, 605-619.

Gratia, E. and Herde, A.D. 2007b. The most efficient position of shading devices in a double-skin facade. Energy and Buildings, 39, 364-373.

Gu, L. 2007. Airflow network modeling in EnergyPlus. Proceeding of Conference for the International Building Performance, Building Simulation 2007, Beijing, China,

September. 2007, 10, 964-971.

Hay, R. and Ostertag, C.P. 2018. Life cycle assessment (LCA) of double-skin façade (DSF) system with fiber-reinforced concrete for sustainable and energy-efficient buildings in the tropics. Building and Environment, 142, 327-341.

He, G., Shu, L., and Zhang, S. 2011. Double skin facades in the hot summer and cold winter zone in China: Cavity open or closed?. Building Simulation, 4, 283–291.

Henninger, R.H., Witte, M.J., and Crawley, D.B. 2004. Analytical and comparative testing of EnergyPlus using IEA HVAC BESTEST E100-E200 test suite. Energy and Buildings, 36, 855–863.

Hyun, I.T., Lee, J.H., Yoon, Y.B., and Lee, K.H. 2014. CO_2 Emission by Heat Pump System using Unused Energy Sources in Large-scale Greenhouse. In Proceedings of the Winter Conference of the Society of Air-Conditioning and Refrigerating Engineers of Korea (SAREK), Seoul, Korea, 340–343.

International Energy Agency. 2019. CO_2 emissions from fuel combustion. Available: https://www.iea.org/reports/co2-emissions-from-fuel-combustion-overview

International Performance Measurement & Verification Protocol (IPMVP). 2002. Concepts and Options for Determining Energy and Water Savings Volume 1, Section 3.4.4.2.

Jang, M.K., Kim, S.M., Song, I.H., and Lee, H.J. 2016. The energy saving effect of existing buildings according to the green remodelling. Proceedings of Conference for The Society of Air-conditioning and Refrigerating Engineers of Korea.

Joe, G.S., Kim, J.H., Yeo, M.S., and Kim, K.W. 2014. An experimental study on thermal performance of double skin façade in residential buildings. Journal of the Architectural Institute of Korea planning & design, 30, 177-184.

Joe, J.W., Choi, W.J., Kwon, H.S., and Huh, J.H. 2013. Load characteristics and operation strategies of building integrated with multi-story double skin façade. Energy and Buildings, 60, 185-198.

Karteris, M., Theodoridou, I., Mallinis, G., and Papadopoulos, A.M. 2014. Façade Photovoltaic systems on multifamily buildings: An urban scale evaluation analysis using geographical information systems. Renewable and Sustainable Energy Reviews, 39, 912-933.

Kim, D., Cox, S.J., Cho, H., and Yoon, J. 2018. Comparative investigation on building energy

performance of double skin façade (DSF) with interior or exterior slat blinds. Journal of Building Engineering, 20, 411-423.

Kim, D.W. and Park, C.S. 2010. Energy performance assessment of a double skin façade with different control strategies. Journal of Architectural Institute of Korea, 26, 389–398.

Kim, D.W. and Park, C.S. 2010. Energy performance assessment of a Double Skin Façade for various configurations. Journal of Architectural Institute of Korea, 26, 379-387.

Kim, G., Schaefer, L., and Kim, J.T. 2012. Development of a double-skin façade for sustainable renovation of old residential buildings, Indoor and Built Environment, 22, 180-190.

Kim, H.I., Kang, G.H., Park, K.E., So, J.H., Yu, G.J., and Suh, S.J. 2009. Analysis of Performance of Balcony Integrated PV System, Journal of the Korean Solar Energy Society, 29, 32-37.

Kim, S.Y. and Oh, C.O. 2012. A study of current status and residents' needs of balcony extension in Korean apartment housing. Journal of the Korean Institute of Interior Design, 21, 152–162.

Kim, T.H., Jung, Y.S., and Jung, H.G. 2016. A trend analysis of greenhouses gas reduction technique development for building sector in Korea. In: Proceedings of the fall conference of the Architectural Institute of Korea. Busan, Republic of Korea.

Kim, Y.J. and Park, C.S. 2010. Calibration of a Nodal Flow Network Simulation model. Journal of Architectural Institute of Korea, 26, 77-85.

Koh, B.B., Moon, J., Yoon, Y.B., Cho, S., and Ahn, Y.H. 2018. Integrated Smart Envelope Module for High-Rise Residential Building Retrofit. Advanced building skin conference, Bern, Switzerland, 28-29 October 2018.

Korea Energy Economics Institute (KEEI). 2016. Monthly Energy Statistics. Available: http://www.keei.re.kr/keei/download/MES1611.pdf

Korea Electric Power Corporation (KEPCO). 2021. Electric Rates Table. Available: http://cyber.kepco.co.kr/ckepco/front/jsp/CY/E/E/CYEEHP00201.jsp

Korea Institute of Energy Research (KIER). 2007. Energy Technology Transfer and Diffusion. Available: http://www.ndsl.kr/ndsl/search/detail/report/reportSearchResultDetail.do?cn=TRKO200800000932&SITE=CLICK, 2007.

Korea Research Institute of Mechanical Facilities Industry (KRIMFI). 2017. Study on heating and cooling load standard per area for apartments in 2017. Available: http://www.krimfi.re.kr/bbs/board.php?bo_table=pu_research_report&wr_id=26 7 August 2019.

Korea Statistical Information Service (KOSIS). 2020. 100 indicators of South Korea. Available: http://kosis.kr/conts/nsportalStats/nsportalStats_0102Body.jsp?menuId=10&NUM=.

Lee, D.Y., Seo, B.M., Hong, S.H., Choi, J.M., and Lee, K.H. 2019. Part load ratio characteristics and energy saving performance of standing column well geothermal heat pump system assisted with storage tank in an apartment. Energy, 174, 1060–1078.

Lee, E.J., Lee, D.Y., Hong, H.K., and Kim, Y.K. 2014. Measurement and Simulation of Heating Energy for Apartments with District Heating. Korean Journal of Air-Conditioning and Refrigeration Engineering, 26, 572-578.

Lee, J.H., Hyun, I.T., Yoon, Y.B., Lee, K.H., and Nam, Y.J. 2015. Energetic and Economic Assessment of Pipe Network Effects on Unused Energy Source System Performance in Large-Scale Horticulture Facilities. Energies, 8, 3328-3350.

Lim, J.H., Han, H.G., and Kang, D.R. 2017. Analysis on green remodeling status, satisfaction, and energy saving effect - Focusing on window replacing of residential buildings, Journal of the Architectural Institute of Korea Structure & Construction, 33, pp.75-80.

Luo, Y., Zhang, L., Wang, X., Xie, L., Liu, Z., Wu, J., Zhang, Y., and He, X. 2017. A comparative study on thermal performance evaluation of a new double skin façade system integrated with photovoltaic blinds. Applied Energy, 199, 281-293.

Ministry of Land, Infrastructure and Transport (MOLIT) and Korea Energy Agency (KEA). 2017. Guidebook of Building Energy Conservation Design Standard.

Ministry of Land, Infrastructure and Transport Statistics system (MOLIT). 2021. Real Estate Trade Management System. Available: http://rtdown.molit.go.kr/

Moon, J.W., Lee, J.H., and Kim, S. 2014a. Application of control logic for optimum indoor thermal environment in buildings with double skin envelope systems. Energy and Buildings, 85, 59-71.

Moon, J.W., Lee, J.H., Yoon, Y., and Kim, S. 2014b. Determining optimum control of double skin envelope for indoor thermal environment based on artificial neural network.

Energy and Buildings, 69, 175-183.

Moon, J.W., Part, J.C., and Kim, S. 2018. Development of control algorithms for optimal thermal environment of double skin envelope buildings in summer. Building and Environment, 144, 657-672.

Morelli, M., Ronby, L., Mikkelsen, S.E., Minzari, M.G., Kildemoes, T., and Tommerup, H.M. 2012. Energy retrofitting of a typical old Danish multi-family building to a "nearly-zero" energy building based on experiences from a test apartment. Energy and Buildings, 54, 395-406.

Oliver, T., Lew, D., Redlinger, R., and Prijyanonda, C. 2001. Global energy efficiency and renewable energy policy options and initiatives. Energy for Sustainable Development, 2, 15–25.

Olivier, J.G.J., Schure, K.M., and Peters, J.A.H.W. 2017. Trends in Global CO_2 and Total Greenhouse Gas Emissions 2017 Report, PBL Netherlands Environmental Assessment Agency.

Pak, R., Ocak, Z., and Sorgüven, E. 2018. Developing a passive house with a double-skin envelope based on energy and airflow performance. Building Simulation, 11, 373-388.

Park, C.Y., Lee, K.H., Yoon, Y.S., and Choi, C.H. 2007. A comparative experimental study on thermal performance of box-typed double skin and curtain wall in cooling period. Journal of the Korean Solar Energy Society, 27, 111-119.

Park, D.J., Yu, K.H., Yoon, Y.S., Kim, K.H., and Kim, S.S. 2015. Analysis of a Building Energy Efficiency Certification System in Korea. Sustainability, 7, 16086-16107.

Pomponi, F., Piroozfar, P.A.E., Southall, R., and Ashton, P. 2015. Life cycle energy and carbon assessment of double skin facades for office refurbishments. Energy and Buildings, 109, 143-156.

Qahtan, A.M. 2019. Thermal performance of a double-skin façade exposed to direct solar radiation in the tropical climate of Malaysia: A case study. Case Studies in Thermal Engineering, 14, 100419.

Raeissi, S. and Taheri, M. 1998. Optimum overhang dimensions for energy saving. Building and Environment, 33, 293-302.

Raftery, P., Lee, K.H, Webster, T., and Bauman, F. 2011. Performance analysis of an integrated UFAD and radiant hydronic slab system. Applied Energy, 90, 250–257.

Seo, B.M. and Lee, K.H. 2016. Detailed analysis on part load ratio characteristics and cooling energy saving of chiller staging in an office building. Energy and Buildings, 119, 309–322.

Seo, B., Yoon, Y.B., Mun, J.H., and Cho, S. 2019. Application of Artificial Neural Network for the Optimum Control of HVAC Systems in Double-Skinned Office Buildings. Energies, 12.

Seoul Energy. 2020. Subsidy information for PV installation on the Balcony. Available: https://www.sunnyseoul.com/citizen/fund.do

Silva, F.M.D., Gomes, M.G., and Rodrigues, A.M. 2015. Measuring and estimating airflow in naturally ventilated double skin facades. Building and Environment, 87, 292-301.

Song, D.S. and Choi, Y.J. 2012. Effect of building regulation on energy consumption in residential buildings in Korea. Renewable and Sustainable Energy Reviews, 16, 1074-1181.

Souza, L.C.O., Souza, H.A., and Rodrigues, E.F. 2018. Experimental and numerical analysis of a naturally ventilated double skin façade. Energy and buildings, 165, 328-339.

Spastri, M., Noble, D., Kensek, K., and Choi, J. 2015. The use of dynamic environment control systems (DECS) in cavities of double skin facades for energy savings. Procedia Engineering, 118, 823-841.

Statistics Korea. 2017. 2016 Population and Housing Census. Available: http://kostat.go.kr/portal/eng/pressReleases/8/7/index.board?bmode=read&bSeq=&aSeq=363132&pageNo=1&rowNum=10&navCount=10&currPg=&searchInfo=&sTarget=title&sTxt=

Statistics Korea. 2019. 2018 Population and Housing Census. Available: http://kostat.go.kr/portal/eng/pressReleases/8/7/index.board?bmode=read&bSeq=&aSeq=378503&pageNo=1&rowNum=10&navCount=10&currPg=&searchInfo=&sTarget=title&sTxt=

Strand, R.K. and Pedersen, C.O. 2002. Modeling radiant systems in an integrated heat balance-based energy simulation program. American Society of Heating, Refrigerating and Air-conditioning Engineers (ASHRAE) Transactions, 108, 979–987.

Sung, Y.M. and Faith, B. 2019. Placing innovation and efficiency at the heart of Korea and the world's energy future. International Energy Agency. Available:

https://www.iea.org/commentaries/placing-innovation-and-efficiency-at-the-heart-of-korea-and-the-worlds-energy-future

Terrenoire, E., Hauglustaine, D.A., Gasser, T., and Penanhoat, O. 2019. The contribution of carbon dioxide emissions from the aviation sector to future climate change. Environmental research letters. 2019. Vol. 14. No. 8. 084019.

Testo Ltd. 2019. Available: https://www.testo.com/en-UK/testo-175-t1-set/p/0572-1750, 3 March 2019.

The official website of Ministry of Land, Infrastructure and Transport Statistics system. 2016. APT House Living Condition Statistics 2016. Available: http://stat.molit.go.kr/portal/cate/statView.do?hRsId=33&hFormId=716&hSelectId=748&hPoint=%5Bobject+HTMLInputElement%5D&hAppr=1&hDivEng=&oFileName=&rFileName=&midpath=&month_yn=N&sFormId=716&sStart=2016&sEnd=2016&sStyleNum=260&sDivEng=N&EXPORT=. 2016

United Nations Framework Convention on Climate Change (UNFCCC). 2015. Submission by the Republic of Korea -Intended Nationally Determined Contribution-. Available: https://www4.unfccc.int/sites/ndcstaging/PublishedDocuments/Republic%20of%20Korea%20First/INDC%20Submission%20by%20the%20Republic%20of%20Korea%20on%20June%2030.pdf

U.S Energy Information Administration (EIA). 2017. Monthly Energy Review April. PSG Facility Services.

U.S. DOE. 2017. EnergyPlus version 8.9, ASHRAE 2005 HOF Materials.idf.

U.S. DOE. 2019. EnergyPlus version 9.0, ASHRAE 2005 HOF Materials.idf.

U.S. DOE. 2019a. EnergyPlus Engineering Reference: the reference to EnergyPlus calculations Version 9.0.

U.S. DOE. 2019b. EnergyPlus input output reference. The encyclopedic reference to Energyplus input and output, version 9.0.

Walton, G.N. AIRNET - A Computer Program for Building Airflow Network Modelling, Washington, DC, 1989.

Winkelmann, F.C. 2011. Modelling windows in EnergyPlus. In: Third National Conference of International Building Performance Simulation Association (IBPSA) (Building Simulation 2001), Rio de Janeiro, Brazil, 457–464.

Won, K.H. and Huh, J.H. 2002. Airtightness Evaluation of Apartments based on their deterioration length. Paper presented at the Society of Air-conditioning and Refrigerating Engineers of Korea, Seoul, South Korea, 508-513.

Yoon, Y.B., Koh, B.B., and Cho, S. 2018. An Analysis of Energy Efficiency of a Smart Envelope Package in Residential Buildings. In Proceeding of Conference for ARCC-EAAE 2018 International Conference, Philadelphia, PA, United States, 2, 27-35.

Yoon, Y.B., Seo, B.M., Koh, B.B., and Cho, S. 2019. Performance analysis of a double-skin façade system installed at different floor levels of high-rise apartment building. Journal of Building Engineering, 26, 100900.

Yu, B.H., Seo, B.M., Moon, J.W., and Lee, J.H. 2015. Analysis of the part load ratio characteristics and gas energy consumption of a hot water boiler in a residential building under Korean climatic conditions. Korean Journal of Air-Conditioning and Refrigeration Engineering, 27, 455–462.

Yuen, B. and Yeh, A.G.O. 2011. High-Rise Living in Asian Cities. Springer.

Zomorodian, Z.S. and Tahsildoost, M. 2018. Energy and carbon analysis of double skin façades in the hot and dry climate. Journal of Cleaner Production, 197, 85-96.